Master's thesis

NTNU
Norwegian University of Science and Technology
Faculty of Natural Sciences
Department of Chemistry

Anders Granli Haraldsen

Investigating synthesis strategies for materials SAPO-40, AlPO-40 and CuAlPO-40

Master's thesis in MSCHEM

Supervisor: Karina Mathisen & Muhammad Mohzin Azim & Guro Sørli

September 2019

NTNU
Norwegian University of Science and Technology

Anders Granli Haraldsen

Investigating synthesis strategies for materials SAPO-40, AlPO-40 and CuAlPO-40

Master's thesis in MSCHEM
Supervisor: Karina Mathisen & Muhammad Mohzin Azim & Guro Sørli
September 2019

Norwegian University of Science and Technology
Faculty of Natural Sciences
Department of Chemistry

NTNU
Norwegian University of
Science and Technology

Abstract

The aim this thesis was to investigate synthesis strategies for materials SAPO-40, AlPO-40 and CuAlPO-40, materials belonging to the *AFR* zeotype system. With a uniquely shaped pore system, potential large surface area, and high hydrothermal stability, the AFR system is a prime candidate for the development of new catalysts. Combining these capabilities with the catalytic power of copper substituted into the framework of zeotypes, made the materials exciting, potential catalysts.

These materials are, to the extent of the author's knowledge, less represented in reported literature when compared to other zeotypes such as SAPO-34 and SAPO-11, and there is a large uncharted territory when it comes to using these materials in catalysis. Both SAPO-40 and AlPO-40 have reportedly been synthesized, while CuAlPO-40 is a completely new material.

No synthesis reported in literature for neither SAPO-40 nor AlPO-40 could be reliably reproduced. Of all the investigated synthesis sources, the AlPO-40 synthesis from Sierra, L. et al was the most successful.

Various physical and chemical parameters were investigated. SAPO-40 was obtained once as a minor phase, though seemingly randomly, and no parameter was found to influence its formation.

For AlPO-40, it was found that washing the liners with concentrated hydrofluoric acid (HF) in order to remove contaminants that could seed byproducts was crucial in order to obtain the desired phase. The water content of the gel was also found to be of upmost importance. Lowering the water content from 37.5 molar equivalents to 32.5, thus lowering the pH to about 6, succeeded in producing a sample where AlPO-40 was the only crystalline phase present. There were some broad peaks in the diffractogram however, indicating that it was not phase pure still. The crystallization time was also found to be important for the crystallization of AlPO-40, with longer time values producing more crystalline and less contaminated samples.

The most promising AlPO-40 sample was calcined and the total surface area was determined to be 528 m^2/g of which 378 $m^2/$ could be attributed to the micropore area. This value was comparable to other, commercialized zeotypes such as SAPO-5.

Finally, phase pure CuAlPO-40 was *not* obtained, but a sample where the AFR phase was the majority phase was obtained. The sample was blue in its as-prepared form and turned a greenish colour upon calcination, possibly indicating successful framework incorporation of copper, but further tests would be needed to confirm this.

Sammendrag

Målet med denne oppgaven var å undersøke syntesestrategier for fremstilling av materialene SAPO-40, AlPO-40 og CuAlPO-40, materialer i AFR zeotyp systemet. På grunn av materialenes unike poresystem, potensiale for høyt overflateareal og høy hydrotermisk stabilitet, så blir AFR systemet ansett som en god kandidat for utvikling av nye katalysatorer. Materialene som oppgaven omhandler er, så langt forfatter kjenner til, mindre representert i litteraturen sammenlignet med andre zeotyper som SAPO-34 og SAPO-11, og det er et stort ukjent territorie i bruken av disse materialene i katalyse. SAPO-40 og AlPO-40 har begge blitt rapportert syntetisert, mens CuAlPO-40 er et helt nytt materiale. Ingen synteser fra litteraturen kunne reproduseres i nevneverdig grad. Av alle syntesene som ble undersøkt, var metoden fra Sierra, L. et al. den mest lovende. Ulike fysiske of kjemiske parametere ble undersøkt. En prøve ga SAPO-40 som den mindre fase, tilsynelatende tilfeldig. Ingen parametere som ble undersøkt så ut til å promotere SAPO-40.

For AlPO-40, ble flere kristiske parametere identifisiert. Reaktoren reaksjonen skjer i, må vaskes med konsentrert flussyre (HF) for å fjerne spor av kontaminerende biprodukter som kan katalysere krysallering av feil produkt. Vanninnholdet i gel-en ble også bestemt som en kritisk parameter. Ved reduksjon fra 37.5 til 32.5 molare ekvivalenter vann, som reduserte pH til ca. 6, så ble en prøve hvor AlPO-40 var eneste krystalline fase oppådd. Diffraktogrammet hadde også brede, uidentifiserte topper, som tydet på at prøven ikke var fullstendig faseren. Krystallisasjontid ble også identifisert som en viktig parameter. Ved økning i tid, så ble mer krystalline prøver, med lavere kontamineringsgrad, oppnådd. Den mest lovende AlPO-40 prøven ble kalsinert og overflate arealet ble undersøkt. Arealet ble funnet til å være på 528 m^2/g hvorav 378 m^2/g kunne attribueres til mikropore-arealet. Til slutt, faseren CuAlPO-40 ble *ikke* oppnådd, men en prøve hvor AFR fasen var største fase ble oppnådd. Prøven var blå i sin tillagde tilstand og endret farge til mer grønnlig etter kalsinering, noe som tyder på vellykket rammeverks-inkorporering. Videre tester er nødvendig for å bekrefte dette.

Aknowledgements

First and foremost, I would like to thank my supervisor, Associate Professor Karina Mathisen, for allowing me to work with such an exciting topic. You have been a great help in guiding me towards being a more hard-working and disciplined person. Your continuous feedback, patience and generosity has helped me immensely throughout the process of the master thesis and for that I am very grateful.

I would also like to thank my co-supervisors, Dr. Muhammad Mohzin Azim and PhD candicate Guro Sørli, for your help with both practical and theoretical problems I faced. Your willingness to always lend a helping hand, has benefited me greatly. Your valuable input and ability to view things from a different angle, has helped me and my project grow.

I would also like to extend my gratitude to the Structural Chemistry group for providing an engaging and caring social environment that functioned as a great support system during the master thesis. I will appreciate all the times we got to share.

My friends and family also deserve a heartfelt thanks. You helped me through my roughest patches of the project and were always there for me to provide love and entertainment. Special thanks goes out to my parents, who were ready to drop everything they were doing in a heartbeat in case I needed them.

The technical personnel that assisted me during the project also deserve a mention. I would like thank Roger Aarvik for his assistance with ordering chemicals. I would also like to Kristin Høydalsvik Wells and Silje Strand Lundgren for their guidance and support with the XRD measurements. I would also like to thank Anuvansh Sharma and Elin Harboe Albertsen for their assistance with BET measurements. Finally, I would like to thank SASOL for providing psuedoboehemite free of charge.

List of symbols

Symbol	Explanation	Unit
n	Integer number	-
d	Interplanar spacing	m
θ	Diffraction angle	-
t_1	Mixing time	h
t_2	Mixing time	h
t_3	Ageing time	h
t_4	Crystallization time	h
T	Crystallization temperature	°C
P	Pressure	bar
P_0	Ambient pressure	bar
V	Volume	cm^3
D	Pore diameter	Å

List of abbreviations

Abbreviation	Explanation
SAPO	silicon aluminophosphate
AlPO	aluminophosphate
CuAlPO	copper aluminophosphate
MeAlPO	metal aluminophosphate
AFR	Aluminophosphate Forty
AFI	Aluminophosphate Five
AFX	Aluminophosphate Fifty six
FAU	Faujasite
CHA	Chabazite
TPAOH	Tetrapropylammonium hydroxide
TPABr	Tetrapropylammonium bromide
TMAOH	Tetramethylammonium hydroxide
TEAOH	Tetraethylammonium hydroxide
SDA	Struture Directing Agent
HF	Hydrofluoric acid
TEOS	tetraethyl orthosilicate
IUPAC	International Union of Pure and Applied Chemistry
XRD	X-ray diffraction
BET	Braunauer, Emmet, Tiller
BJH	Barret, Joyner, Halenda
σ	Sigma Aldrich
α	Alfa Aesar
S40	silicon aluminophosphate 40
A40	aluminophosphate 40
CuA40	copper aluminophosphate 40
D	Dumont
S	Sierra
L	Lourenço
B	Before
A	After

Contents

Chapter 1

Introduction

Innovation has always been one of humanities best survival tools. The ability to adapt and evolve our technology in tandem with our changing environment and to meet the challenges we face head on, has been detrimental to our success as a species.

Perhaps the greatest challenges of our time, are climate change and resource scarcity.[1,2] These issues are tightly interwoven as in order to resolve climate change, new technologies have to be developed. To make these new technologies, smarter ways of using non-renewable resources must be considered. Humanity is currently starting to exhaust several rare metal reservoirs in our never-ending quest for improvement and efficiency. If some this innovation could be done with more abundant materials, we as a species would greatly benefit from it.

For the purposes of this thesis, the main focus will be the investigation of synthesis strategies for the development of new catalysts using cheaper and more common materials. These catalysts could potentially be used in processes such as the making of bio diesel or conversion of NO_x gases to less harmful substances.

Catalysts are used in a wide variety of reactions in order to facilitate desired chemical pathways.[3] Working by altering activation energy needed in a reaction, catalysts need a favourable electronic structures in order to have the desired interactions with the reactants. As a consequence of this, many catalysts use transition metals.[4] There are stark differences in the transition metals when it comes to price and availability. Some are cheap and widespread, such as iron or copper, while others are expensive and rare, such as platinum or iridium.[5]

One set of catalysts that utilizes the capabilities of transition metal cations, are zeotypes with metal ions either in the matrix or supported on it.[6] Zeotypes are a class of material with a range of interesting physical and potential chemical capabilities. They can form in many different structural configurations with nano-

scale channels, enabling their use as molecular sieves.[7] Furthermore, zeotypes typically have a very large surface area, often above 300 m^2/g.[8] Due to the many different zeotype structures and the possibilities of supporting transition metal cations with varying catalytic abilities, there is a large potential research field into making novel catalysts that can replace traditional catalysts used today.

One such example, is replacing the standard platinum catalyst used to convert methane to methanol, with a copper based catalyst supported on a specific zeotype.[9,10] This has a multitude of advantages. The traditional catalyst uses the expensive and limited metal platinum, and replacing this with the much cheaper and much more abundant copper, is beneficial. The greater surface area of the zeotype can also add to the reactivity of the catalyst by increasing the amount of active sites. The methanol produced with transition metal containing zeotypes can then be used in the production of precursors for bio-diesel and other simple organic molecules, and various organic transformation reactions.[11,12]

The main focus of this thesis will not be catalysis itself, but rather the development of synthesis pathways for novel catalyst materials. The zeotype which will be synthesized as the framework are the AlPO-40 and SAPO-40 zeotypes, a zeotype with a characteristic intersecting pore network of multiple pore sizes.[7] It has been stated to be more hydrothermally stable than other more established, closely related zeotypes such as SAPO-34 and SAPO-11.[13] To the extent of the author knowledge, there is limited literature into transition metal containing AlPO-40 and SAPO-40. Only two metals, zinc and cobalt, seem to have been supported successfully on the system.[12,14]

There is large, untapped potential into supporting transition metals in SAPO-40 and AlPO-40, and this will be focus of this thesis. The main aim of the thesis will be to investigate synthesis strategies for making SAPO-40, AlPO-40 and CuAlPO-40. The materials could potentially have a variety of interesting and new catalytic properties when compared to other similar materials; and if efficient and reproducible synthesis pathways can be discovered, a new frontier of catalysis science can be explored.

Chapter 2

Theory

2.1 Zeotypes

Zeotypes are molecular structures which resemble zeolites in structure, but vary in chemical composition. Traditional zeolites contain interlinked alumina and silica tetrahedra connected by oxygen bridges. These tetrahedra are arranged in particular ways, allowing for microscopic pores and cages to form. The pores that form are classified according to ring size, ranging from as small as 4-ring pores[7] to as large 18-ring pores.[15] The ring "size" is in turn determined by the amount of tetrahedra atoms (aluminium, phosphorus and silicon) in the ring. Pores can be classified according to IUPAC, in a different system when only the overall size range is considered, these are presented in Table 2.1 below.[16]

Table 2.1: Table showing the different pore classification according to IUPAC.[16]

Pore type	Size range
Micropores	Below 2 nm
Mesopores	Between 2 and 50 nm
Macropores	Above 50 nm

Replacing the aluminium or silicon in the zeolite framework with phosphorus will result in a wide range of materials hereafter referred to as zeotypes. In the 1980's, Wilson et al.[17] experimented with replacing either aluminium or silicon with phosphorus, resulting in two new material classes, aluminophosphates (AlPO) and silica-aluminosphosphates (SAPO).

Zeotypes are common materials in catalysis due to their large surface area and possibility for shape selectivity of reactants and products due to their unique

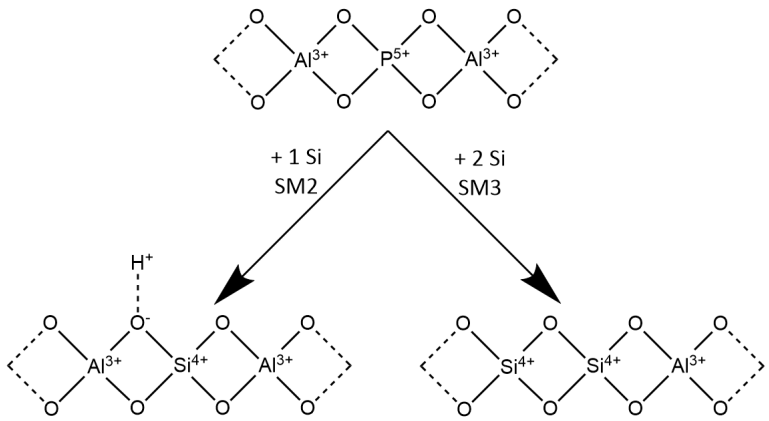

Figure 2.1: Figure showcasing the SM2 and SM3 substitution reactions when silicon is incorporated into the

nano-scale pore structures and molecular sieve properties.[8,18]

2.1.1 AlPOs and SAPOs

Aluminophosphates are a class of zeotypes where no silicon is present in framework. Instead, they are constructed only from equivalent amounts of phosphate- and alumina-tetrahedra and as a result they have no net framework charge.[19]

When silicon is inserted into the framework by replacing phosphorus during the synthesis, referred to as an SM2 substitution, a charge deficiency is created.[20] Silicon can also replace a set of adjacent aluminium and phosphorus ions, creating a small silica island in the network, this is referred to as a SM3 substitution.[21] These two substitutions are illustrated in Figure 2.1 below. Silicon can also solely replace an aluminium ion, but this is exceedingly rare due to the hypothetical formation of energetically unfavourable Si-O-P bonds..[21]

AlPO frameworks are charge neutral while SAPO frameworks contain a net negative charge. This negative charge is balanced by cationic template molecules prior to calcination, and hydrogen ions afterwards. These hydrogen ions create *Brønsted acid sites*,[22] sites of varying acidic strength depending on the chemical environment. These acid sites can act as catalytic seats in a variety of reactions.[13,23]

2.1.2 Nomenclature

These new materials are structurally classified within a system where a number (n) after the composition (AlPO/SAPO) denotes the structure. These numbers are equal across the material types, making them independent of the composition. Any framework also has its own associated three-letter framework code. This code is assigned to a material based on its pore systems and can be shared across different material classes.[7] These codes can be named in various ways; either after the organization who discovered the framework, the natural zeolite of which it resembles, or after the chronological order its aluminophosphate variant was discovered. Examples of this are the framework codes CHA and FAU named after the naturally occuring (CHA)bazite and (FAU)jasite minerals respectively, or AFI and AFR which are shorted versions of (A)luminophosphate (FI)ve and (A)luminophosphate (F)ou(R)ty.

2.1.3 Synthesis of zeotypes

Zeotypes are most commonly synthesized through a *hydrothermal* method which involved subjecting a gel to high temperatures and pressures over prolonged amounts of time ranging from a couple of hours to several weeks.[17] Parameters which are critical for specific zeotype formation will be described in detail in subsequent sections, but a short summary is listed in Table 2.2 below.

Table 2.2: Table showcasing parameters that are critical for zeotype formation in regards to effect on synthesis conditions, yield, purity and specific material that is obtained.

Parameter	Roles
Gel chemistry (molar ratios)	Structure specification, crystallization rate
Templates used	Structure direction and blocking, pH control
pH	Structure specification, crystallization rate
Ageing time	pH control, crystallization rate, homogeneity
Crystallization time	Structure specification, yield and crystallinity
Crystallization temperature	Structure specification, kinetic control, crystallinity

2.1.3.1 Reactants and ratios, gel chemistry

For the purposes of this thesis, SAPOs, AlPOs and MeAlPOs will be discussed. All gels are composed of dissolved precursors, mineralizers that help dissolve precursors, templates and a solvent. Other additions to gels include small quantities of metal ions that ideally replaces some of the framework atoms (In the case of

MeAlPOs), seeds in order facilitate faster crystallization of specific phases, and a salt that can aid in structure direction and stabilization.[6,24]

The aluminium is most commonly introduced as alumina (i. e. pseudoboehemite) or as aluminium isopropoxide in certain syntheses. Phosphorus is the second important framework atom, commonly introduced as ortho-phosphoric acid to serve a dual purpose as both a reactant and a pH controller.[25] If silicon is being introduced into the gel, there are a variety of common silicon sources that have been used, the most common being tetraethyl orthosilicate (TEOS), fumed silica and colloidal silica. Which source that should be used in the synthesis is dependent on the purity requirement of the synthesis.[26]

Ratios between the different reactants are often given in their molar oxide forms such as in the example given below.

$$1\mathrm{Al_2O_3} : 1\mathrm{P_2O_5} : x(\mathrm{SiO_2}) : y\mathrm{H_2O} : z\mathrm{R_2O} : a(\mathrm{MeO})$$

where R is a template molecule in its ionic form, x is the molar fraction of silicon if present, y is the molar fraction of water, z is the molar fraction template and a is the molar fraction of metal if present. Considering the ratios, there are a few baselines present which set the ground for many syntheses. Al and P almost always appear in equimolar amounts in order to ensure the crystallization of a framework that is charge neutral, unless dopants such as silicon or transition metals are present. Many syntheses use a base of 10 H_2O per framework atom in order to satisfy proper solvation and mixability of the gel, but this has also been reported as both higher and lower ratios as well.[19,25]

Ageing is a central part of many zeotype syntheses, it ensures homogeneity and proper availability of reactants in a gel. Extended stirring from initial mixing will facilitate dissolution of reactants in the gel and proper monomerization.[27,28] Tied to this is the pH of the gel, as a higher grade of dissolution and complexation of reactants in a zeotype gel, will in most cases give an increase in the pH to a plateau.[29] The time needed to achieve this pH-plateau when most alumina and phosphate units have complexed together, is dependent on the source of the respective framework molecule and their solubility in the solvent used.

2.1.3.2 Templates

By far the most critical component of any synthesis of microporous systems, is the template. Templates work as structure directing agents for the nano-scale morphology of the system, usually by dictating pore channel size, direction and inter-connectivity. In zeotypes, the most common templates are organic additives, typically amines or quaternary ammonium ions.[19,30]

Templates, especially quaternary ammonium ions, can also act as a pH-controller in the synthesis.[19] This is done either through the presence of a counter

anion as in the case of the quaternary ammonium ions,[31] or through a free electron pair on the nitrogen that can pick a proton, as in the case of amines.

Interactions between the template and the gel can be sorted into two categories, electronic and steric. Electronic interactions are interactions between free electrons or charges on the template molecule and charges or electrons in the framework that is developing. In the case of SAPO systems, the framework charge is readily available as Brønsted acid sites; but for the AlPO systems, a framework charge arises when OH-bridges temporarily forms between Al and P-ions.[19]

Steric effects are more easily visualized, as templates can fill out various channels and cages in a microporous material depending on their shape and kinetic diameter.[32] Steric effects are not absolute; there is no template that is specific to only one structure. However, there are variations in how many templates that can be used to make specific structures, ranging from well over 70 different molecules for the AFI system, to only one for the AFR and AFX (AlPO-56 and SAPO-56) systems.[19] Some templates can template multiple different structures, such as tetraethylammonium hydroxide (TEAOH) which can template both SAPO-5[33] and SAPO-34[34] under different reaction conditions.

2.1.3.3 Kinetics of formation, physical parameters

When a zeotype is forming it is usually through a transformation of a gel consisting of complexed reactants and templates, into a solid via a reaction at temperatures up to 200 °C and 75-200 bar. There are several physical parameters that can affect the kinetics of formation. The most easily identified are crystallization time and temperature which will directly affect reaction rate, product distribution and yield through their influence on the thermodynamics of the system.[24]

2.1.3.4 Work-up, calcination and cleaning procedures

After a hydrothermal synthesis is complete, the final product needs to be recovered from the reaction vessel. Recovery is typically done through a separation of powder from the effluent liquid followed by a washing procedure. The effluent liquid often contains leftover reactants such as alumina and phosphate, as well as decomposition products from the templates that have been used.[24] The most common way of separating the powder and the effluent liquid is through centrifuging. After the first cycle, the powder then has to be washed with deionized water in order to remove any excess effluent liquid and other bi-products adsorbed on the surface of the powder.

As-prepared zeotypes can then be further treated in order remove excess organic moieties, water and other undesired products in the zeotype. This is done through a process called *calcination*. In calcination, the as-prepared material is

slowly heated to a specified temperature and kept at this temperature for a certain amount of time.[35] Calcination of microporous materials uses temperatures up to 600 °C in order to achieve a range of reactions. Among these are the cracking and decomposition of larger organic molecules into smaller moieties such as short chain hydrocarbons and ammonia, in turn followed by either combustion or desorption of these smaller molecules, as well as removal of water through dehydration.[35] The breakdown and removal of these molecules will happen at different temperatures and can be tracked by measuring the weight of the sample across a heating range in a process known as thermogravimetric analysis.[36]

In addition to removing unwanted molecules, calcination can also serve as a purification for the desired phase in the zeotype by transforming inter-grown phase impurities.[37] While most zeotypes are materials with a relatively high thermal resistance, care must still be taken when elevating the temperature. If the temperature is raised too quickly or to a too high level, the structure could partially or completely collapse.[35]

The reactor used in the synthesis will have to be washed in-between syntheses in order to avoid cross-contamination effects.[24] Zeotype residues in the reactor can induce crystallization of erroneous phases through induced crystallization from microscopic crystallites. Several cleaning procedures can be used in order to avoid this issue, all of them involving strong bases or acids in order to dissolve any remaining material. One such method is to partially fill the reaction vessel with 1M sodium hydroxide (NaOH) and subjecting the vessel to elevated pressures at about 160 °C for 1 hour.[24] If the caustic wash should deem insufficient, acids can also be used. The first these acids is a concentrated solution of 5M nitric acid (HNO_3) which is added to vessel and kept there for at least 24 hours. Stronger acids that also can be used are Aqua Regia and hydrofluoric acid (HF), both in their concentrated forms.

2.2 The AFR system

AlPO- and SAPO-40 both belong to the system described by the AFR framework code.[7,38,39] The AFR framework is characterized by interlocked 12- and 8-ring channels, forming a three dimensional pore network. There are also 6- and 4-ring channels present in the framework, but these are not as prominent in the structure. This can be seen in Figure 2.2.[7,39] Through its 12-ring channels with a diameter of 6.9 Å, it can be classified as a *large pore zeotype*, and with its interconnected 8-ring channels it carries a high available volume compared to other zeotypes.[7]

Figure 2.2: A graphical representation of the AFR structure viewed normal to the [001] direction with the interconnected 12- and 8-ring channels. Figure was obtained from [http://www.iza-structure.org]. Reprinted with permission from Baerlocher, C. and McCusker, L. B.[7]

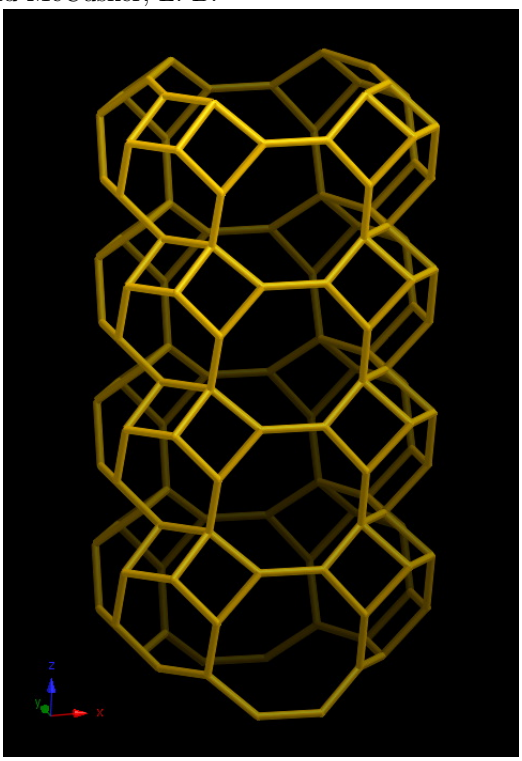

A large surface area also can be found for the AFR systems, with the potential of reaching up to 600 m^2/g. This stands in contrast to a fairly similar zeotype, SAPO-5, which has an average surface area of around 350 m^2/g.[8]

Both AlPO-40 and SAPO-40 have shown great hydrothermal stability at high temperature in both dry and humid air, tolerating temperatures up to 700 °C for several hours without experiencing much structural decay or defect generation.[12,40] In certain catalytic reactions such as the dehydration of glycerol to acrolein, when compared to other commercialized SAPO-class materials such as SAPO-34 and SAPO-11, SAPO-40 showed similar activity towards the reaction as the commercialized zeotypes, but a greater resistance towards coke formation and thus deactivation. Additionally, the structure of SAPO-40 showed less structural damage when subjected to catalyst regeneration, removal of the deactivating

coke phase, in comparison to SAPO-34 and SAPO-11.[13]

The combined high surface area, similar activity towards certain catalytic reactions as other SAPO-systems, great hydrothermal stability, and resistance against structural decay upon regeneration, makes the AFR systems highly interesting as potential catalytic materials on a wider scale.

2.2.1 AlPO-40 synthesis

Synthesis of AlPO-40 has mostly been reported in the works of Lourenço et al.[12,14] and Sierra et al..[38,41] Similarly to most other zeotypes, AlPO-40 is synthesized via a hydrothermal method with water as a solvent, pseudoboehemite as an aluminium source and ortho-phosphoric acid as a phosphorous source. The *Tetrapropylammonium cation* (TPA^+) is used as the main template as it is the only reported template for the synthesis of the AFR-system. While most commonly used in its hydroxide form (TPAOH), other anionic counter-ions such as the bromide form (TPABr) can be used as well.[12,19,39,41] The structure of TPAOH is given in Figure 2.3 below.

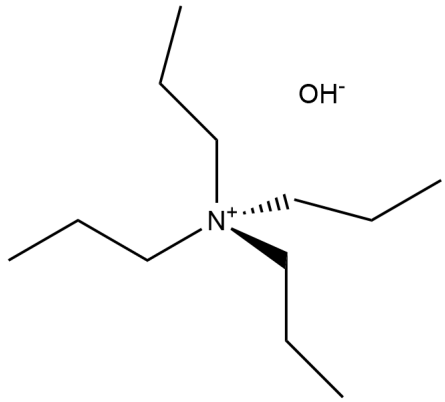

Figure 2.3: Figure showing the molecular structure of TPAOH.

All reported syntheses of AlPO-40 use a ratio of TPAOH to *tetrapropylammonium bromide* (TPABr) in order to get a better control of the pH in the gel.[14,38] The pH has been reported as a critical factor in the synthesis of the AFR-systems, generally only giving successful syntheses at a pH-level of about 6.5.[41] Other factors that will affect the pH are the amount of ortho-phosphoric acid and water.

Another critical factor to ensure a successful synthesis of AlPO-40, is the addition of a small amount of TMAOH to the gel, as it seems to have a suppressing effect on the competing AFI phase.[41]

AlPO-40 has been reported to form across a wide temperature and time scale, from as low as 120 °C up to 170 °C with crystallization times varying between 23 and 140 hours.[14,41]

2.2.2 SAPO-40 synthesis

Dumont et al.[39] were among the first to synthesize a SAPO-40 phase free of any other crystalline phases, and only using TPAOH as a template. Fumed silica was used as a silicon source in all reported syntheses of SAPO-40 due to it having less chemical impurities than the otherwise more convenient colloidal solution of silica.[26]

As detailed by Sierra et al.,[41] AlPO-40 materials with small amounts of a dopant atom in the framework such as silicon, have a preference for crystallizing at higher temperatures. This is in agreement with most successful reported syntheses of SAPO-40 which are carried out at temperatures ranging from 170 °C to 200 °C.[13,39,41] Dumont et al.[39] also noted that increasing the temperature further, to 215 °C, had no apparent effect.

2.2.3 Competition between the AFR and AFI phases

First described by Wilson, S. et al.[17] and Lok, B. et al.[25] in their original patents on AlPOs and SAPOs, there is a competition between two distinct phases in most AFR-structure syntheses. The template used in all AFR-system syntheses, TPAOH, also readily templates the AFI-phase and there have been several investigations on how to suppress this competing phase. Through studies performed by Dumont et al.[39] on the SAPO-40 system it was discovered that the AFI-phase was the kinetic product in the reaction and thus measures to avoid the kinetic phase were investigated. Through experimentation with different parameters it was discovered that either small amounts of alkali cations in the gel, or a dilution of the gel with deionized water, could suppress the AFI-phase.[39]

Weyda, et al.[42] first observed that in the presence of too high a concentration of sodium ions, SAPO-5 would not crystallize even after 24 hours. Dumont, N. et al.[39] continued to investigate this and found that about 0.01 mol Na to 1 mol Al would suppress the AFI-phase, but at the cost of an unidentified amorphous phase forming. Due to this unwanted phase formation, further investigations were conducted by Dumont, N. et al.[39] to see if there were any other ways to prevent AFI-phase formation. By diluting the gel at a constant H_2O/TPAOH molar ratio of 35 and keeping the H_2O/(Al+P) molar ratio above 17.5, SAPO-40 would more readily crystallize with fewer impurities. This was explained to be the case

because a dilution would reduce the overall concentration of phosphoric acid and thus increasing the pH in the system. An increase of the pH in the system would increase the solubility of alumina and phosphate and thus making crystallization slower, favouring the thermodynamic product in the reaction.[27,28,39]

Transformation of the AFI-phase to an AFR-phase at prolonged crystallization times was not observed in the works of Dumont, N. et al.[39] On the contrary, it was stated that once an AFI phase is obtained, it was impossible to obtain a phase pure SAPO-40 sample free of any other crystalline phases.[39] The SAPO-5 phase was deemed to form irreversibly in the reactor as the kinetic product, thus initiating a cascade effect which further nucleated the bi-product in the reaction.

When it comes to the synthesis of SAPO-40, the addition of tetramethylammonium hydroxide (TMAOH) is not crucial to obtaining a pure AFR-phase. Instead, there seems to a much bigger dependency on the total water and silicon content as reported by Dumont, N. et al.[3939] The silicon added to the synthesis was suspected of playing the role of an acid in the gel, thus lowering the pH without the necessary addition of TPABr.[41] However, at silicon levels below 0.2 mol silicon to 1 mol aluminium, the system generally favours the crystallization of SAPO-5.[39] If the silicon level is too high, crystallization of any crystalline phase becomes more difficult yielding an amorphous phase instead. In case of the water content, increasing the total amount of water seemed to favour the SAPO-40 phase and suppress the SAPO-5 phase, but the level of increase required is tied to the total amount of silicon.

It was observed that AlPO-40 would not form under the circumstances described by Dumont, N. et al.[39] In turn, most of the published developments on the AlPO-40 system have been made by the research teams of Sierra, L. et al[38,41] and Lourenço, J. P. et al.[14] Two factors that were found to be essential to the successful formation of AlPO-40, and sufficient suppression of AlPO-5, were the TMAOH content in the gel, and the pH. It was found that a TMA^+/TPA^+ molar ratio equal to approximately 0.02-0.045 was crucial in obtaining a pure AFR-phase.[14,41] A lower value would typically yield an AFI phase, while a higher value would produce a FAU phase.[41,43] The exact mechanism for as to why TMAOH can suppress the AFI phase is unknown, due to the black-box nature of the hydrothermal reaction and therefore inability to obtain an in-situ observation of the reaction pathway.

The gel's pH level upon transfer to the reaction vessel was also found to be a critical parameter. As described earlier, a higher pH-level results in a high solubility of reactants and a slowing of the crystallization reaction. An optimal pH-value of about 6.5 holds true for the reported syntheses of AlPO-40 as well, and to achieve this some of the TPAOH is replaced by the similar *tetrapropylammonium bromide* (TPABr).[14,41] This substitution leads to a replacement of the strongly basic OH^- ions with the weaker Br^- thereby lowering the pH-value,

without introducing any other foreign cations into the gel that might affect the crystallization process. Different sources report different working ratios of TPABr to TPAOH; with Sierra, L. using a molar ratio range of about 0.35 to 0.75, while Lourenço, J. P. et al.[14] only used a molar ratio of 1.1. It is important to view the total amount of TPA^+ in relation to both the amount of ortho-phosphoric acid and the amount of water in the gel as these ratios will greatly impact the crystallization course. An overview of the different ratios reported is shown in Table 2.3

Table 2.3: Table showing values for the different reactant ratios that can influence the pH in the gel when synthesizing AlPO-40, with values from Sierra, L. et al.[41] and Lourenço, J. P. et al.[14]

Literature	$\frac{TPABr}{TPAOH}$	$\frac{TMA^+}{TPA^+}$	$\frac{H_2O}{TPA^+}$	$\frac{TPA^+}{H_3PO_4}$	$\frac{H_2O}{H_3PO_4}$
Lourenço[14]	1.1	0.02	40	1.25	50
Sierra (29)[41]	0.36	0.045	39	0.97	37.5

Lourenço, J. P. et al.[14] were not able to reproduce the results presented by Sierra, L. et al.,[41] instead they opted to optimize their own synthesis with a much higher Br/OH^- ratio and a higher water content in comparison to the amount of acid added to the gel. The exact interactions between the different species in the gel are hereto unknown, but it worth pointing out that to the extent of the author's knowledge there have been no significant advances in the synthesis of AlPO-40 in the past 15 to 20 years.

There are a wide variety of factors that can influence the promotion of the AFR phase. Some of the most essential are summarized below.

- pH at about 6.5 (Both)
- Gel dilution while keeping H_2O/TPAOH ratio constant (SAPO-40)
- Longer crystallization time (Both)
- Addition of TMAOH to the gel (AlPO-40)
- Slow heating rate (Both)
- Addition of alkali cations (SAPO-40)
- Higher crystallization temperature (SAPO-40)
- Higher amount of silicon (SAPO-40)

2.3 Metal containing zeotypes, copper incorporation

Zeotype materials are not restricted to using silicon, aluminium and phosphorus as framework materials. Incorporation of elements outside the traditional silicon, aluminium and phosphorus into AlPOs and SAPOs is possible and has been documented since the mid 1990's.[6] Of special interest is the incorporation of transition metal cations into the framework both of AlPOs and SAPOs due to their potential uses in catalysis.[44]

2.3.1 Ion-exchange and framework incorporation

When talking about the presence of transition metal cations in the framework, it is very important to distinguish between *ion-exchanged* and *framework incorporated* metal cations. Ion exchanged cations can adhere to negatively charged framework oxygen in the zeotype, effectively replacing the H^+ cations in the Brønsted acid sites on the surface.[45] Framework incorporated cations are cations which have substituted other framework elements, typically either aluminium or silicon depending on the matrix in question and the nature of the substituting cation.[6] The framework element which is substituted is dependent on the size and valency of the substituting transition metal cation. When a transition metal is introduced into the framework, framework strain will be generated due to the difference in structural geometry preferences and atomic sizes between the substituting cation and the cation being substituted. The system will generally try to aim towards existing in a low-strain state, and the transition metal cations will therefore replace the framework ion closest in size and structural geometry preference.[46]

There are distinct differences between zeotypes which are ion-exchanged and zeotypes which have framework incorporated cations. Proper ion exchange is only possible in matrices with permanent Brønsted acidity, and therefore is most common in SAPOs.[6,47] The ion exchanged samples remove the general acidic activity of the acid sites in the framework due to the replacement of H^+, but gain the red-ox reaction properties of the ion exchanged transition metal cation. The synergistic effect obtained from this can be used to catalyze a variety of reactions including selective reduction of NO_x gases using hydrocarbons,[48] the methanol to olefins reaction,[11] and many more.[6] Ion-exchange is also regarded as a more straight-forward method of introducing transition metals to the matrix when compared to framework incorporation.[6,49] The downside to ion-exchanged samples are their longevity, matrix type restrictions and limitations in catalysis as a consequence of their active site.[50]

On the other hand, frameworks with incorporated metal cations are generally

harder to synthesize, but in return they are new materials that can have widely different catalytic properties when compared to the plain matrix variants.[6] Furthermore, framework incorporated cations are more stable to both hydrothermal and chemical treatments, and can be in a wider variety of frameworks due to the lack of a need for Brønsted acid sites.[50,51] Should for example a divalent cation such as Cu^{2+} replace Al^{3+}, Brønsted acid sites can be generated in the framework.[14]

2.3.2 Copper in the framework

When copper in the form of Cu^{2+} is substituted into the framework of AlPOs and SAPOs, it will reportedly replace the Al^{3+} cation.[47,52] This will alter the overall structure of the surrounding area due to the different steric geometry preferences of the cations.[33,36] Copper in its divalent form does not readily form tetrahedral geometries, instead it prefers a tetragonally distorted octahedral symmetry due to the Jahn-Teller effect.[36] As prepared samples of copper-incorporated SAPOs and AlPOs reportedly adapt a tetragonally distorted octahedral copper geometry through formation of a hexaquacopper(II) complex connected to oxobridges in the framework.[33,53] A light-blue to turquoise colour of the sample in question, combined with a colourless effluent liquid, is usually indicative of the successful formation of the hexaquacopper complex.[33] When calcined, the copper ion shifts into the matrix proper, changing the overall geometry and chemical environment of the copper ion and altering the colour to a greenish colour.[47,54]

An important distinction for the purposes of this thesis is the classification of the single site substitution. Ideally, the substituting copper ions should not form any copper metal clusters as this will impede the overall effectiveness of the system in regards to catalysis.[33,51] A single site, for the purposes of this thesis, is a framework incorporated copper ion that is not connected to another copper in its immediate neighborhood either through a direct connection or through oxygen bridges. This is to ensure both higher activity due to optimal chemical environments, as well as to prevent the expulsion and separation of copper oxide during calcination.[47,55]

Once incorporated, copper can readily take part in red-ox reactions by reversibly reducing to copper(I) under the right circumstances.[53] Furthermore, the replacement of Al^{3+} with the lower valency Cu^{2+} generated negative framework charges and in turn Brønsted acid sites.

2.3.3 Method of incorporation

By far the most common way of introducing copper into the framework of a zeotype, is to add it during the early stages of the synthesis.[52,53,56] In order to obtain a successful product, several factors have to be considered. Among

these are the type of template used, the crystallization temperature and the total copper content in the synthesis gel.[55]

Perhaps the most crucial parameter is the template that is being used to synthesize the zeotype. As stated earlier, many zeotypes are structure directed by amines, however there structure directing agents can have an adverse effect on the copper in solution as well as in the intermediate stages of formation. The template must not be able to bind the copper ions in solution lest it would be able to be reduce the copper to copper oxide.[57] Additionally the template should also be free of strongly complexing anions such as halogen ions in order to avoid the potential isolation and precipitation of copper salts.[55] In order to avoid this effect, a quaternary ammonium ion should ideally be used as the template.

Another equally as important parameter is the crystallization temperature. At temperatures above 190 °C, copper(II) auto-reduces to metallic copper and forms a dispersed colloidal copper phase in the effluent liquid.[55] When incorporating transition metals into the framework, the optimal temperature for obtaining phase pure samples can vary depending on the framework in question.[41]

Considering the total amount of copper in the synthesis, it is reportedly less detrimental to the success of the synthesis than the template and temperature effects. Mathisen , K. et al[53] reported that an increase in the copper content resulted in both active and non-active sites in the framework being filled. Due to copper being larger than the other framework atoms, it distorts the framework upon incorporation. The effect of this, is the reduction of crystallinity in samples with high copper content compared to other samples with lower amounts of copper in the framework.

2.3.3.1 Incorporation of metals in the AFR system

To the extent of the author's knowledge, only two transition metals have been successfully incorporated into SAPO-40 and AlPO-40. Lourenço, J. P. et al.[12,14] reported successful incorporation of cobalt and zinc into both SAPO-40 and AlPO-40. In both cases, successful incorporation resulted in generation of Brønsted acid sites and a lower hydrothermal stability when compared to the plain matrices. The synthesis method largely followed the standard synthesis pathway of using a two solution method. The metal cation was introduced as the acetate salt by dissolving it in the phosphoric acid.

2.4 Characterization

2.4.1 XRD

X-ray diffraction, XRD, is a powerful characterization method for crystalline solids.[58] It utilizes scattering of electromagnetic light with wavelengths approaching the order of atomic spacing. The incident beams can be elastically scattered by the electrons in a solid phase to obtain constructive interference at specific wavelengths and incident beam angles. The angle of diffraction θ directly correlates to the inter-atomic spacing between two adjacent planes in a solid via *Bragg's law*:[58]

$$n \cdot \lambda = 2 \cdot d \cdot \sin\theta \tag{2.1}$$

where n is the order of reflection and can be any integer (n = 1, 2, 3...), λ is the incident radiation wavelength, θ is the angle between the horizontal direction of the plane and the incident radiation and d is is the interplanar spacing.

There exists two main techniques for diffraction, the powder method and the single-crystal diffraction method.[36] Common for both is the use of a *diffractometer* that determines the angles at which diffraction occurs. In the first method, a poly-crystalline powder is scanned over a range of angles and the intensity of the diffracted x-rays is recorded against the corresponding *diffraction angle*, 2θ to produce a diffractogram. The second method, single-crystal diffraction, uses a single uniform crystal of a material to gain a thorough understanding of the structure of an inorganic solid by applying the same principles used in the powder method.

Assuming a random distribution and orientation of planes in the crystals in the powder bulk, then a mapping of all the planes in the relevant material is possible. In turn this enables XRD to be used as a "fingerprint"-identification method for inorganic solids.[36]

Each peak represents the relative intensity of diffracted x-rays with respect to the diffracting plane. The interplanar spacing, d, is a function of the lattice length and the Miller indices for the plane in question. As a result of this, nearly all crystalline materials will have a material-specific set of peaks that can be used for identification.[58]

Of special interest in microporous systems like SAPOs, is the domain below 10 °for 2θ. In this domain, micropores in the system tend to give strong signals and enables the rapid identification of different zeotypes.[7] In regards to the SAPO-40 (AFR) system, the presence of a double peak near the 7.4 value is a distinguishing feature that separates it from similar structures like SAPO-5 (AFI) and SAPO-37 (FAU). This is highlighted in Figure 2.4 below.

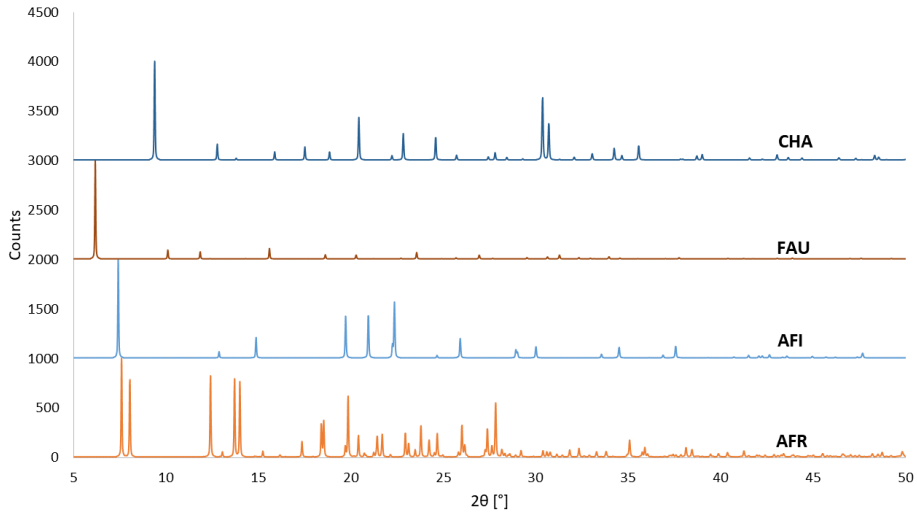

Figure 2.4: An overview over the different competing phases that can be present during the synthesis of AFR samples.

XRD will therefore be used as the primary identification tool for determination of phases and phase purity.

2.4.2 Nitrogen adsorption, BET and BJH models

BET is an analytical technique that utilizes the fundamentals of BET adsorption descriptions for multi-layer adsorption in order to map various physical characteristics of a solid material.[59] First developed as an extension to the traditional Langmuir isotherm of adsorption, it sought to describe adsorption in multiple layers on non-ideal surfaces.[60]

The most widespread application of this theory is in BET- nitrogen adsorption. Here, nitrogen gas is used to study the surface area of a solid material as well as the nature of potential pores in the system.[16] By using a volumetric method where the quantity of adsorbed gas is measured in relation to the relative pressure inside the measuring vessel under isothermal conditions, information about the surface area of the material can be obtained. When gas is being adsorbed on the surface of the material, the pressure inside the vessel drops. The adsorbing process can then be assumed to be complete when the pressure inside the vessel is equal to the ambient pressure of the adsorbate gas at the specified temperature, that is, when the relative pressure is approximately unity. The total surface area of the sample can determined from the data through insertion and manipulation

of the linear BET equation.[16,59] This equation will not be covered in detail in this thesis, as BET only constitutes a very small portion of the thesis.

More interestingly is the shape of the isotherm that is obtained. The shape of the isotherm reveals the "progress" of adsorption as the pressure increases. Different surfaces will have differently shaped isotherms. IUPAC has defined a set of six distinct, theoretical isotherm shapes, each corresponding to a class of materials.

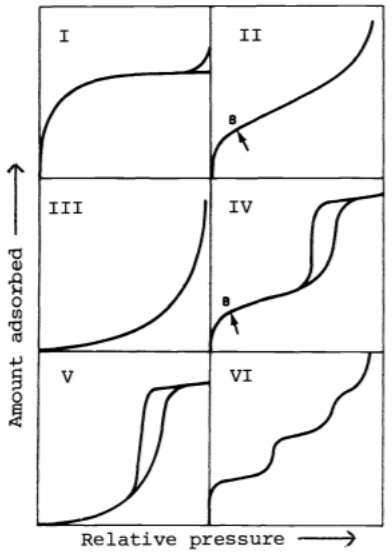

Figure 2.5: Figure detailing the different theoretical isotherm shapes in the BET-nitrogen adsorption, as defined by IUPAC. Figure made by Sing, K. S. W. Reprinted with permission from Sing, K. S. W.[16]

Of special interest in this thesis are the type 1 and type 4 isotherms. Type 1 is an isotherm that is characteristic of a microporous solid in which the micropore area is larger than the external surface area. Type 4 is an isotherm characteristic of mesoporous materials. The hysteresis loop that forms is a result of capillary condensation in larger pores lowering the overall pressure in the system and making the desorption plot deviate from the adsorption plot. While most common in mesoporous materials, hysteresis can also occur in materials with sufficient interparticle voids.

IUPAC has also categorized different hysteresis loops that can be present in porous materials. These are showcased in Figure 2.6

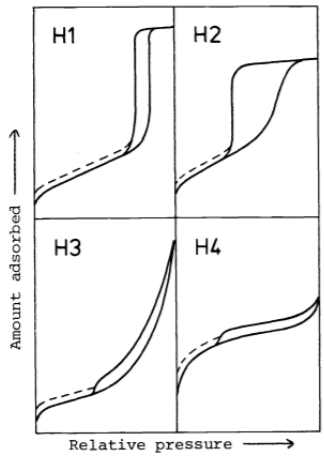

Figure 2.6: Figure detailing the different hysteresis loops in the BET-nitrogen adsorption, as defined by IUPAC. Figure made by Sing, K. S. W. Reprinted with permission from Sing, K. S. W.[16]

The hysteresis loops that are relevant to this thesis are H3 and H4. H1 and H2 are mainly present in mesoporous materials with narrow pore distributions, of which will not be covered in this thesis. Type H4 however, is a hysteresis loop that can be produced in analyses microporous materials. The shallow slope of hysteresis loop is often associated with either slit-like pores or a wide pore distribution.[16]

Pore distribution can also be mapped using a method developed by Barrett, J. P. et al.[61] Through computational methods, the cumulative pore volume over specified pore size intervals, can then be plotted against the pore size to illustrate the pore size distribution.

Chapter 3

Experimental methods

For the syntheses of SAPO-40 and AlPO-40, the experimental sections are split up for easier readability due to a large amount of different parameters being tested. These are reproduction of literature, chemical parameter experiments, physical parameter experiments, and finally combined physical and chemical parameter experiments. These subsections correspond to the subsections detailed in the Results chapter of this thesis.

Generally, all syntheses presented in this thesis can be sorted into two categories, based on how the reactants are mixed together. An illustration of both methods is shown in Figure 3.1 One is the *two solution method*, which involves mixing the aluminium-, phosphorus- and potentially the copper-source together with water in one reaction vessel for t_1 hours; while the templates and silicon-source is mixed in another reaction vessel for t_2 hours. When homogeneity is achieved in both reactant mixtures, the solutions are combined and aged under continuous stirring for t_3 hours. The contents are then transferred to a 50mL Teflon-lined, stainless steel autoclave and subjected to hydrothermal treatment at T °C for t_4 hours.

The other is the *one-pot method*, which involves mixing all reactants together in the same reaction vessel in sequential order. For the purposes of this thesis, the first step involved mixing water together with the aluminium-source and the phosphorus-source and stirring it for t_1 hours until the mixture becomes homogeneous. Then the templates are added and the mixture is further stirred until homogeneity again for t_2 hours, before finally, the silicon-source is added and the mixture is aged for t_3 hours. The final gel is transferred to a 50mL Teflon-lined, stainless steel autoclave and subjected to hydrothermal treatment at T °C for t_4 hours.

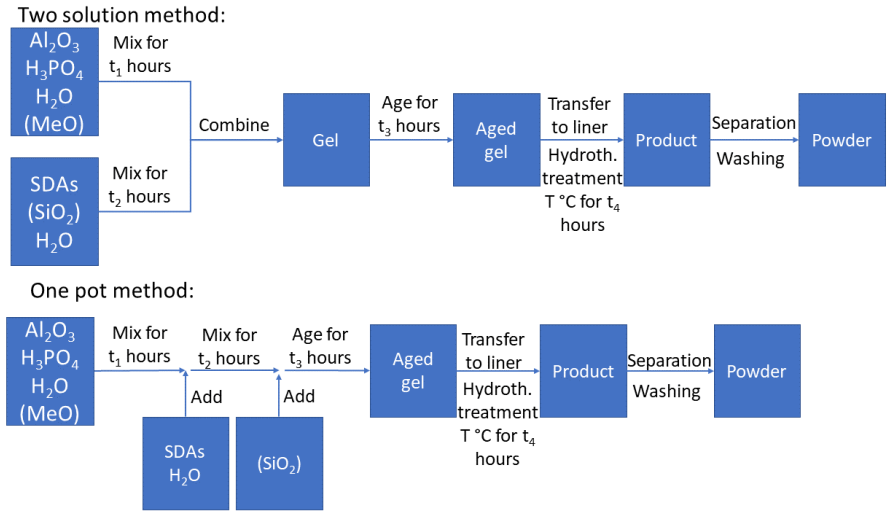

Figure 3.1: Figure detailing the two main synthesis schematics, the two solution method (twosol) and and the one pot method (onepot). Chemicals in parentheses are not always included in the syntheses, but if they are present, they are included at their respective steps. SDAs is an umbrella term for all structure directing chemicals (templates).

All liquids were measured out directly in the reaction vessels in order to minimize loss and error. All solid reactants were measured out in plastic weighing boats, before transfer to the reaction vessel, in order to minimize contamination.

Calcination of samples was done by heating the sample in air to 550 °C at 1 °C per minute then keeping the sample at 550 °C for 16 hours before cooling the sample back down to 25 °C.

For the attempted syntheses of SAPO-40, three different methods were employed. The as-reported syntheses, with appropriate parameters are presented in Table 3.1 below.

Table 3.1: Comparison between the parameters in the different syntheses used as starting points in the synthesis of SAPO-40.

Source	Al	P	H_2O	Si	TMAOH	TPABr	TPAOH	Ageing [h]	Fill grade	T [°C]	t_4 [h]
Dumont[39]	1	1	39.8	0.35	-	-	1	t_1 : 4 t_2 : 2 t_3 : 1.5	50	200	144
Lourenço[12]	1	1	33.33	0.15	0.017	0.37	0.463	t_1 : 4 t_2 :2 t_3 : 1.5	33	200	144
Sierra[41]	1	1	39	0.235	0.05	0.26	0.74	t_1 : 7 t_2 : 2 t_3 : 23	40	170	30

For the attempted syntheses of AlPO-40, two different methods were employed.

Table 3.2: Comparison between the parameters in the different syntheses used as starting points in the synthesis of AlPO-40.

Source	Al	P	H_2O	TMAOH	TPABr	TPAOH	Ageing [h]	Fill grade	T [°C]	t_4 [h]
Sierra[41]	1	1	37.5	0.045	0.26	0.71	t_1 : 6 t_2 : 2 t_3 : 17	45	150	23
Lourenço[14]	0.8	0.8	40	0.02	0.52	0.48	t_1 : 4 t_2 : 2 t_3 : 18	45	150	120

3.1 SAPO-40 synthesis

An overview of all conducted plain SAPO-40 syntheses are given in the following table. For a standard synthesis from Dumont, N. et al[13,39] using a 45 mL liner in a stainless steel autoclave; about 1.5 grams of psudeoboehemite (Al_2O_3 PLURAL B, 75%, SASOL) was dissolved in a mixture of 2.5 grams of ortho-phosphoric acid (H_3PO_4, 85 %, Merck) and 10 grams of distilled water, and stirred for a specific amount of time (t_1). Another mixture of 0.9 grams of fumed silica (SiO_2, 99%, Sigma Aldrich) dispersed via mixing for t_2 hours in 7 grams of tetrapropylammonium hydroxide (TPAOH, 40 %, Sigma Aldrich), was added to the alumina mixture and the two were set to age for a specific amount of time (t_3). About 20 grams were then transferred to a liner and hydrothermally treated for t_4 hours at T °C. The final product was recovered via centrifuging with distilled water (3 x 60 mL) and dried for 24 hours at 70 °C.

3.1.1 Reproduction

First, a reproduction of established literature was performed. No parameters were varied in this instance.

Table 3.3: Table detailing the experimental parameters of the reproduction of syntheses reported by Dumont, N. et al.[39] and Sierra, L. et al.[41] Method of mixing was always two solution.

Entry	Parameter varied	Al	P	H_2O	Si	TMAOH	TPABr	TPAOH	Ageing [h]	Fill grade	T[°C]	t_4 [h]
1	None	1	1	39.8	0.35	0	0	1.08	t_1 : 4 t_2 : 2 t_3 : 1.5	50	200	144
2	None	1	1	39	0.235	0.05	0.26	0.74	t_1 : 7 t_2 : 2 t_3 : 23	40	170	30
3	None	1	1	39	0.235	0.05	0.26	0.74	t_1 : 7 t_2 : 2 t_3 : 23	40	170	30
4	None	1	1	39	0.235	0.05	0.26	0.74	t_1 : 7 t_2 : 2 t_3 : 23	40	170	30

3.1.2 Chemical parameter experiments

Next, chemical parameters were investigated based on reported findings into what could promote the formation of an AFR phase. Only a few tests were performed, testing for the addition of either water or TMAOH, two additions which had been reported as beneficial for the formation of an AFR phase.

Table 3.4: Table detailing the experimental parameters of the chemical parameter variations in the synthesis of SAPO-40. Parameters being varied are bolded for visibility. Method of mixing was always two solution, filling grade was constant at 50 %

Entry	Parameter varied	Al	P	H_2O	Si	TMAOH	TPABr	TPAOH	Ageing [h]	T[°C]	t_4 [h]
5	None	1	1	39.8	0.35	0	0	1.08	t_1 : 4 t_2 : 2 t_3 : 1.5	200	144
6	H_2O	1	1	**43**	0.35	0	0	1.08	t_1 : 4 t_2 : 2 t_3 : 1.5	200	144
7	TMAOH	1	1	39.8	0.35	**0.011**	0	**1.07**	t_1 : 4 t_2 : 2 t_3 : 1.5	200	144

3.1.3 Physical parameter experiments

The physical parameter experiments were done mainly done in the synthesis adapted from Dumont, N. et al.,[39] but one test was done with an adapted synthesis from Lourenço, J. P.[12] The physical parameter experiments were mainly concerned with experimenting with the crystallization temperature and time due to their influence on the thermodynamics of the system; and one experiment set up to study the influence of filling grade of the liners.

Table 3.5: Table detailing the experimental parameters of the physical parameter variations in the synthesis of SAPO-40. Parameters being varied are bolded for visibility. Method of mixing was always two solution.

Entry	Parameter varied	Al	P	H_2O	Si	TMAOH	TPABr	TPAOH	Ageing [h]	Fill grade	T[°C]	t_4 [h]
8	Cryst. time. (t_4) and temp.	1	1	33.3	0.15	0.017	0.37	0.463	t_1 : 4 t_2 : 2 t_3 : 1.5	33	200	144
9	Cryst. time. (t_4) and temp.	1	1	33.3	0.15	0.017	0.37	0.463	t_1 : 4 t_2 : 2 t_3 : 1.5	33	200	**288**
10	Cryst. time. (t_4) and temp.	1	1	33.3	0.15	0.017	0.37	0.463	t_1 : 4 t_2 : 2 t_3 : 1.5	33	**150**	144
11	Cryst. time. (t_4) and temp.	1	1	33.3	0.15	0.017	0.37	0.463	t_1 : 4 t_2 : 2 t_3 : 1.5	33	**150**	**288**
12	Cryst. time. (t_4) and temp.	1	1	39.8	0.35	0	0	1.08	t_1 : 4 t_2 : 2 t_3 : 1.5	40	200	144
13	Cryst. time. (t_4) and temp.	1	1	39.8	0.35	0	0	1.08	t_1 : 4 t_2 : 2 t_3 : 1.5	40	200	**288**
14	Cryst. time. (t_4) and temp.	1	1	39.8	0.35	0	0	1.08	t_1 : 4 t_2 : 2 t_3 : 1.5	40	**150**	144
15	Cryst. time. (t_4) and temp.	1	1	39.8	0.35	0	0	1.08	t_1 : 4 t_2 : 2 t_3 : 1.5	40	**150**	**288**
16	Filling, Cryst. time. (t_4) and temp.	1	1	39.8	0.35	0	0	1.08	t_1 : 4 t_2 : 2 t_3 : 1.5	**33**	**150**	**72**
17	Filling, Cryst. time. (t_4) and temp.	1	1	39.8	0.35	0	0	1.08	t_1 : 4 t_2 : 2 t_3 : 1.5	**33**	200	**72**

Table 3.5: Table detailing the experimental parameters of the physical parameter variations in the synthesis of SAPO-40. Parameters being varied are bolded for visibility. Method of mixing was always two solution.

Entry	Parameter varied	Al	P	H_2O	Si	TMAOH	TPABr	TPAOH	Ageing [h]	Fill grade	T[°C]	t_4 [h]
18	Filling, Cryst. time. (t_4) and temp.	1	1	39.8	0.35	0	0	1.08	t_1 : 4 t_2 : 2 t_3 : 1.5	**33**	**150**	**216**
19	Filling, Cryst. time. (t_4) and temp.	1	1	39.8	0.35	0	0	1.08	t_1 : 4 t_2 : 2 t_3 : 1.5	**33**	200	**216**
20	Filling, Cryst. time. (t_4) and temp.	1	1	39.8	0.35	0	0	1.08	t_1 : 4 t_2 : 2 t_3 : 1.5	**67**	150	**72**
21	Filling, Cryst. time. (t_4) and temp.	1	1	39.8	0.35	0	0	1.08	t_1 : 4 t_2 : 2 t_3 : 1.5	**67**	200	**72**
22	Filling, Cryst. time. (t_4) and temp.	1	1	39.8	0.35	0	0	1.08	t_1 : 4 t_2 : 2 t_3 : 1.5	**67**	150	**216**
23	Filling, Cryst. time. (t_4) and temp.	1	1	39.8	0.35	0	0	1.08	t_1 : 4 t_2 : 2 t_3 : 1.5	**67**	200	**216**
24	Filling, Cryst. time. (t_4) and temp.	1	1	39.8	0.35	0	0	1.08	t_1 : 4 t_2 : 2 t_3 : 1.5	50	**175**	144
25	Filling, Cryst. time. (t_4) and temp.	1	1	39.8	0.35	0	0	1.08	t_1 : 4 t_2 : 2 t_3 : 1.5	50	**175**	144
26	Filling, Cryst. time. (t_4) and temp.	1	1	39.8	0.35	0	0	1.08	t_1 : 4 t_2 : 2 t_3 : 1.5	50	**175**	144

3.1.4 Combined chemical and physical parameter experiments

Finally, the effect of mixing method and silicon source were investigated in order to see if the methods from reported literature could be replaced with less demanding solutions.

Table 3.6: Table detailing the experimental parameters of the combined chemical and physical parameter variations in the synthesis of SAPO-40. Parameters being varied are bolded for visibility. A '*' next to the amount of silicon in the synthesis indicates that the silicon source was colloidal silica (LUDOX). Filling grade grade was constant at 45 %

Entry	Parameter varied	Al	P	H_2O	Si	TMAOH	TPABr	TPAOH	Method	Ageing [h]	T[°C]	t_4 [h]
27	Method and silicon source	1	1	39.8	0.35 *	0	0	1.08	Onepot	t_1 : 4 t_2 : 2 t_3 : 1.5	200	144
28	Method and silicon source	1	1	39.8	0.35	0	0	1.08	Onepot	t_1 : 4 t_2 : 2 t_3 : 1.5	200	144
29	Method and silicon source	1	1	39.8	0.35 *	0	0	1.08	Twosol	t_1 : 4 t_2 : 2 t_3 : 1.5	200	144
30	Method and silicon source	1	1	39.8	0.35	0	0	1.08	Twosol	t_1 : 4 t_2 : 2 t_3 : 1.5	200	144

3.2 AlPO-40 synthesis

An overview of all conducted plain AlPO-40 syntheses are given in the following table. For a standard synthesis from Sierra, L. et al[41] using a 45 mL liner in a stainless steel autoclave; about 1.75 grams of psudeoboehemite (Al_2O_3 PLURAL B, 75%, SASOL) was dissolved in a mixture of 3 grams of ortho-phosphoric acid (H_3PO_4, 85 %, Merck) and 10 grams of distilled water, and stirred for a specific amount of time (t_1). Another mixture of 1.8 grams of tetrapropylammonium bromide (TPABr, 98%, Sigma Aldrich) dissolved in 9 grams of tetrapropylammonium hydroxide (TPAOH, 40 %, Sigma Aldrich) and 0.4 grams of tetramethylammonium hydroxide (TMAOH, 25 %, Sigma Aldrich), mixed for t_2 hours, was added to the alumina mixture and the two were set to age for a specific amount

of time (t_3). About 20 grams were then transferred to a liner and hydrothermally treated for t_4 hours at T °C. The final product was recovered via centrifuging with distilled water (3 x 60 mL) and dried for 24 hours at 70 °C.

3.2.1 Reproduction

First a reproduction of established literature was performed. The crystallization time was varied in the synthesis from Lourenço, J. P. et al.[14] due to two time values being reported. The 140 hours reported in literature was changed to 144 hours due to logistical reasons.

Table 3.7: Table detailing the experimental parameters of the reproduction attempts of the syntheses of AlPO-40 reported by Sierra, L. et al.[41] and Lourenço, J. P. et al..[14] Parameters being varied are bolded for visibility. The filling grade of the liners was always 45 %.

Entry	Parameter varied	Al	P	H_2O	TMAOH	TPABr	TPAOH	Ageing [h]	HF wash	T [°C]	t_4 [h]
31	None	1	1	37.5	0.045	0.26	0.71	t_1 : 6 t_2 : 2 t_3 : 17	Yes	150	23
32	None	1	1	37.5	0.045	0.26	0.71	t_1 : 6 t_2 : 2 t_3 : 17	Yes	150	23
33	None	1	1	37.5	0.045	0.26	0.71	t_1 : 6 t_2 : 2 t_3 : 17	Yes	150	23
34	None	1	1	50	0.025	0.65	0.6	t_1 : 4 t_2 : 2 t_3 : 18	No	150	120
35	Cryst. time (t_4)	1	1	50	0.025	0.65	0.6	t_1 : 4 t_2 : 2 t_3 : 18	No	150	**144**

3.2.2 Chemical parameter experiments

Then, investigations of the effect of various chemical parameters was done. With the main focus being manipulation of the pH via two different methods, both altering the ratio between TPAOH and TPABr as well as changing the total amount of TPA^+ the gel. TMAOH content was lowered to see the response of

the system. These were all done in lieu of washing with HF as a dual attempt at producing AlPO-40 without the need for intensive washing procedures.

Table 3.8: Table detailing the experimental parameters of the chemical parameter variations in the synthesis of AlPO-40. Parameters being varied are bolded for visibility. The filling grade of the liners was always 45 %.

Entry	Parameter varied	Al	P	H_2O	TMAOH	TPABr	TPAOH	Ageing [h]	HF wash	T [°C]	t_4 [h]
36	Br^-/OH^- ratio	1	1	37.5	0.045	0.26	0.71	t_1 : 6 t_2 : 2 t_3 : 17	No	150	23
37	Br^-/OH^- ratio	1	1	37.5	0.045	0.335	0.645	t_1 : 6 t_2 : 2 t_3 : 17	No	150	23
38	Br^-/OH^- ratio	1	1	37.5	0.045	0.39	0.58	t_1 : 6 t_2 : 2 t_3 : 17	No	150	23
39	TMAOH	1	1	37.5	0.02	0.26	0.71	t_1 : 6 t_2 : 2 t_3 : 17	No	150	23
40	TPA^+ content	1	1	37.5	0.045	0.215	0.585	t_1 : 6 t_2 : 2 t_3 : 17	No	150	23
41	TPA^+ content	1	1	37.5	0.045	0.245	0.665	t_1 : 6 t_2 : 2 t_3 : 17	No	150	23
42	TPA^+ content	1	1	37.5	0.045	0.297	0.803	t_1 : 6 t_2 : 2 t_3 : 17	No	150	23
43	TPA^+ content	1	1	37.5	0.045	0.325	0.875	t_1 : 6 t_2 : 2 t_3 : 17	No	150	23

3.2.3 Physical parameter experiments

Working further, various physical parameters were investigated in order to map the response to a variety of changes. Crystallization time and crystallization

temperature were varied in order to study if the AFR phase had a preference for either higher crystallization times or temperatures. Several ageing times were investigated to see if the prolonged ageing times from literature could be shorted, as well as to study the system's dependence on the ageing if the gel.

Table 3.9: Table detailing the experimental parameters of the physical parameter variations in the synthesis of AlPO-40. Parameters being varied are bolded for visibility. The filling grade of the liners was always 45 %.

Entry	Parameter varied	Al	P	H_2O	TMAOH	TPABr	TPAOH	Ageing [h]	HF wash	T [°C]	t_4 [h]
44	Cryst. time (t_4)	1	1	37.5	0.045	0.26	0.71	t_1 : 6 t_2 : 2 t_3 : 17	No	150	**47**
45	None	1	1	37.5	0.045	0.26	0.71	t_1 : 6 t_2 : 2 t_3 : 17	No	150	23
46	Cryst. time (t_4)	1	1	37.5	0.045	0.26	0.71	t_1 : 6 t_2 : 2 t_3 : 17	No	150	**47**
47	Cryst. temp.	1	1	37.5	0.045	0.26	0.71	t_1 : 6 t_2 : 2 t_3 : 17	No	**170**	23
48	Cryst. time (t_4) and temp.	1	1	37.5	0.045	0.26	0.71	t_1 : 6 t_2 : 2 t_3 : 17	No	**170**	**47**
49	Ageing time (t_3)	1	1	37.5	0.045	0.26	0.71	**t_1 : 6** **t_2 : 2** **t_3 : 41**	No	150	23
50	Mixing and ageing time (t_1, t_2, t_3)	1	1	37.5	0.045	0.26	0.71	**t_1 : 1.5** **t_2 : 1.5** **t_3 : 2**	No	150	23
51	Mixing and ageing time (t_1, t_2, t_3)	1	1	37.5	0.045	0.26	0.71	**t_1 : 1.5** **t_2 : 1.5** **t_3 : 4**	No	150	23
52	Mixing and ageing time (t_1, t_2, t_3)	1	1	37.5	0.045	0.26	0.71	**t_1 : 1.5** **t_2 : 1.5** **t_3 : 6**	No	150	23

Table 3.9: Table detailing the experimental parameters of the physical parameter variations in the synthesis of AlPO-40. Parameters being varied are bolded for visibility. The filling grade of the liners was always 45 %.

Entry	Parameter varied	Al	P	H_2O	TMAOH	TPABr	TPAOH	Ageing [h]	HF wash	T [°C]	t_4 [h]
53	Cryst. time	1	1	37.5	0.045	0.26	0.71	**t_1 : 1.5 t_2 : 1.5 t_3 : 4**	No	150	**24**
54	Cryst. time	1	1	37.5	0.045	0.26	0.71	**t_1 : 1.5 t_2 : 1.5 t_3 : 4**	No	150	**48**
55	Cryst. time	1	1	37.5	0.045	0.26	0.71	**t_1 : 1.5 t_2 : 1.5 t_3 : 4**	No	150	**72**
56	Cryst. time	1	1	37.5	0.045	0.26	0.71	**t_1 : 1.5 t_2 : 1.5 t_3 : 4**	No	150	**96**
57	Cryst. time	1	1	37.5	0.045	0.26	0.71	**t_1 : 1.5 t_2 : 1.5 t_3 : 4**	No	150	**120**
58	Ageing time (t_3)	1	1	37.5	0.045	0.26	0.71	**t_1 : 6 t_2 : 2 t_3 : 0.5**	No	150	23

3.2.4 Combined chemical and physical parameter experiments

Finally, both physical and chemical parameters were studied simultaneously alongside washing the liners with HF in order to determine critical parameters in the synthesis of AlPO-40. The main parameters that were investigated were the TPAOH source to see if there were any differences between the two sources. A revisit of crystallization time when the liners had been washed with HF was also performed in order to study if the AFR phase would form at greatly extended crystallization times. The total water content was lowered in order to lower the pH of the system without introducing more template or phosphoric acid molecules, as well to make the gel less watery.

Table 3.10: Table detailing the experimental parameters of the combined chemical and physical parameter variations in the synthesis of AlPO-40. Parameters being varied are bolded for visibility. A '*' next to the amount of TPAOH in the synthesis indicates that the TPAOH was sourced from Alfa Aesar rather than Sigma Aldrich. The filling grade of the liners was always 45 %.

Entry	Parameter varied	Al	P	H_2O	TMAOH	TPABr	TPAOH	Ageing [h]	HF wash	T [°C]	t_4 [h]
59	None	1	1	37.5	0.045	0.26	0.71	t_1 : 6 t_2 : 2 t_3 : 17	Yes	150	23
60	Cryst. temp.	1	1	37.5	0.045	0.26	0.71	t_1 : 6 t_2 : 2 t_3 : 17	Yes	**170**	23
61	TPAOH source and Cryst. time (t_4)	1	1	50	0.025	0.65	**0.6 ***	t_1 : 4 t_2 : 2 t_3 : 18	Yes	150	120
62	TPAOH source and Cryst. time (t_4)	1	1	50	0.025	0.65	**0.6 ***	t_1 : 4 t_2 : 2 t_3 : 18	Yes	150	**144**
63	TPAOH source and Cryst. time (t_4)	1	1	50	0.025	0.65	**0.6 ***	t_1 : 4 t_2 : 2 t_3 : 18	Yes	150	**168**
64	TPAOH source and Cryst. time (t_4)	1	1	50	0.025	0.65	**0.6 ***	t_1 : 4 t_2 : 2 t_3 : 18	Yes	150	**192**
65	TPAOH source and Cryst. time (t_4)	1	1	50	0.025	0.65	**0.6 ***	t_1 : 4 t_2 : 2 t_3 : 18	Yes	150	**216**
66	TPAOH source and Cryst. time (t_4)	1	1	50	0.025	0.65	**0.6 ***	t_1 : 4 t_2 : 2 t_3 : 18	Yes	150	**240**
67	TPAOH source and Cryst. time (t_4)	1	1	50	0.025	0.65	**0.6**	t_1 : 4 t_2 : 2 t_3 : 18	Yes	150	120

Table 3.10: Table detailing the experimental parameters of the combined chemical and physical parameter variations in the synthesis of AlPO-40. Parameters being varied are bolded for visibility. A '*' next to the amount of TPAOH in the synthesis indicates that the TPAOH was sourced from Alfa Aesar rather than Sigma Aldrich. The filling grade of the liners was always 45 %.

Entry	Parameter varied	Al	P	H_2O	TMAOH	TPABr	TPAOH	Ageing [h]	HF wash	T [°C]	t_4 [h]
68	TPAOH source and Cryst. time (t_4)	1	1	50	0.025	0.65	**0.6**	t_1 : 4 t_2 : 2 t_3 : 18	Yes	150	**144**
69	TPAOH source and Cryst. time (t_4)	1	1	50	0.025	0.65	**0.6**	t_1 : 4 t_2 : 2 t_3 : 18	Yes	150	**168**
70	TPAOH source and Cryst. time (t_4)	1	1	50	0.025	0.65	**0.6**	t_1 : 4 t_2 : 2 t_3 : 18	Yes	150	**192**
71	TPAOH source and Cryst. time (t_4)	1	1	50	0.025	0.65	**0.6**	t_1 : 4 t_2 : 2 t_3 : 18	Yes	150	**216**
72	TPAOH source and Cryst. time (t_4)	1	1	50	0.025	0.65	0.6	t_1 : 4 t_2 : 2 t_3 : 18	Yes	150	**240**
73	Cryst. time (t_4)	1	1	50	0.025	0.65	0.6 *	t_1 : 4 t_2 : 2 t_3 : 18	Yes	150	**24**
74	Cryst. time (t_4)	1	1	50	0.025	0.65	0.6 *	t_1 : 4 t_2 : 2 t_3 : 18	Yes	150	**48**
75	Cryst. time (t_4)	1	1	50	0.025	0.65	0.6 *	t_1 : 4 t_2 : 2 t_3 : 18	Yes	150	**72**
76	Cryst. time (t_4)	1	1	50	0.025	0.65	0.6 *	t_1 : 4 t_2 : 2 t_3 : 18	Yes	150	**96**

Table 3.10: Table detailing the experimental parameters of the combined chemical and physical parameter variations in the synthesis of AlPO-40. Parameters being varied are bolded for visibility. A '*' next to the amount of TPAOH in the synthesis indicates that the TPAOH was sourced from Alfa Aesar rather than Sigma Aldrich. The filling grade of the liners was always 45 %.

Entry	Parameter varied	Al	P	H_2O	TMAOH	TPABr	TPAOH	Ageing [h]	HF wash	T [°C]	t_4 [h]
77	None	1	1	37.5	0.045	0.26	0.71	t_1 : 6 t_2 : 2 t_3 : 17	Yes	150	23
78	TPAOH Source	1	1	37.5	0.045	0.26	**0.71 ***	t_1 : 6 t_2 : 2 t_3 : 17	Yes	150	23
79	None	1	1	37.5	0.045	0.26	0.71 *	t_1 : 6 t_2 : 2 t_3 : 17	Yes	150	23
80	Cryst. time (t_4)	1	1	37.5	0.045	0.26	0.71 *	t_1 : 6 t_2 : 2 t_3 : 17	Yes	150	**71**
81	Cryst. time (t_4)	1	1	37.5	0.045	0.26	0.71 *	t_1 : 6 t_2 : 2 t_3 : 17	Yes	150	**119**
82	Cryst. time (t_4)	1	1	37.5	0.045	0.26	0.71 *	t_1 : 6 t_2 : 2 t_3 : 17	Yes	150	**167**
83	None	1	1	37.5	0.045	0.26	0.71 *	t_1 : 6 t_2 : 2 t_3 : 17	Yes	150	23
84	H_2O	1	1	**35**	0.045	0.26	0.71 *	t_1 : 6 t_2 : 2 t_3 : 17	Yes	150	23
85	H_2O	1	1	**32.5**	0.045	0.26	0.71 *	t_1 : 6 t_2 : 2 t_3 : 17	Yes	150	23
86	H_2O	1	1	**30**	0.045	0.26	0.71 *	t_1 : 6 t_2 : 2 t_3 : 17	Yes	150	23

Table 3.10: Table detailing the experimental parameters of the combined chemical and physical parameter variations in the synthesis of AlPO-40. Parameters being varied are bolded for visibility. A '*' next to the amount of TPAOH in the synthesis indicates that the TPAOH was sourced from Alfa Aesar rather than Sigma Aldrich. The filling grade of the liners was always 45 %.

Entry	Parameter varied	Al	P	H_2O	TMAOH	TPABr	TPAOH	Ageing [h]	HF wash	T [°C]	t_4 [h]
87	HF wash	1	1	37.5	0.045	0.26	0.71 *	t_1 : 6 t_2 : 2 t_3 : 17	**No**	150	23
88	H_2O and HF wash	1	1	**32.5**	0.045	0.26	0.71 *	t_1 : 6 t_2 : 2 t_3 : 17	**No**	150	23
89	H_2O	1	1	**32.5**	0.045	0.26	0.71 *	t_1 : 6 t_2 : 2 t_3 : 17	Yes	150	23
90	H_2O and Cryst. time (t_4)	1	1	**32.5**	0.045	0.26	0.71 *	t_1 : 6 t_2 : 2 t_3 : 17	Yes	150	**71**
91	H_2O and Cryst. time (t_4)	1	1	**32.5**	0.045	0.26	0.71 *	t_1 : 6 t_2 : 2 t_3 : 17	Yes	150	**119**
92	H_2O and Cryst. time (t_4)	1	1	**32.5**	0.045	0.26	0.71 *	t_1 : 6 t_2 : 2 t_3 : 17	Yes	150	**167**

3.3 CuAlPO-40 syntheses

An overview of all conducted CuAlPO-40 syntheses are given in the following table. For an adapted synthesis from Sierra, L. et al[41] using a 45 mL liner in a stainless steel autoclave; about 1.75 grams of psudeoboehemite (Al_2O_3 CATAPAL B, 75%, SASOL), and either 0.1 grams of copper oxide (CuO, 99%, VWR chemicals) or 0.3 grams of copper acetate mono-hydrate ($Cu(Ac)_2 \cdot H_2O$, 99 %, Fluka), were dissolved in a mixture of 3 grams of ortho-phosphoric acid (H_3PO_4, 85 %, Merck) and 10 grams of distilled water, then stirred for a specific amount of time (t_1). Another mixture of 1.8 grams of tetrapropylammonium bromide (TPABr, 98%, Sigma Aldrich) dissolved in 9 grams of tetrapropylammonium hy-

droxide (TPAOH, 40 %, Sigma Aldrich) and 0.4 grams of tetramethylammonium hydroxide (TMAOH, 25 %, Sigma Aldrich), mixed for t_2 hours, was added to the alumina mixture and the two were set to age for a specific amount of time (t_3). About 20 grams were then transferred to a liner and hydrothermally treated for t_4 hours at T °C. The final product was recovered via centrifuging with distilled water (3 x 60 mL) and dried for 24 hours at 70 °C.

Only a few CuAlPO-40 syntheses were run. In these syntheses, the effects of copper source, copper to aluminium ratio, washing the liner with Hf and crystallization temperature. Which copper was used could influence the synthesis due to the different properties of the counter ion. The copper to aluminium ratio could affect the amount of copper being incorporated due to copper theoretically replacing aluminium. The HF was done to see a stronger washing procedure was necessary and the temperature was investigated due to the reported benefit of increasing the temperature when trying to incorporate transition metals ions into AlPO-40.

Table 3.11: Table detailing all CuAlPO-40 syntheses, with selected parameters important to the synthesis. Parameters being changed are bolded for visibility. A '*' next to the copper amount indicates that the copper source was copper acetate. The filling grade of the liners was always 45 %.

Entry	Parameter varied	Al	P	H_2O	Cu	TMAOH	TPABr	TPAOH	Ageing [h]	HF wash	T [°C]	t_4 [h]
93	Copper source and aluminium content	**1**	1	37.5	**0.05**	0.045	0.26	0.71	t_1 : 6 t_2 : 2 t_3 : 17	No	150	23
94	Copper source and aluminium content	**0.95**	1	37.5	**0.05**	0.045	0.26	0.71	t_1 : 6 t_2 : 2 t_3 : 17	No	150	23
95	Copper source and aluminium content	**1**	1	37.5	**0.05 ***	0.045	0.26	0.71	t_1 : 6 t_2 : 2 t_3 : 17	No	150	23
96	Copper source and aluminium content	**0.95**	1	37.5	**0.05 ***	0.045	0.26	0.71	t_1 : 6 t_2 : 2 t_3 : 17	No	150	23
97	Cryst. temp.	1	1	37.5	0.05	0.045	0.26	0.71	t_1 : 6 t_2 : 2 t_3 : 17	**Yes**	**150**	23

Table 3.11: Table detailing all CuAlPO-40 syntheses, with selected parameters important to the synthesis. Parameters being changed are bolded for visibility. A '*' next to the copper amount indicates that the copper source was copper acetate. The filling grade of the liners was always 45 %.

Entry	Parameter varied	Al	P	H_2O	Cu	TMAOH	TPABr	TPAOH	Ageing [h]	HF wash	T [°C]	t_4 [h]
98	Cryst. temp.	1	1	37.5	0.05	0.045	0.26	0.71	t_1 : 6 t_2 : 2 t_3 : 17	**Yes**	**170**	23

3.4 Instrumentation

Two instrumentation methods were employed in the thesis, XRD and nitrogen adsorption, details for each method are detailed in their respective subsections.

3.4.1 XRD

Diffractograms were obtained using a Bruker D8 A25 DaVinci X-ray Diffractometer with CuKα radiation, LynxEye™ SuperSpeed Detector, and 90 position sample changer. The samples were run at a 5-60 °, 15 minute program with a variable slit. Copper containing samples were run at a 5-60 °, 15 minute program with a fixed slit. The step size was 0.0133 °C. The counting time was approximately 5.3 * 10^{-5} seconds per step.

3.4.2 Nitrogen adsorption, BET and BJH models

BET and BJH data were obtained using a 3Flex 3500 Surface Area and Porosity and Chemisorption Analyzer instrument with nitrogen gas as the adsorbent gas. Samples were run at isothermal conditions at 77 K through use of liquid nitrogen and an isothermal jacket around the sample tube. A filler rod was inserted into the sample tube in order to promote static conditions during the analysis.

Before analysis, the samples were degassed using a Smartprep Programmable Degas System. The degas program was a three-step program starting with a gradual increase of temperature from room temperature up to 300 °C over 8 hours, followed by an isothermal treatment at 300 °C for 5 hours and finally a decrease of temperature from 300 °C to 30 °C over 8 hours.

Chapter 4

Results

The nomenclature of the descriptive names of samples used in the results chapter follow the following rules:

- S40, A40 and CuA40 denotes SAPO-40, AlPO-40 and CuAlPO-40 respectively.
- The letter following the system name denotes which synthesis was used as a source. D, L and S, represents Dumont, Lourenço and Sierra respectively.
- Text connected by a ":" is tied to each other as parameter descriptors, with the number in front representing the value of the parameter and the work after representing the parameter itself.
- The distinction between "age" and "mix" is that "age" only edits the final gel ageing time, while "mix" alters each mixing time.

The results are sectioned as in the experimental section. With an overview of obtained results given in the beginning of each section.

4.1 SAPO synthesis results

Presented in the following table is an overview of all the conducted syntheses for plain SAPO-40 with pH values and obtained zeotype phases given to the right in the table.

Table 4.1: Table showcasing SAPO results, with selected parameters important for the overall synthesis schemes. A '*' indicated that the silicon source was colloidal silica. In the pH column, B means for "Before", A means for "After".

Entry	Parameter varied	Al	P	H_2O	Si	TMAOH	TPABr	TPAOH	Method	Ageing [h]	Fill grade	T[°C]	t_4 [h]	pH	Resulting zeotype(s)
1	None	1	1	39.8	0.35	0	0	1.08	Twosol	t_1 : 4 t_2 : 2 t_3 : 1.5	50	200	144	B: 6.5 A: 8	AFI
2	None	1	1	39	0.235	0.05	0.26	0.74	Twosol	t_1 : 7 t_2 : 2 t_3 : 23	40	170	30	B: 5.5 A: 7	AFI
3	None	1	1	39	0.235	0.05	0.26	0.74	Twosol	t_1 : 7 t_2 : 2 t_3 : 23	40	170	30	B: 5.5 A: 7	AFI
4	None	1	1	39	0.235	0.05	0.26	0.74	Twosol	t_1 : 7 t_2 : 2 t_3 : 23	40	170	30	B: 5.5 A: 7	AFI
5	H_2O	1	1	**39.8**	0.35	0	0	1.08	Twosol	t_1 : 4 t_2 : 2 t_3 : 1.5	50	200	144	B: 6 A: 8	AFI + AFR
6	H_2O	1	1	**43**	0.35	0	0	1.08	Twosol	t_1 : 4 t_2 : 2 t_3 : 1.5	50	200	144	B: 6.5 A: 8	AFI

Table 4.1: Table showcasing SAPO results, with selected parameters important for the overall synthesis schemes. A '*' indicated that the silicon source was colloidal silica. In the pH column, B means for "Before", A means for "After".

Entry	Parameter varied	Al	P	H_2O	Si	TMAOH	TPABr	TPAOH	Method	Ageing [h]	Fill grade	T[°C]	t_4 [h]	pH	Resulting zeotype(s)
7	TMAOH	1	1	39.8	0.35	0.011	0	1.065	Twosol	$t_1 : 4$ $t_2 : 2$ $t_3 : 1.5$	50	200	144	B: 6.5 A: 8	AFI + FAU
8	Cryst. time. (t_4) and temp.	1	1	33.3	0.15	0.017	0.37	0.463	Twosol	$t_1 : 4$ $t_2 : 2$ $t_3 : 1.5$	33	**200**	**144**	B: 4.5 A: 8	AFI
9	Cryst. time. (t_4) and temp.	1	1	33.3	0.15	0.017	0.37	0.463	Twosol	$t_1 : 4$ $t_2 : 2$ $t_3 : 1.5$	33	**200**	**288**	B: 4.5 A: 9	AFI + FAU
10	Cryst. time. (t_4) and temp.	1	1	33.3	0.15	0.017	0.37	0.463	Twosol	$t_1 : 4$ $t_2 : 2$ $t_3 : 1.5$	33	**150**	**144**	B: 4.5 A: 7.5	AFI + FAU
11	Cryst. time. (t_4) and temp.	1	1	33.3	0.15	0.017	0.37	0.463	Twosol	$t_1 : 4$ $t_2 : 2$ $t_3 : 1.5$	33	**150**	**288**	B: 4.5 A: 8	AFI
12	Cryst. time. (t_4) and temp.	1	1	39.8	0.35	0	0	1.08	Twosol	$t_1 : 4$ $t_2 : 2$ $t_3 : 1.5$	40	**200**	**144**	B: 6.5 A: 8	AFI + FAU

Table 4.1: Table showcasing SAPO results, with selected parameters important for the overall synthesis schemes. A '*' indicated that the silicon source was colloidal silica. In the pH column, B means for "Before", A means for "After".

Entry	Parameter varied	Al	P	H_2O	Si	TMAOH	TPABr	TPAOH	Method	Ageing [h]	Fill grade	T[°C]	t_4 [h]	pH	Resulting zeotype(s)
13	Cryst. time. (t_4) and temp.	1	1	39.8	0.35	0	0	1.08	Twosol	t_1 : 4 t_2 : 2 t_3 : 1.5	40	**200**	**288**	B: 6.5 A: 9	AFI
14	Cryst. time. (t_4) and temp.	1	1	39.8	0.35	0	0	1.08	Twosol	t_1 : 4 t_2 : 2 t_3 : 1.5	40	**150**	**144**	B: 6.5 A: 7.5	None
15	Cryst. time. (t_4) and temp.	1	1	39.8	0.35	0	0	1.08	Twosol	t_1 : 4 t_2 : 2 t_3 : 1.5	40	**150**	**288**	B: 6.5 A: 7.5	None
16	Filling, Cryst. time. (t_4) and temp.	1	1	39.8	0.35	0	0	1.08	Twosol	t_1 : 4 t_2 : 2 t_3 : 1.5	**33**	**150**	**72**	B: 6.5 A: 7.5	None
17	Filling, Cryst. time. (t_4) and temp.	1	1	39.8	0.35	0	0	1.08	Twosol	t_1 : 4 t_2 : 2 t_3 : 1.5	**33**	**200**	**72**	B: 6.5 A: 7.5	AFI + FAU
18	Filling, Cryst. time. (t_4) and temp.	1	1	39.8	0.35	0	0	1.08	Twosol	t_1 : 4 t_2 : 2 t_3 : 1.5	**33**	**150**	**216**	B: 6.5 A: 7.5	None

Table 4.1: Table showcasing SAPO results, with selected parameters important for the overall synthesis schemes. A '*' indicated that the silicon source was colloidal silica. In the pH column, B means for "Before", A means for "After".

Entry	Parameter varied	Al	P	H_2O	Si	TMAOH	TPABr	TPAOH	Method	Ageing [h]	Fill grade	T[°C]	t_4 [h]	pH	Resulting zeotype(s)
19	Filling, Cryst. time. (t_4) and temp.	1	1	39.8	0.35	0	0	1.08	Twosol	t_1 : 4 t_2 : 2 t_3 : 1.5	**33**	**200**	**216**	B: 6.5 A: 7.5	FAU
20	Filling, Cryst. time. (t_4) and temp.	1	1	39.8	0.35	0	0	1.08	Twosol	t_1 : 4 t_2 : 2 t_3 : 1.5	**67**	**150**	**72**	B: 6.5 A: 7.5	None
21	Filling, Cryst. time. (t_4) and temp.	1	1	39.8	0.35	0	0	1.08	Twosol	t_1 : 4 t_2 : 2 t_3 : 1.5	**67**	**200**	**72**	B: 6.5 A: 7.5	AFI + FAU
22	Filling, Cryst. time. (t_4) and temp.	1	1	39.8	0.35	0	0	1.08	Twosol	t_1 : 4 t_2 : 2 t_3 : 1.5	**67**	**150**	**216**	B: 6.5 A: 7.5	None
23	Filling, Cryst. time. (t_4) and temp.	1	1	39.8	0.35	0	0	1.08	Twosol	t_1 : 4 t_2 : 2 t_3 : 1.5	**67**	**200**	**216**	B: 6.5 A: 8	AFI

Table 4.1: Table showcasing SAPO results, with selected parameters important for the overall synthesis schemes. A '*' indicated that the silicon source was colloidal silica. In the pH column, B means for "Before", A means for "After".

Entry	Parameter varied	Al	P	H_2O	Si	TMAOH	TPABr	TPAOH	Method	Ageing [h]	Fill grade	T[°C]	t_4 [h]	pH	Resulting zeotype(s)
24	Filling, Cryst. time. (t_4) and temp.	1	1	39.8	0.35	0	0	1.08	Twosol	t_1 : 4 t_2 : 2 t_3 : 1.5	**50**	**175**	**144**	B: 6.5 A: 7.5	None
25	Filling, Cryst. time. (t_4) and temp.	1	1	39.8	0.35	0	0	1.08	Twosol	t_1 : 4 t_2 : 2 t_3 : 1.5	**50**	**175**	**144**	B: 6.5 A: 7.5	None
26	Filling, Cryst. time. (t_4) and temp.	1	1	39.8	0.35	0	0	1.08	Twosol	t_1 : 4 t_2 : 2 t_3 : 1.5	**50**	**175**	**144**	B: 6.5 A: 7.5	None
27	Method and silicon source	1	1	39.8	**0.35 ***	0	0	1.08	Onepot	t_1 : 4 t_2 : 2 t_3 : 1.5	45	200	144	B: 6.5 A: 9	AFI
28	Method and silicon source	1	1	39.8	**0.35**	0	0	1.08	Onepot	t_1 : 4 t_2 : 2 t_3 : 1.5	45	200	144	B: 6.5 A: 9	AFI
29	Method and silicon source	1	1	39.8	**0.35 ***	0	0	1.08	Twosol	t_1 : 4 t_2 : 2 t_3 : 1.5	45	200	144	B: 6.5 A: 8	AFI

Table 4.1: Table showcasing SAPO results, with selected parameters important for the overall synthesis schemes. A '*' indicated that the silicon source was colloidal silica. In the pH column, B means for "Before", A means for "After".

Entry	Parameter varied	Al	P	H_2O	Si	TMAOH	TPABr	TPAOH	Method	Ageing [h]	Fill grade	T[°C]	t_4 [h]	pH	Resulting zeotype(s)
30	Method and silicon source	1	1	39.8	**0.35**	0	0	1.08	Twosol	t_1 : 4 t_2 : 2 t_3 : 1.5	45	200	144	B: 6.5 A: 9	AFI

In order to get a better overview when comparing results, the synthesis entries where given longer, more descriptive names in order to highlight differences better.

Table 4.2: Table correlating entry numbers from the SAPO-40 syntheses to their longer, more descriptive names.

Entry	Sample
1	S40-D-reprod
2	S40-S-reprod1
3	S40-S-reprod2
4	S40-S-reprod3
5	S40-D-39.8:H_2O
6	S40-D-43:H_2O
7	S40-D-0.011:TMA
8	S40-L-200°C-144h
9	S40-L-200°C-288h
10	S40-L-150°C-144h
11	S40-L-150°C-288h
12	S40-D-200°C-144h
13	S40-D-200°C-288h
14	S40-D-150°C-144h
15	S40-D-150°C-288h
16	S40-D-33%-150°C-72h
17	S40-D-33%-150°C-288h
18	S40-D-33%-200°C-72h
19	S40-D-33%-200°C-288h
20	S40-D-67%-150°C-72h
21	S40-D-67%-150°C-288h
22	S40-D-67%-200°C-72h
23	S40-D-67%-200°C-288h
24	S40-D-50%-175°C-144h-1

Table 4.2: Table correlating entry numbers from the SAPO-40 syntheses to their longer, more descriptive names.

Entry	Sample
25	S40-D-50%-175°C-144h-2
26	S40-D-50%-175°C-144h-3
27	S40-D-onepot-LUDOX
28	S40-D-onepot-fumed
29	S40-D-twosol-LUDOX
30	S40-D-twosol-fumed

4.1.1 Reproduction of literature

To start, a synthesis originally developed by Dumont, N. et al[39] and optimized by Lourenço, J. P. et al.[13] was attempted. Only an AFI phase could be seen in the diffractogram that was obtained.

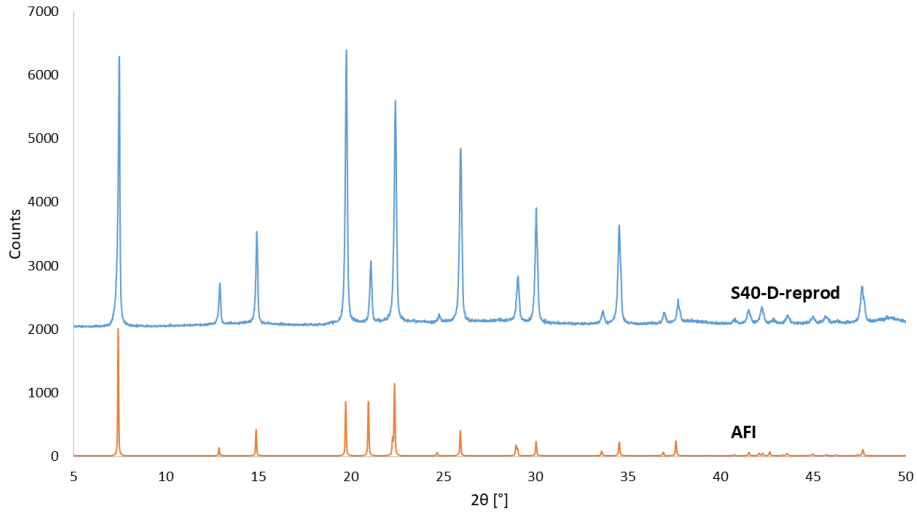

Figure 4.1: Diffractogram showing the attempted reproduction of the synthesis developed by Dumont, N. et al..[39] The syntheses reported corresponds to entries 1 to 3 in Table 4.1.

Due to the reproduction not yielding any visible AFR phases, a different base synthesis was attempted this time from Sierra, L. et al..[41] Here, a reproducibility test was also conducted.

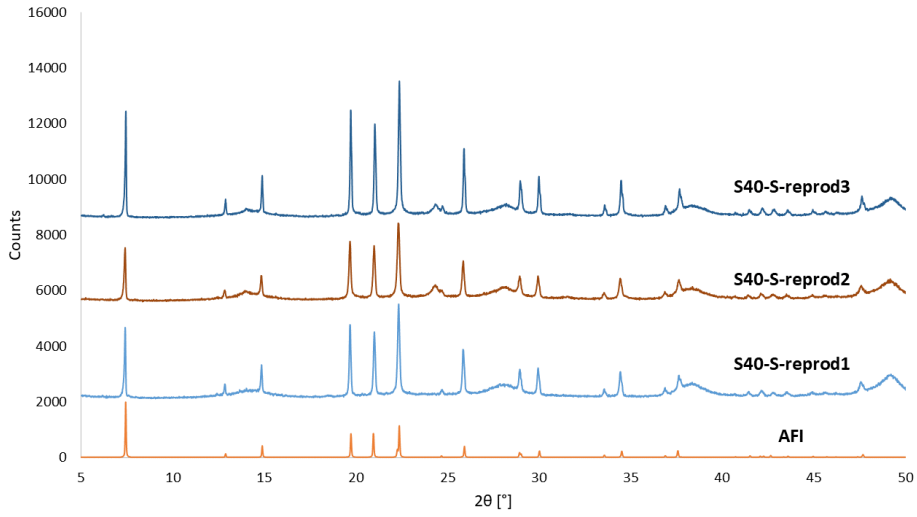

Figure 4.2: Diffractogram showing the attempted reproduction of the synthesis developed by Sierra, L. et al.[41] The synthesis reported corresponds to entry 4 in Table 4.1.

The Sierra based synthesis also only yielded an AFI phase, in all three reproductions. Interesting to note was also the generally lower crystallinity when compared to the Dumont synthesis, as well as the presence of broad, flatter peaks at multiple points in the diffractogram. These peaks were assigned to a ambiguously defined aluminophosphate phase.

4.1.2 Chemical parameter experiments

Due to the Dumont synthesis yielding better conditions in regards to zeotype formation, it was chosen as the synthesis for further investigation. In their original report, Dumont, N. et al.[39] pointed to a favourable interaction between gel dilution and AFR phase formation. Thus, a probe experiment, seeking to see the effect of increasing the water content was conducted.

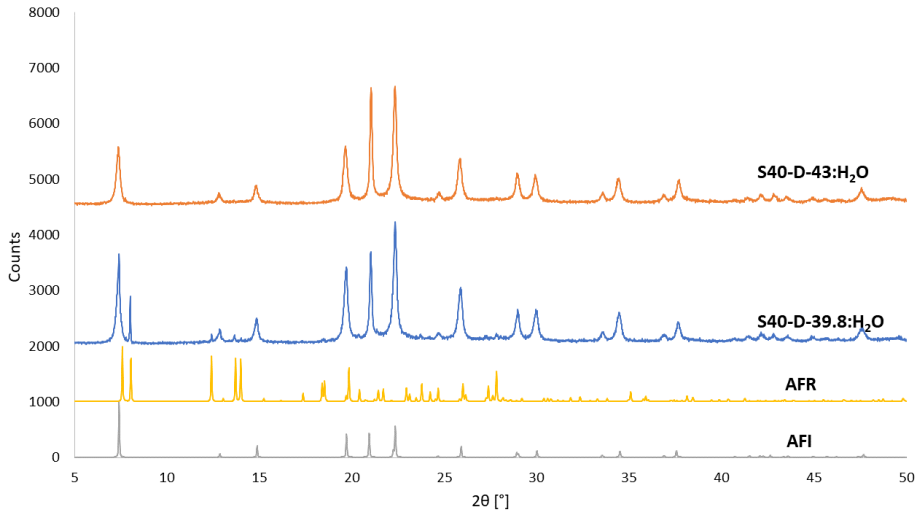

Figure 4.3: Diffractogram showing the effect of diluting the gel with additional water in the Dumont synthesis. The syntheses reported corresponds to entries 5 and 6 in Table 4.1.

As can be seen in Figure 4.3, an increase in water from 39.8 molar equivalents to 43 molar equivalents in did not favour any AFR phase formation. There was an AFR phase forming in the sample with 39.8 molar equivalents of water, but this phase was still eclipsed by the more dominant AFI phase.

Several sources, including the aforementioned Sierra based synthesis, highlighted the benefit of using TMAOH in order to suppress the AFI phase in the synthesis. A synthesis seeking to investigate the effect of a small addition of TMAOH was therefore conducted.

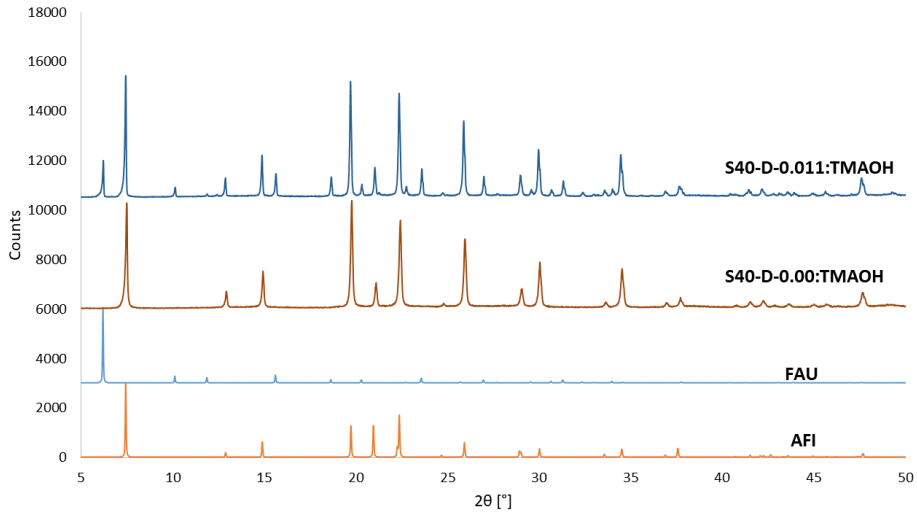

Figure 4.4: Diffractogram showcasing the effect of a small addition of TMAOH to the Dumont based synthesis. The synthesis reported corresponds to entry 4 in Table 4.1. The synthesis reported corresponds to entry 7 in Table 4.1. Entry 1 in Table 4.1 was used as a reference.

There were two phases forming upon addition of TMAOH to the gel. These were identified as the AFI phase and FAU phase respectively.

4.1.3 Physical parameter experiments

By modifying a synthesis from Lourenço, J. P. et al.[12] by omitting the added transition metal cation, an adapted SAPO synthesis was developed. This synthesis was also subjected to a study on the effects of crystallization time and temperature.

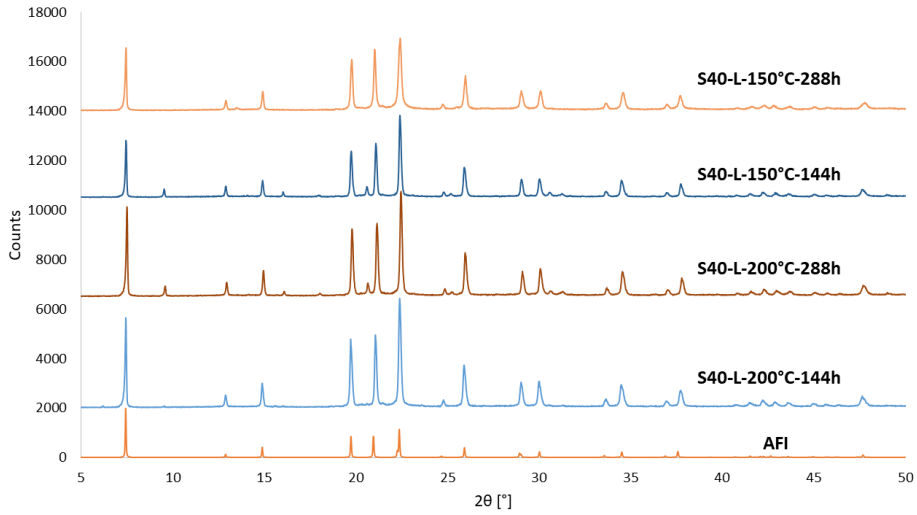

Figure 4.5: Diffractogram showcasing the effect of lowering the crystallisation temperature, while extending the crystallization time in the adapted Lourenço based synthesis. The syntheses reported corresponds to entries 8 to 11 in Table 4.1.

No AFR phase was formed in any of the syntheses. Instead, an AFI phase was formed, with traces of a CHA phase. There was no observable pattern to when the CHA trace formed with respect to temperatures and times used in the synthesis .

For the sake of completion, the same study of the effect of crystallization time and temperature was performed for the Dumont synthesis.

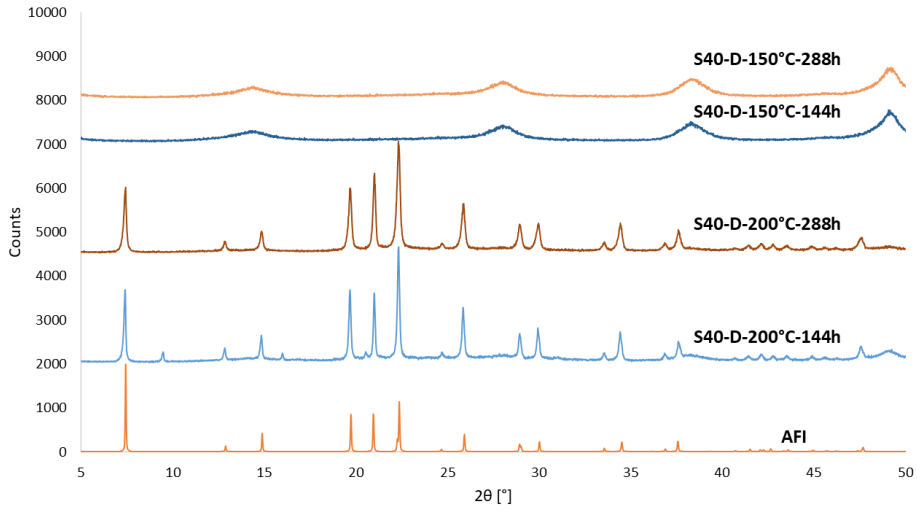

Figure 4.6: Diffractogram showcasing the effect of lowering the crystallisation temperature, while extending the crystallization time in the Dumont based synthesis. The syntheses reported corresponds to entries 12 to 15 in Table 4.1.

Figure 4.6 shows that at lower temperature values in the Dumont synthesis, no zeotype phase was obtained. For the syntheses performed at 200 °C, mainly an AFI was formed with a trace of a CHA phase.

To further study the effect of physical parameters in the Dumont synthesis, the effect of filling grade and in turn pressure in the reaction vessel during the synthesis, was investigated in tandem with the crystallization temperature and time. The obtained diffractogram can be viewed in Appendix A.1 Figure A.1.

At a 33 % filling grade, no zeotypes form at 150 °C. Like many of the aforementioned experimental results, an AFI phase readily forms at 200 °C as.An exception existed for sample S40-D-33%:fill-200°C-216h (Entry 19), the only zeotype phase seems to be the CHA phase.

With regards to a 67 % filling grade, the obtained diffractogram can be viewed in Appendix A.1 FigureA.2

From Figure A.2, the main phase in the 200°C syntheses seems to be the AFI phase. Even at the 67 % filling grade, the syntheses at 150 °C still failed to produce a zeotype phase.

As a control, a set of three identical syntheses were performed at the average value of time temperature and filling grade. The obtained diffractogram is shown in Appendix A.1 Figure A.3

No synthesis parallel at 175°C succeeded in producing any observable zeo-

types.

4.1.4 Combined chemical and physical parameter experiments

The final set of parameters that were investigated in regards to the SAPO-40 synthesis, was the method of gel formation as well as the Si-source. The two methods were the two-solution method, which involved the combination of two separately mixed reactant mixtures to a gel, and the one-pot method in which all reactants were mixed in the same vessel. The two silicon sources that were investigated were fumed silica and colloidal silica solution (LUDOX).

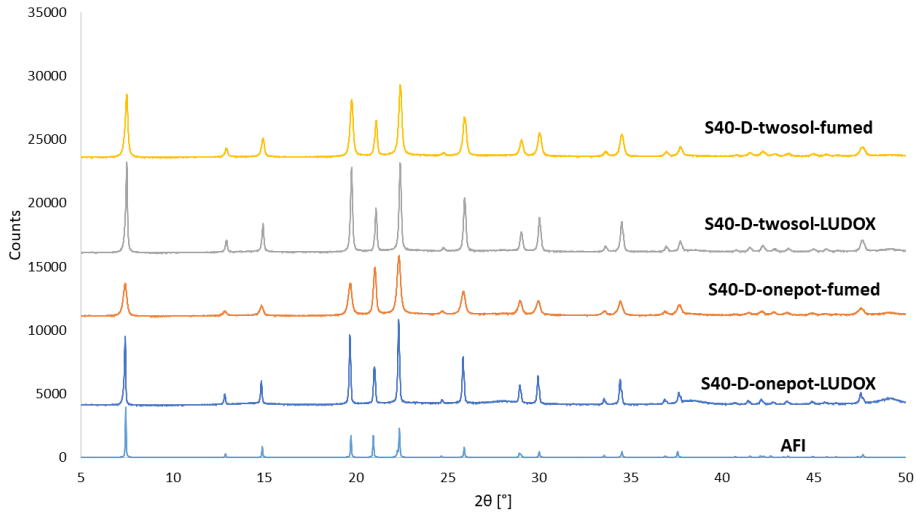

Figure 4.7: Diffractogram showing the influence of mixing method and silicon source on the Dumont synthesis. The syntheses reported corresponds to entries 27 to 30 in Table 4.1.

Only an AFI phase was obtained, regardless of the method and silicon source used. The two solution method with colloidal silica did produce the sample with the highest crystallinity, and samples with colloidal silica had generally higher crystallinities than their fumed silica counterparts.

4.2 AlPO synthesis results

Presented in the following table in an overview of all the conducted syntheses for plain AlPO-40 with pH values and obtained zeotype phases given to the right in the table.

Table 4.3: Table detailing all AlPO-40 synthesis and their respective results in zeotypes formed as well as pH values before and after the reaction had taken place. Filling grade was always kept constant at 45 %. A '*' next to the amount of TPAOH. In the pH column, B means for "Before", A means for "After".

Entry	Parameter varied	Al	P	H_2O	TMAOH	TPABr	TPAOH	Ageing [h]	HF wash	T [°C]	t_4 [h]	pH	Resulting zeotype(s)
1	None	1	1	37.5	0.045	0.26	0.71	t_1 : 6 t_2 : 2 t_3 : 17	Yes	150	23	B: 6 A: 7.5	AFR
2	None	1	1	37.5	0.045	0.26	0.71	t_1 : 6 t_2 : 2 t_3 : 17	Yes	150	23	B: 6 A: 7.5	AFI
3	None	1	1	37.5	0.045	0.26	0.71	t_1 : 6 t_2 : 2 t_3 : 17	Yes	150	23	B: 6 A: 7.5	AFI
4	Cryst. time (t_4)	0.8	0.8	40	0.02	0.52	0.48	t_1 : 4 t_2 : 2 t_3 : 18	No	150	**120**	B: 5.5 A: 7.5	AFI
5	Cryst. time (t_4)	0.8	0.8	40	0.02	0.52	0.48	t_1 : 4 t_2 : 2 t_3 : 18	No	150	**144**	B: 5.5 A: 7.5	AFI + AFR
6	Br^-/OH^- ratio	1	1	37.5	0.045	**0.26**	**0.71**	t_1 : 6 t_2 : 2 t_3 : 17	No	150	23	B: 6.5 A: 7	AFI

Table 4.3: Table detailing all AlPO-40 synthesis and their respective results in zeotypes formed as well as pH values before and after the reaction had taken place. Filling grade was always kept constant at 45 %. A '*' next to the amount of TPAOH. In the pH column, B means for "Before", A means for "After".

Entry	Parameter varied	Al	P	H_2O	TMAOH	TPABr	TPAOH	Ageing [h]	HF wash	T [°C]	t_4 [h]	pH	Resulting zeotype(s)
7	Br^-/OH^- ratio	1	1	37.5	0.045	**0.335**	**0.645**	t_1 : 6 t_2 : 2 t_3 : 17	No	150	23	B: 6 A: 7	AFI
8	Br^-/OH^- ratio	1	1	37.5	0.045	**0.39**	**0.58**	t_1 : 6 t_2 : 2 t_3 : 17	No	150	23	B: 5.5 A: 6.5	AFI
9	TMAOH	1	1	37.5	**0.02**	0.26	0.71	t_1 : 6 t_2 : 2 t_3 : 17	No	150	23	B: 6.5 A: 7	AFI
10	TPA^+ content	1	1	37.5	0.045	**0.215**	**0.585**	t_1 : 6 t_2 : 2 t_3 : 17	No	150	23	B: 5.5 A: 7	AFI
11	TPA^+ content	1	1	37.5	0.045	**0.245**	**0.665**	t_1 : 6 t_2 : 2 t_3 : 17	No	150	23	B: 6 A: 7	AFI
12	TPA^+ content	1	1	37.5	0.045	**0.297**	**0.803**	t_1 : 6 t_2 : 2 t_3 : 17	No	150	23	B: 7 A: 7.5	AFI

Table 4.3: Table detailing all AlPO-40 synthesis and their respective results in zeotypes formed as well as pH values before and after the reaction had taken place. Filling grade was always kept constant at 45 %. A '*' next to the amount of TPAOH. In the pH column, B means for "Before", A means for "After".

Entry	Parameter varied	Al	P	H_2O	TMAOH	TPABr	TPAOH	Ageing [h]	HF wash	T [°C]	t_4 [h]	pH	Resulting zeotype(s)
13	TPA^+ content	1	1	37.5	0.045	**0.325**	**0.875**	t_1 : 6 t_2 : 2 t_3 : 17	No	150	23	B: 7.5 A: 8	None
14	Cryst. time (t_4)	1	1	37.5	0.045	0.26	0.71	t_1 : 6 t_2 : 2 t_3 : 17	No	150	**47**	B: 6.5 A: 7	AFR + AFI + unknown
15	None	1	1	37.5	0.045	0.26	0.71	t_1 : 6 t_2 : 2 t_3 : 17	No	150	23	B: 6.5 A: 7	AFI
16	Cryst. time (t_4)	1	1	37.5	0.045	0.26	0.71	t_1 : 6 t_2 : 2 t_3 : 17	No	150	**47**	B: 6.6 A: 7.5	AFI
17	Cryst. temp.	1	1	37.5	0.045	0.26	0.71	t_1 : 6 t_2 : 2 t_3 : 17	No	**170**	23	B: 6.5 A: 7	AFI
18	Cryst. time (t_4) and temp.	1	1	37.5	0.045	0.26	0.71	t_1 : 6 t_2 : 2 t_3 : 17	No	**170**	**47**	B: 6.5 A: 7.5	AFI

Table 4.3: Table detailing all AlPO-40 synthesis and their respective results in zeotypes formed as well as pH values before and after the reaction had taken place. Filling grade was always kept constant at 45 %. A '*' next to the amount of TPAOH. In the pH column, B means for "Before", A means for "After".

Entry	Parameter varied	Al	P	H_2O	TMAOH	TPABr	TPAOH	Ageing [h]	HF wash	T [°C]	t_4 [h]	pH	Resulting zeotype(s)
19	Ageing time (t_3)	1	1	37.5	0.045	0.26	0.71	**t_1 : 6** **t_2 : 2** **t_3 : 41**	No	150	23	B: 6.5 A: 7	AFI
20	Mixing and ageing time (t_1, t_2, t_3)	1	1	37.5	0.045	0.26	0.71	**t_1 : 1.5** **t_2 : 1.5** **t_3 : 2**	No	150	23	B: 6.5 A: 6.5	None
21	Mixing and ageing time (t_1, t_2, t_3)	1	1	37.5	0.045	0.26	0.71	**t_1 : 1.5** **t_2 : 1.5** **t_3 : 4**	No	150	23	B: 6.5 A: 7	None
22	Mixing and ageing time (t_1, t_2, t_3)	1	1	37.5	0.045	0.26	0.71	**t_1 : 1.5** **t_2 : 1.5** **t_3 : 6**	No	150	23	B: 6.5 A: 7	None
23	Cryst. time	1	1	37.5	0.045	0.26	0.71	**t_1 : 1.5** **t_2 : 1.5** **t_3 : 4**	No	150	24	B: 6.5 A: 7	AFI
24	Cryst. time	1	1	37.5	0.045	0.26	0.71	**t_1 : 1.5** **t_2 : 1.5** **t_3 : 4**	No	150	**48**	B: 6.5 A: 7	AFI

Table 4.3: Table detailing all AlPO-40 synthesis and their respective results in zeotypes formed as well as pH values before and after the reaction had taken place. Filling grade was always kept constant at 45 %. A '*' next to the amount of TPAOH. In the pH column, B means for "Before", A means for "After".

Entry	Parameter varied	Al	P	H_2O	TMAOH	TPABr	TPAOH	Ageing [h]	HF wash	T [°C]	t_4 [h]	pH	Resulting zeotype(s)
25	Cryst. time	1	1	37.5	0.045	0.26	0.71	**t_1 : 1.5 t_2 : 1.5 t_3 : 4**	No	150	**72**	B: 6.5 A: 7	AFI
26	Cryst. time	1	1	37.5	0.045	0.26	0.71	**t_1 : 1.5 t_2 : 1.5 t_3 : 4**	No	150	**96**	B: 6.5 A: 7	AFI
27	Cryst. time	1	1	37.5	0.045	0.26	0.71	**t_1 : 1.5 t_2 : 1.5 t_3 : 4**	No	150	**120**	B: 6.5 A: 8	AFI
28	Ageing time (t_3)	1	1	37.5	0.045	0.26	0.71	**t_1 : 6 t_2 : 2 t_3 : 0.5**	No	150	23	B: 6 A: 7	AFI
29	Cryst. temp.	1	1	37.5	0.045	0.26	0.71	t_1 : 6 t_2 : 2 t_3 : 17	Yes	150	23	B: 6.5 A: 7	AFI
30	Cryst. temp.	1	1	37.5	0.045	0.26	0.71	t_1 : 6 t_2 : 2 t_3 : 17	Yes	**170**	23	B: 6.5 A: 7.5	AFI

Table 4.3: Table detailing all AlPO-40 synthesis and their respective results in zeotypes formed as well as pH values before and after the reaction had taken place. Filling grade was always kept constant at 45 %. A '*' next to the amount of TPAOH. In the pH column, B means for "Before", A means for "After".

Entry	Parameter varied	Al	P	H_2O	TMAOH	TPABr	TPAOH	Ageing [h]	HF wash	T [°C]	t_4 [h]	pH	Resulting zeotype(s)
31	TPAOH source and Cryst. time (t_4)	1	1	50	0.025	0.65	**0.60 ***	t_1 : 4 t_2 : 2 t_3 : 18	Yes	150	120	B: 6 A: 7	AFI + AFR
32	TPAOH source and Cryst. time (t_4)	1	1	50	0.025	0.65	**0.60 ***	t_1 : 4 t_2 : 2 t_3 : 18	Yes	150	**144**	B: 6 A: 7	AFI
33	TPAOH source and Cryst. time (t_4)	1	1	50	0.025	0.65	**0.60 ***	t_1 : 4 t_2 : 2 t_3 : 18	Yes	150	**168**	B: 6 A: 7.5	AFI
34	TPAOH source and Cryst. time (t_4)	1	1	50	0.025	0.65	**0.60 ***	t_1 : 4 t_2 : 2 t_3 : 18	Yes	150	**192**	B: 6 A: 7.5	AFI
35	TPAOH source and Cryst. time (t_4)	1	1	50	0.025	0.65	**0.60 ***	t_1 : 4 t_2 : 2 t_3 : 18	Yes	150	**216**	B: 6 A: 8	AFI

Table 4.3: Table detailing all AlPO-40 synthesis and their respective results in zeotypes formed as well as pH values before and after the reaction had taken place. Filling grade was always kept constant at 45 %. A '*' next to the amount of TPAOH. In the pH column, B means for "Before", A means for "After".

Entry	Parameter varied	Al	P	H_2O	TMAOH	TPABr	TPAOH	Ageing [h]	HF wash	T [°C]	t_4 [h]	pH	Resulting zeotype(s)
36	TPAOH source and Cryst. time (t_4)	1	1	50	0.025	0.65	**0.60 ***	t_1 : 4 t_2 : 2 t_3 : 18	Yes	150	**240**	B: 6 A: 7.5	AFI
37	TPAOH source and Cryst. time (t_4)	1	1	50	0.025	0.65	0.60	t_1 : 4 t_2 : 2 t_3 : 18	Yes	150	120	B: 6 A: 7	AFI + AFR
38	TPAOH source and Cryst. time (t_4)	1	1	50	0.025	0.65	0.60	t_1 : 4 t_2 : 2 t_3 : 18	Yes	150	**144**	B: 6 A: 7	AFI + AFR
39	TPAOH source and Cryst. time (t_4)	1	1	50	0.025	0.65	0.60	t_1 : 4 t_2 : 2 t_3 : 18	Yes	150	**168**	B: 6 A: 7.5	AFI
40	TPAOH source and Cryst. time (t_4)	1	1	50	0.025	0.65	0.60	t_1 : 4 t_2 : 2 t_3 : 18	Yes	150	**192**	B: 6 A: 7.5	AFI

Table 4.3: Table detailing all AlPO-40 synthesis and their respective results in zeotypes formed as well as pH values before and after the reaction had taken place. Filling grade was always kept constant at 45 %. A '*' next to the amount of TPAOH. In the pH column, B means for "Before", A means for "After".

Entry	Parameter varied	Al	P	H_2O	TMAOH	TPABr	TPAOH	Ageing [h]	HF wash	T [°C]	t_4 [h]	pH	Resulting zeotype(s)
41	TPAOH source and Cryst. time (t_4)	1	1	50	0.025	0.65	0.60	t_1 : 4 t_2 : 2 t_3 : 18	Yes	150	**216**	B: 6 A: 8	AFI
42	TPAOH source and Cryst. time (t_4)	1	1	50	0.025	0.65	0.60	t_1 : 4 t_2 : 2 t_3 : 18	Yes	150	**240**	B: 6 A: 7.5	AFI
43	Cryst. time (t_4)	1	1	50	0.025	0.65	0.60 *	t_1 : 4 t_2 : 2 t_3 : 18	Yes	150	**24**	B: 6 A: 6.5	AFI
44	Cryst. time (t_4)	1	1	50	0.025	0.65	0.60 *	t_1 : 4 t_2 : 2 t_3 : 18	Yes	150	**48**	B: 6 A: 6.5	AFI
45	Cryst. time (t_4)	1	1	50	0.025	0.65	0.60 *	t_1 : 4 t_2 : 2 t_3 : 18	Yes	150	**72**	B: 6 A: 6.5	AFI
46	Cryst. time (t_4)	1	1	50	0.025	0.65	0.60 *	t_1 : 4 t_2 : 2 t_3 : 18	Yes	150	**96**	B: 6 A: 7	AFI

Table 4.3: Table detailing all AlPO-40 synthesis and their respective results in zeotypes formed as well as pH values before and after the reaction had taken place. Filling grade was always kept constant at 45 %. A '*' next to the amount of TPAOH. In the pH column, B means for "Before", A means for "After".

Entry	Parameter varied	Al	P	H_2O	TMAOH	TPABr	TPAOH	Ageing [h]	HF wash	T [°C]	t_4 [h]	pH	Resulting zeotype(s)
47	TPAOH Source	1	1	37.5	0.045	0.26	0.71	t_1 : 6 t_2 : 2 t_3 : 17	Yes	150	23	B: 6.5 A: 7	AFI
48	TPAOH Source	1	1	37.5	0.045	0.26	**0.71 ***	t_1 : 6 t_2 : 2 t_3 : 17	Yes	150	23	B: 6.5 A: 7	AFI
49	Cryst. time (t_4)	1	1	37.5	0.045	0.26	0.71 *	t_1 : 6 t_2 : 2 t_3 : 17	Yes	150	**23**	B: 6.5 A: 7	None
50	Cryst. time (t_4)	1	1	37.5	0.045	0.26	0.71 *	t_1 : 6 t_2 : 2 t_3 : 17	Yes	150	**71**	B: 6.5 A: 7.5	AFI
51	Cryst. time (t_4)	1	1	37.5	0.045	0.26	0.71 *	t_1 : 6 t_2 : 2 t_3 : 17	Yes	150	**119**	B: 6.5 A: 7.5	AFI + AFR
52	Cryst. time (t_4)	1	1	37.5	0.045	0.26	0.71 *	t_1 : 6 t_2 : 2 t_3 : 17	Yes	150	**167**	B: 6.5 A: 7.5	AFI + AFR

Table 4.3: Table detailing all AlPO-40 synthesis and their respective results in zeotypes formed as well as pH values before and after the reaction had taken place. Filling grade was always kept constant at 45 %. A '*' next to the amount of TPAOH. In the pH column, B means for "Before", A means for "After".

Entry	Parameter varied	Al	P	H_2O	TMAOH	TPABr	TPAOH	Ageing [h]	HF wash	T [°C]	t_4 [h]	pH	Resulting zeotype(s)
53	H_2O	1	1	37.5	0.045	0.26	0.71 *	t_1 : 6 t_2 : 2 t_3 : 17	Yes	150	23	B: 6.5 A: 6.5	None
54	H_2O	1	1	**35**	0.045	0.26	0.71 *	t_1 : 6 t_2 : 2 t_3 : 17	Yes	150	23	B: 6.5 A: 6.5	AFI
55	H_2O	1	1	**32.5**	0.045	0.26	0.71 *	t_1 : 6 t_2 : 2 t_3 : 17	Yes	150	23	B: 6 A: 6.5	AFR
56	H_2O	1	1	**30**	0.045	0.26	0.71 *	t_1 : 6 t_2 : 2 t_3 : 17	Yes	150	23	B: 6 A: 6.5	AFR + AFI
57	H_2O and HF wash	1	1	37.5	0.045	0.26	0.71 *	t_1 : 6 t_2 : 2 t_3 : 17	No	150	23	B: 6.5 A: 7	None
58	H_2O and HF wash	1	1	**32.5**	0.045	0.26	0.71 *	t_1 : 6 t_2 : 2 t_3 : 17	No	150	23	B: 6 A: 7	AFI

Table 4.3: Table detailing all AlPO-40 synthesis and their respective results in zeotypes formed as well as pH values before and after the reaction had taken place. Filling grade was always kept constant at 45 %. A '*' next to the amount of TPAOH. In the pH column, B means for "Before", A means for "After".

Entry	Parameter varied	Al	P	H_2O	TMAOH	TPABr	TPAOH	Ageing [h]	HF wash	T [°C]	t_4 [h]	pH	Resulting zeotype(s)
59	H_2O and Cryst. time (t_4)	1	1	**32.5**	0.045	0.26	0.71 *	t_1 : 6 t_2 : 2 t_3 : 17	Yes	150	23	B: 6.5 A: 7	AFI
60	H_2O and Cryst. time (t_4)	1	1	**32.5**	0.045	0.26	0.71 *	t_1 : 6 t_2 : 2 t_3 : 17	Yes	150	**71**	B: 6.5 A: 7	AFI + AFR
61	H_2O and Cryst. time (t_4)	1	1	**32.5**	0.045	0.26	0.71 *	t_1 : 6 t_2 : 2 t_3 : 17	Yes	150	**119**	B: 6.5 A: 7.5	AFI + AFR
62	H_2O and Cryst. time (t_4)	1	1	**32.5**	0.045	0.26	0.71 *	t_1 : 6 t_2 : 2 t_3 : 17	Yes	150	**167**	B: 6.5 A: 8	AFR + AFI

In order to get a better overview when comparing results, the synthesis entries where given longer, more descriptive names in order to highlight differences better.

Table 4.4: Table correlating specific sample names used in upcoming diffractograms to entry numbers in experimental and result overview sections for AlPO-40.

Entry	Sample
31	A40-S-reprod1
32	A40-S-reprod2
33	A40-S-reprod3
34	A40-L-noHF-120h
35	A40-L-noHF-144h
36	A40-S-0.37:Br^-/OH^-
37	A40-S-0.52:Br^-/OH^-
38	A40-S-0.67:Br^-/OH^-
39	A40-S-0.02:TMA
40	A40-S-0.8:TPA^+
41	A40-S-0.9:TPA^+
42	A40-S-1.1:TPA^+
43	A40-S-1.2:TPA^+
44	A40-S-47h
45	A40-S-150°C-23h
46	A40-S-150°C-47h
47	A40-S-170°C-23h
48	A40-S-170°C-47h
49	A40-S-41h:age
50	A40-S-lowmix-2h
51	A40-S-lowmix-4h
52	A40-S-lowmix-6h
53	A40-S-4h:mix-24h
54	A40-S-4h:mix-48h

Table 4.4: Table correlating specific sample names used in upcoming diffractograms to entry numbers in experimental and result overview sections for AlPO-40.

Entry	Sample
55	A40-S-4h:mix-72h
56	A40-S-4h:mix-96h
57	A40-S-4h:mix-120h
58	A40-S-0.5:age
59	A40-S-150 °C
60	A40-S-170 °C
61	A40-L-αTPA-120h
62	A40-L-αTPA-144h
63	A40-L-αTPA-168h
64	A40-L-αTPA-192h
65	A40-L-αTPA-216h
66	A40-L-αTPA-240h
67	A40-L-σTPA-120h
68	A40-L-σTPA-144h
69	A40-L-σTPA-168h
70	A40-L-σTPA-192h
71	A40-L-σTPA-216h
72	A40-L-σTPA-240h
73	A40-L-24h
74	A40-L-48h
75	A40-L-72h
76	A40-L-96h
77	A40-S-σTPA
78	A40-S-αTPA
79	A40-S-23h
80	A40-S-71h

Table 4.4: Table correlating specific sample names used in upcoming diffractograms to entry numbers in experimental and result overview sections for AlPO-40.

Entry	Sample
81	A40-S-119h
82	A40-S-167h
83	A40-S-37.5:H_2O
84	A40-S-35:H_2O
85	A40-S-32.5:H_2O
86	A40-S-30:H_2O
87	A40-S-noHF-37.5:H_2O
88	A40-S-noHF-32.5:H_2O
89	A40-S-32.5:H_2O-23h
90	A40-S-32.5:H_2O-71h
91	A40-S-32.5:H_2O-119h
92	A40-S-32.5:H_2O-167h

4.2.1 Reproduction of literature

As can be seen in Figure 4.8, initial attempts at reproducing a reported synthesis from Sierra et al.[41] resulted in a product dominated by the AFR phase, but that carried an unidentified phase impurity marked by a star in the diffractogram. This could only be reproduced once, the remaining two parallels did not yield any AFR phase.

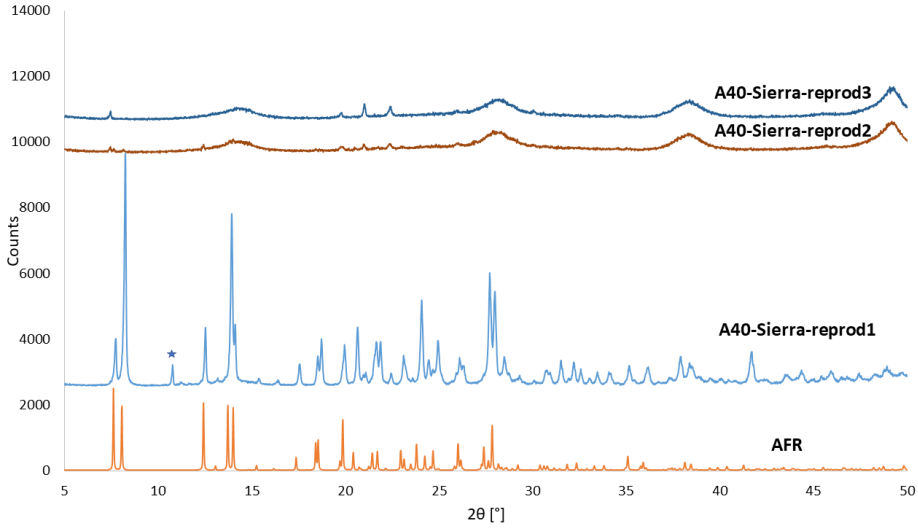

Figure 4.8: Diffractogram showcasing the attempted reproduction of the synthesis reported by Sierra, L. et al.[41] as well as a study of reproducibility. The syntheses reported corresponds to entries 31 to 33 in Table 4.3.

Calcining this sample in an effort to remove the impurity yielded the following:

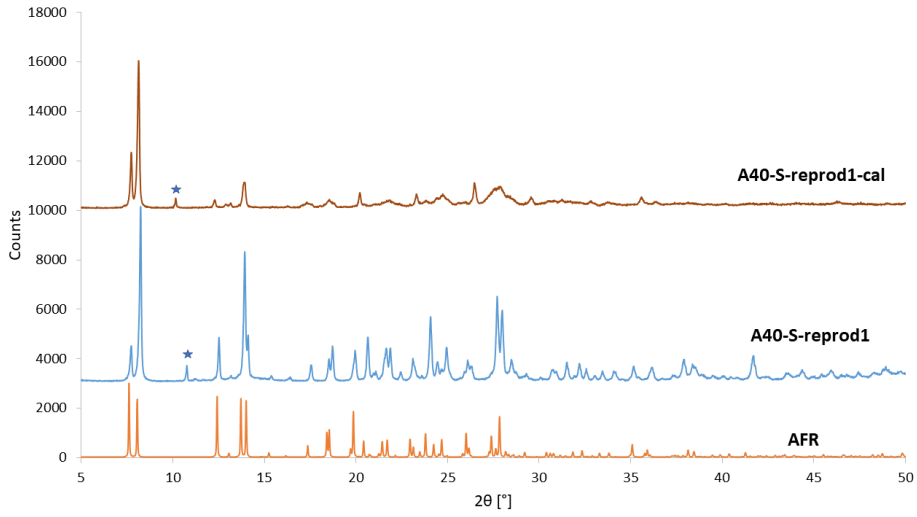

Figure 4.9: Diffractogram showcasing the calcination the partial successful synthesis of AlPO-40 as represented by the A40-S-reprod1-cal sample. The synthesis reported corresponds to entry 31 Table 4.3 and its calcined version.

Working further, another replication of literature was executed, this time using the synthesis of Lourenço, J. P. et al.,[14] testing both reported crystallization times.

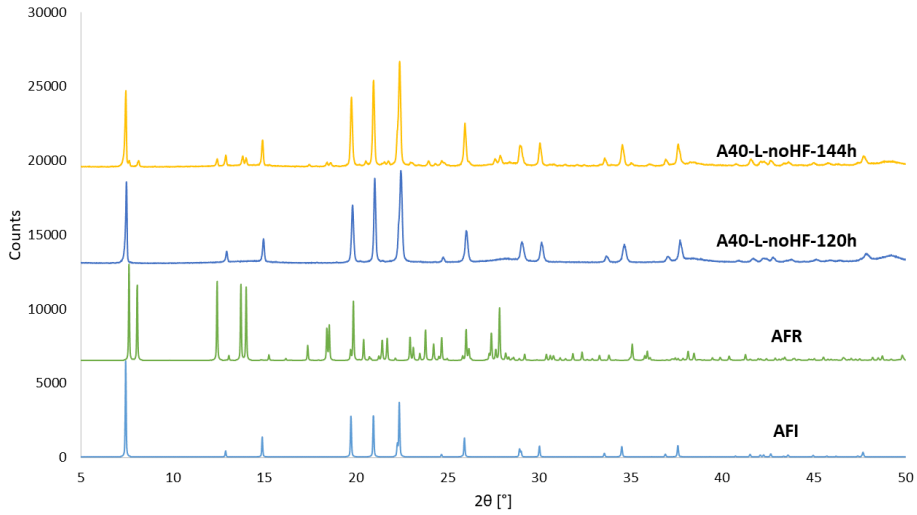

Figure 4.10: Diffractogram detailing the attempted reproduction of syntheses reported by Lourenço, J. P. et al.[14] The syntheses reported corresponds to entries 34 and 35 in Table 4.3.

Neither of the samples were able to produce any significant AFR phase, as can be seen in Figure 4.10. There was a small signal from an AFR phase in the sample subjected to a 144 hour crystallization period, but it was deemed too small to constitute a successful replication.

4.2.2 Chemical parameter experiments

Working with the Sierra based synthesis that resulted in a partially successful AlPO-40 production, several probe studies were performed, investigating the effect of changing various parameters. The first of these was an increase of the Br^-/OH^- ratio to both 0.52 and 0.67 respectively, in an effort to study the baseline effect of the ratio within the constraints specified in the original work.

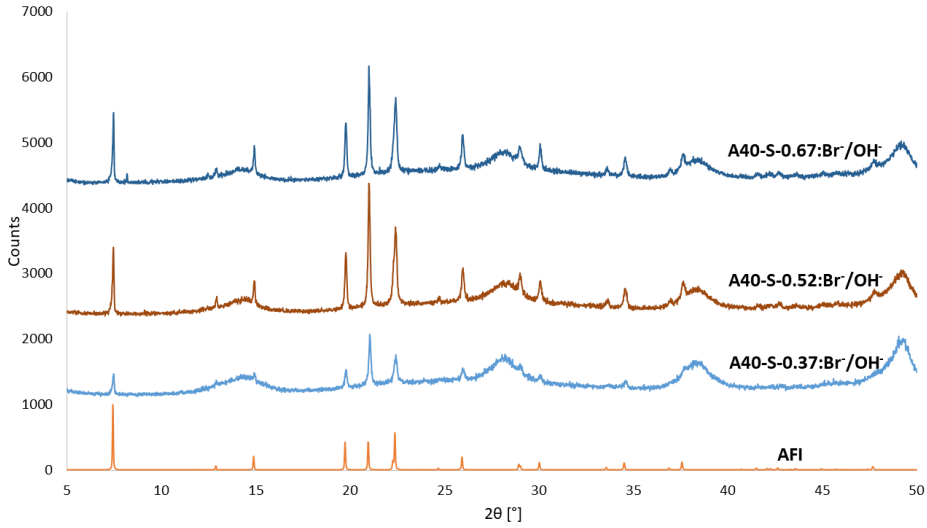

Figure 4.11: Diffractogram showcasing the effect of an increased Br^-/OH^- ratio. The syntheses reported corresponds to entries 36 to 38 in Table 4.3.

Increasing the Br^-/OH^- ratio only intensified the already present AFI phase, with a small possible AFR peak appearing in the sample with a Br^-/OH^- of 0.67. Sample A40-S-0.37:Br^-/OH^- (Entry 36 in Table 4.3) was used as a reference sample in diffractograms with probe studies, as it represented a base line synthesis.

In the Sierra method, the TMAOH content is at 0.045 molar equivalents to 0.97 molar equivalents of TPA^+. Increasing this number was reported to result in contamination of the AFR phase with other zeotype phases. Therefore, a probing testing was conducted by roughly halving the TMAOH content from 0.045 to 0.02 molar equivalents.

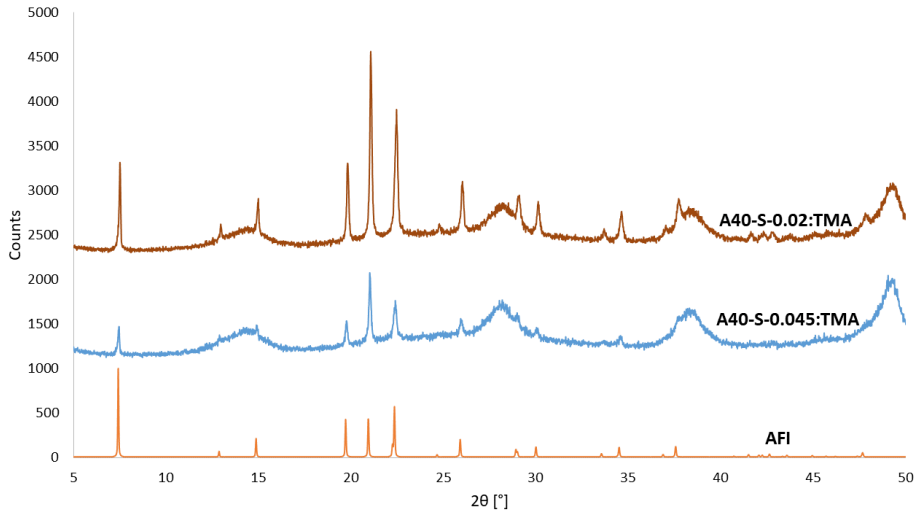

Figure 4.12: Diffractogram showcasing the effect of halving the TMAOH content in the gel in order to see if an AFR phase could be obtained. Entry 36 in Table 4.3 was used as a reference sample in the diffractogram. Here represented as A40-S-0.045:TMA. The syntheses reported corresponds to entries 36 (0.045 TMAOH) and 39 (0.02 TMAOH) in Table 4.3.

As can be seen in Figure 4.12, halving the TMAOH content only served to intensify the already present AFI phase, and did nothing to improve on the crystallization of an AFR phase in either of the samles. Sample A40-S-0.37:Br^-/OH^- (Entry 36) was used as a reference sample in the diffractogram.

The next experiment set that was performed, was a study of a varying total TPA^+ concentration without a change to the Br^-/OH^- ratio in order to alter the overall pH-value in the gel without disturbing the halide ion to hydroxide ion ratio. The diffractogram can be viewed in Appendix A.2 Figure A.4 At higher concentrations of TPA^+, crystallinity gradually decreases until no zeotypes visibly form. At lower concentrations, only the AFI phase forms.

4.2.3 Physical parameter experiments

Moving to physical parameters; ageing times, crystallization times and crystallization temperatures, were varied in order to see if any AFR phases could form.

First, the crystallization time was doubled from 23 to 47 hours, in order to see if either an AFR phase would directly form, or be converted from a formed AFI phase.

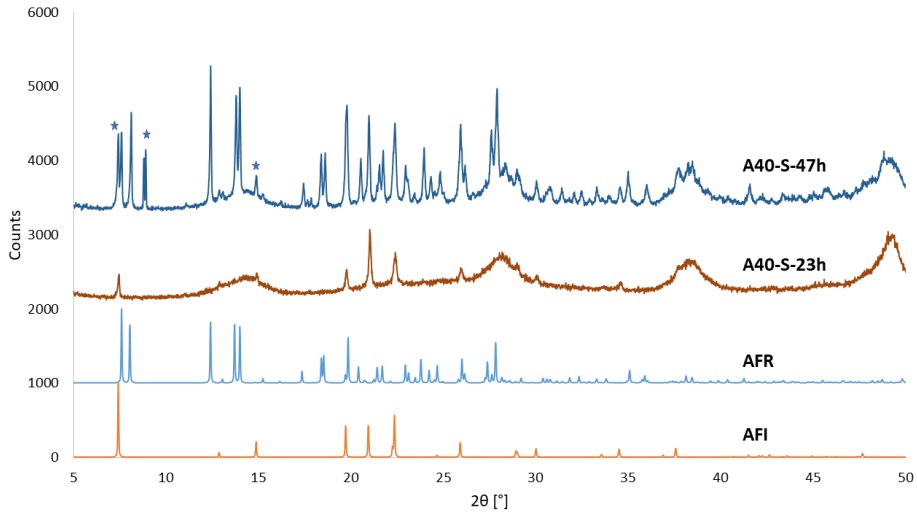

Figure 4.13: Diffractogram showing the effect of doubling the crystallization time. Entry 36 in Table4.3 was used as a reference sample in the diffractogram, here represented as A40-S-23h. The syntheses reported corresponds to entries 36 (23 hours) and 44 (47 hours) in Table 4.3.

Increasing the crystallization time produced a significant AFR signal, but with high contamination signals from both an AFI phase and an unidentified phase. Entry 36 in Table 4.3 was used as a reference sample in the diffractogram, here represented as A40-S-23h.

To study the combined effect of crystallization time and crystallization temperature, a 4-sample experiment was performed. The experiment only investigated increased parameters, as this was highlighted in the original paper to more easily produce phase pure samples of AlPO-40. The obtained diffractogram can be viewed in Appendix A.2 Figure A.5. Another synthesis with a 47 hour crystallization time at 150 °C, failed to reproduce the earlier obtained result that was shown in Figure 4.13. Furthermore, increasing either parameter did not yield any sign of an AFR phase, only yielding the common impurity phase instead. Combining the parameters did result in an increase in crystallinity, however.

With no distinctively positive results from increasing the crystallization time and temperature, the focus was shifted to the ageing process. First, an extension from 17 hours to 41 hours was performed.

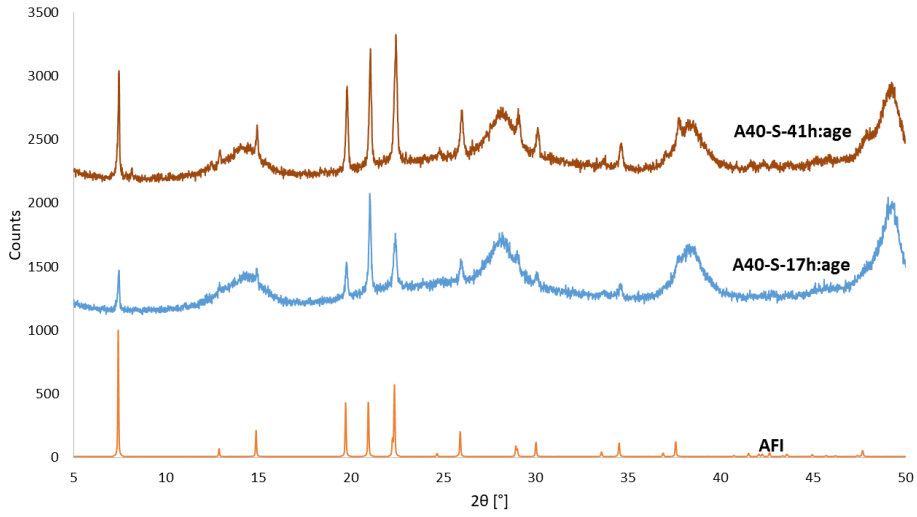

Figure 4.14: Diffractogram showing the effect of increasing the ageing time of the gel from 17 for 41 hours. Entry 36 was used as a reference sample in the diffractogram, here represented as A40-S-17h:age. The syntheses reported corresponds to entries 36 (17 hours) and 49 (41 hours) in Table 4.3.

No visible AFR phase was formed when the ageing time was extended. Entry 36 in Table 4.3 was used as a reference sample in the diffractogram, here represented as A40-S-17h:age.

Therefore, a synthesis set that reduced the overall ageing in the system was conducted. This included the mixing stages before the final combination into a gel, working under the assumption that only a homogeneous mixture was needed, and not a predetermined, specific mixing time.

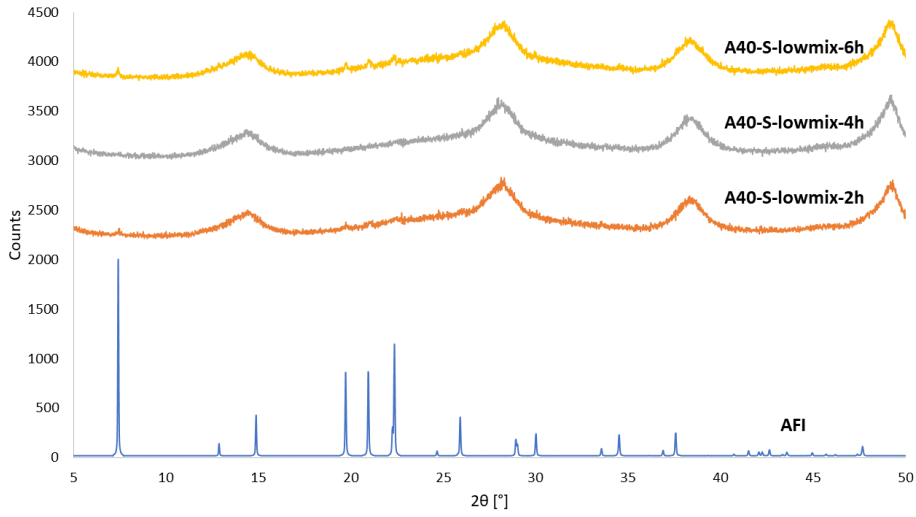

Figure 4.15: Diffractogram showcasing the effect of reducing the overall ageing time including the time used for mixing the reactants. The syntheses reported corresponds to entries 50 to 52 in Table 4.3.

Common for all tested mixing times, was a failure to crystallize any significant zeotype phase, with only a small AFI peak appearing in the sample subjected to a 6 hour ageing period.

To determine if the formation of zeotype phases was a question of time needed to crystallize, the crystallization time was extended in a five sample experiment to a maximum of 120 hours as this had proven to be effective in previous experiments. The obtained diffractogram can be vied in Appendix A.2 Figure A.6.

Similar to results reported earlier, increasing the crystallization time only served to increase the crystallinity of the AFI phase. As a final attempt on reducing the ageing time, only the ageing in the final gel was reduced, to see if the reactant mixing times were crucial.

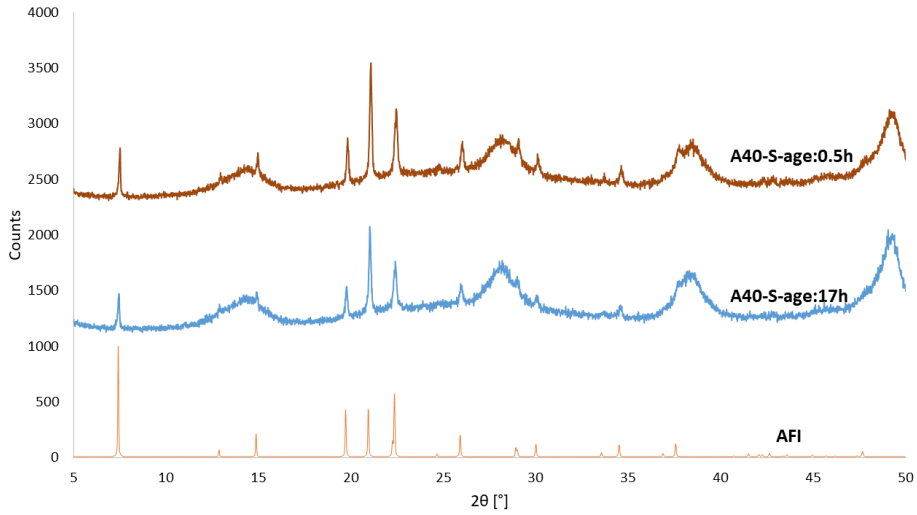

Figure 4.16: Diffractogram showing the effect of ageing the gel only until homogeneous (roughly corresponding to 30 minutes). Entry 36 in Table 4.3 was used as a reference, here represented as A40-S-age:17h. The syntheses reported corresponds to entries 36 (17 hours) and 58 (0.5 hours) in Table 4.3.

As can be seen in Figure 4.16, no significant AFR phase is obtained even when dropping the ageing time to a value where homogeneity in the gel has barely occurred.

4.2.4 Combined chemical and physical parameter experiment

After a correspondence with Lourenço, J. P., it was discovered that washing equipment with HNO_3 was not sufficient. Instead, HF had to be used in order to fully purge the liners used of any contaminating remnants of AFI that could seed the reaction. The first synthesis performed with systematically HF-washed liners was a new study on the sole effect of a raised crystallization temperature in the Sierra based synthesis.

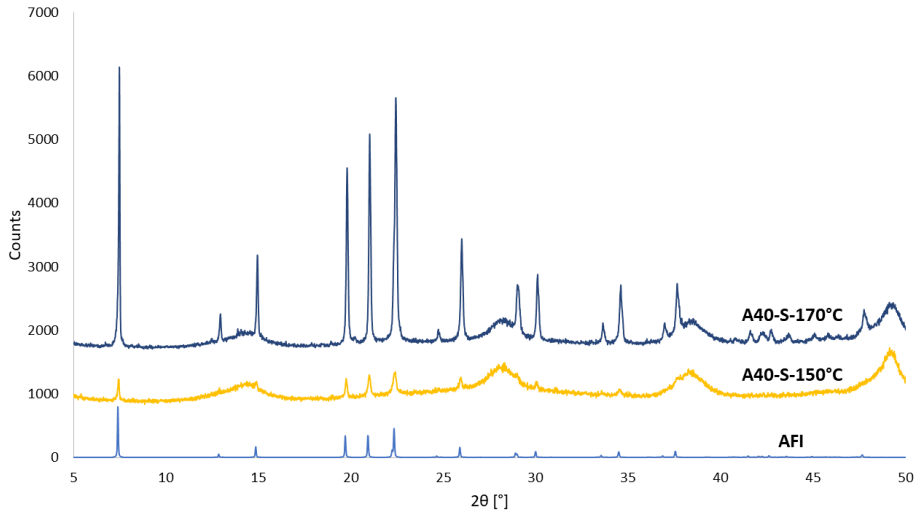

Figure 4.17: Diffractogram showing the effect of an increased crystallization temperature in the Sierra based synthesis, as well as reproducibility when washing the liners with HF. The syntheses reported correspond to entries 59 and 60 in Table 4.3.

When Figure 4.17 was compared to the diffractogram presented in Figure 4.8, it could be seen that despite liners being washed with HF and the syntheses being followed exactly as reported, the syntheses was still only partially successful in one case. Raising the crystallization temperature to 170 °C also did nothing to improve on this.

Another parameter that was highlighted by Lourenço, J. P. in regards to obtaining their results, was the production source of the TPAOH molecule. Up until this point a TPAOH solution sourced from Sigma Aldrich had been used. Noted by Lourenço, J. P. was that the Sigma Aldrich provided TPAOH was too impure, instead they opted to use a TPAOH solution sourced from Alfa Aesar. As such the effect of TPAOH source in the Lourenço based synthesis was tested, along with extended crystallization times. Both obtained diffractograms can be viewed in Appendix A.2 Figure A.7 and Figure A.8

From the two diffractograms shown above, there does not seem to be any significant benefit of choosing one template source over the other. There is a very small signal of an AFR phase in the A40-L-αTPA-120h sample, but this peak seems to disappear at higher crystallization times. Also, worth noting is that there seems to be little benefit in regards increasing crystallinity when the crystallization time is increased in the Lourenço based synthesis.

Seeing as the template source had little effect on phase distribution, only one source was used to study the effect of lowering the crystallization time in the Lourenço synthesis.

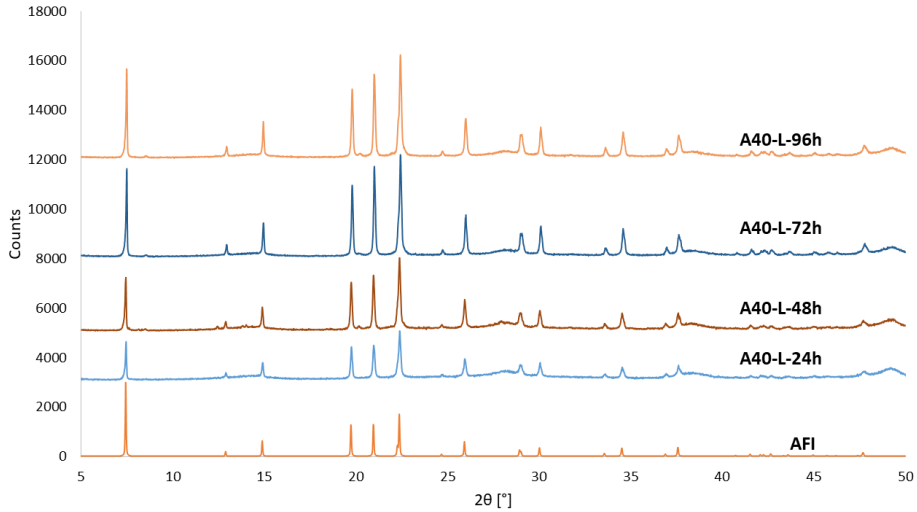

Figure 4.18: Diffractogram showing the effect of lowering the crystallization time in the Lourenço based synthesis. The TPAOH source was Alfa Aesar. Liners were washed with HF. The syntheses reported corresponds to entries 73 to 76 in Table 4.3.

Reducing the crystallization time in Lourenço also did little to promote any formation of an AFR phase, only serving to lessen the crystallinity in the system instead as the time was decreased.

Effects of the TAPOH source were investigated in the Sierra based synthesis as well, yielding the following diffractogram.

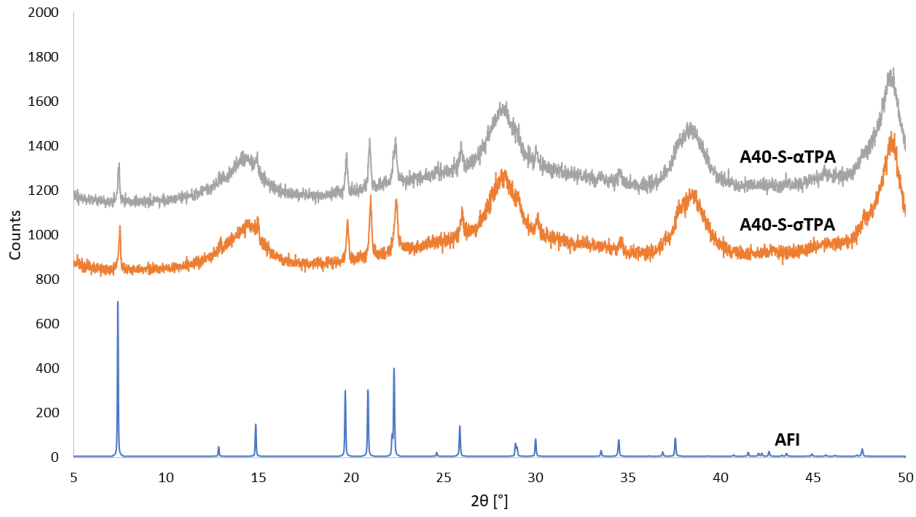

Figure 4.19: Diffractogram showing the effect of TPAOH sources in the Sierra based synthesis. The syntheses reported corresponds to entries to 48 in Table 4.3.

As can be seen in Figure 4.19, the TPAOH source used did not influence the synthesis, with both syntheses only yielding a weak AFI phase.

Due to consistently low crystallinity values, regardless of actual phase obtained, when working with the Sierra synthesis, a set of experiments were performed aiming to increase the crystallization time to higher values than previously tested.

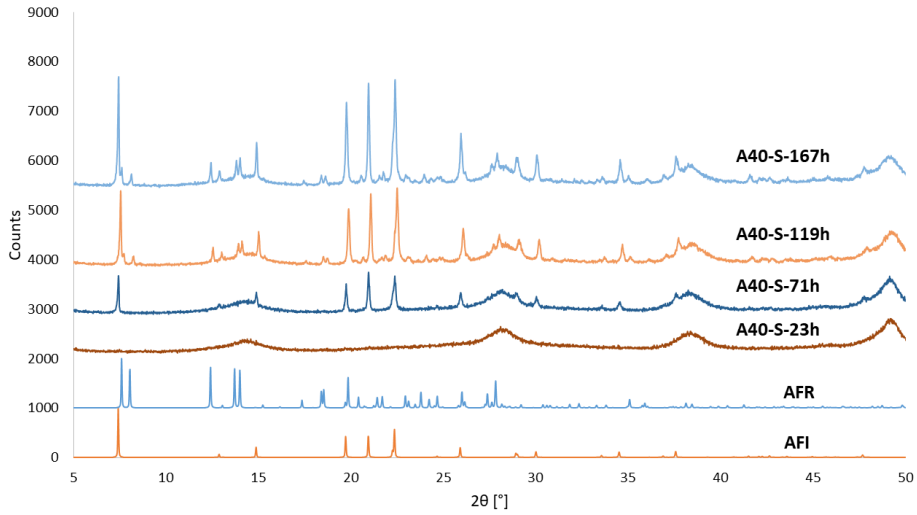

Figure 4.20: Diffractogram showcasing the effect of pushing the crystallization time in the Sierra based synthesis to more extreme lengths. The syntheses reported corresponds to entries 79 to 82 in Table 4.3.

At 119 hours and 167 hours, a distinctive AFR phase could be seen forming. While still dwarfed in comparison to AFI phase present, it still showed a small growth with increasing crystallization time indicating a synergistic relationship between AFR phase formation and greatly extended crystallization times.

The gels until this point had a watery consistency and a set of experiments investigating the influence of the total amount of water in the system were conducted. The data from the experiments are presented in the diffractogram below.

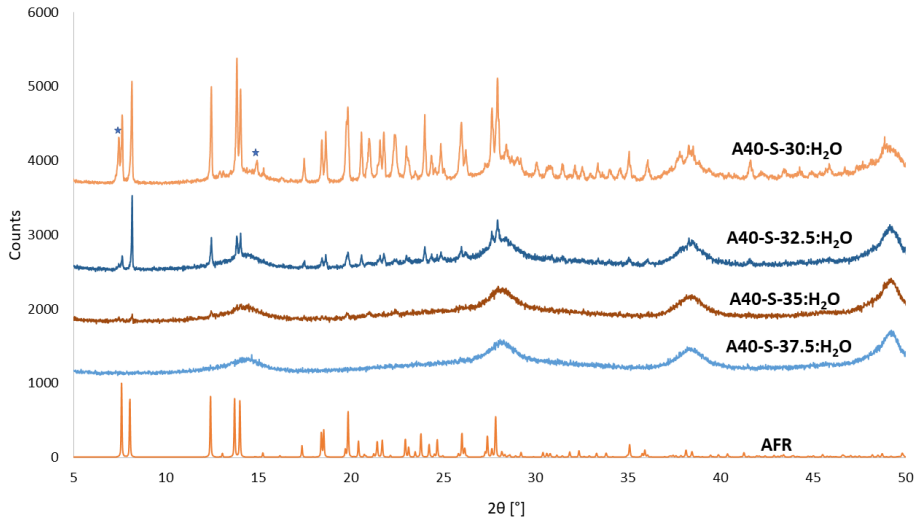

Figure 4.21: Diffractograms showcasing the effect of lowering the water content in the Sierra synthesis while keeping all other parameters the same and washing the liner with HF. The syntheses reported corresponds to entries 83 to 86 in Table 4.3.

At the literature reported water content of 37.5 molar equivalents,[41] no zeotype phases form. As the water content decreases, an AFR phase starts to form. This can be seen in Figure 4.21. At 35 molar equivalents, a very small AFR peak starts to appear, and this peak is increased in size as the water content is equal to 32.5 molar equivalents. At 30 molar equivalents, and AFI phase starts to form as well. All samples obtained had a low crystallinity as can be seen from the low count values and broad peaks.

To see if the HF wash was crucial to obtaining an AFR phase, samples A40-S-37.5:H_2O (Entry 83 in Table 4.3) and A40-S-32.5:H_2O (Entry 85 in Table 4.3) were repeated without the HF wash.

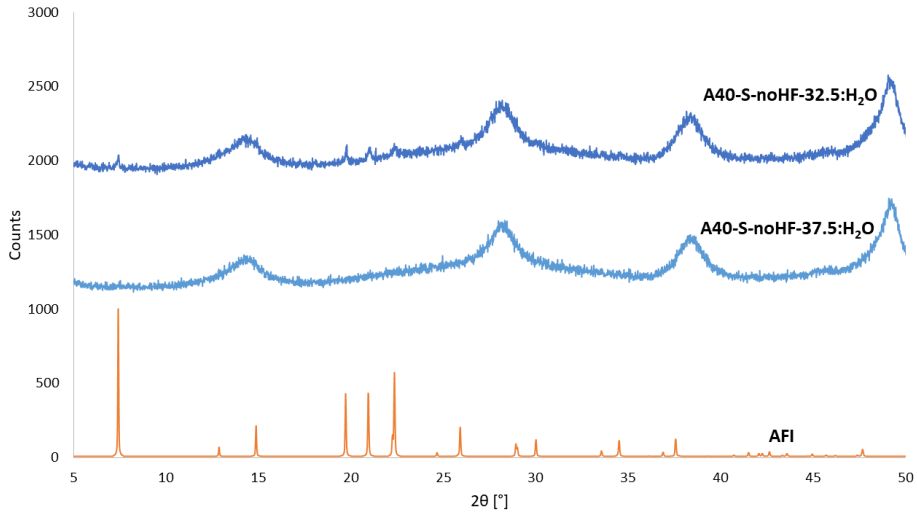

Figure 4.22: Diffractogram showing the effect of not washing the liners with HF when the water content is lowered. The syntheses reported corresponds to entries 87 to 88 in Table 4.3.

Figure 4.22 showed no sign of any AFR phase, even at a lower water content which had produced a clear AFR phase when the liner was washed with.

Finally, to see if any synergistic effects were present between the water content and the crystallization time, a combination study was conducted.

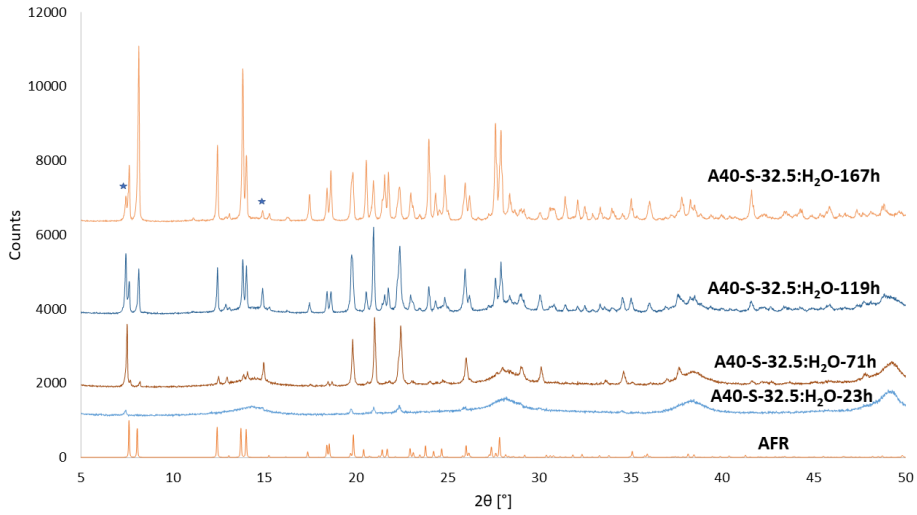

Figure 4.23: Diffractogram showcasing the effect of lowering the water content in the Sierra synthesis as well as extending the crystallization time. The syntheses reported corresponds to entries 89 to 92 in Table 4.3.

As illustrated by the diffractogram in Figure 4.23, there seemed to be a distinct AFR phase forming when subjecting the synthesis with 32.5 molar equivalents of water to longer crystallization times. The sample subjected a 167 hour (7 days) reaction period, while not phase pure, shows only a 13 % contamination of the AFI phase, which was deemed to be sufficiently low in regards to further investigation of the material. As a comparison, the sample which was subjected to a 119 hour (5 days) treatment, showed a significantly higher contamination grade of 57 %.

Sample A40-32.5:H_2O-167h (Entry 92 in Table 4.3) was calcined in order to see if the contamination could either be suppressed or transformed and the following diffractogram was obtained.

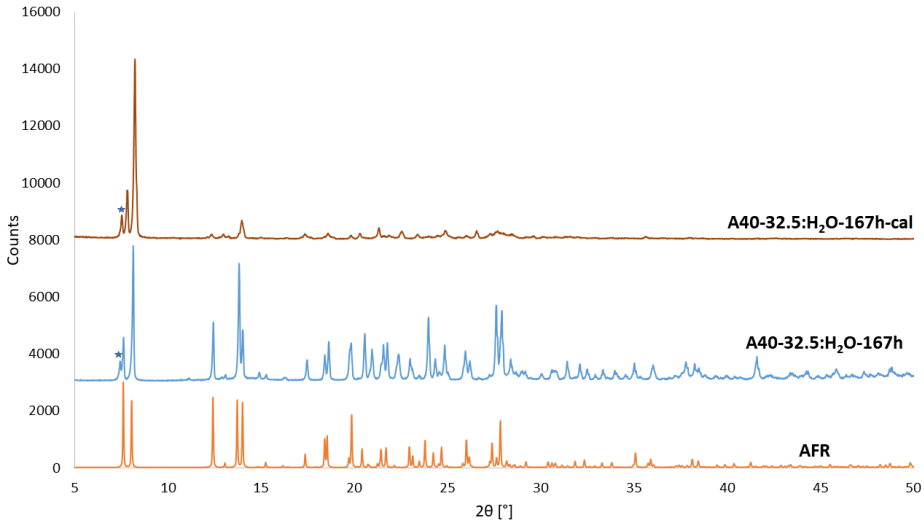

Figure 4.24: Diffractograms of the calcined and as prepared A40-32.5:H_2O-167h sample with a theoretical AFR diffractogram for reference.The synthesis reported corresponds to entry 92 in Table 4.3. and its calcined version.

The AFI-impurity did not disappear, but an increase in crystallinity was observed. The structure maintained the characteristic double peak of the AFR system, although shifted slightly.

Simultaneously, BET and BJH measurements were conducted on the calcined A40-32.5:H_2O-167h sample (Entry 92 in Table 4.3). The quantity adsorbed was plotted against the relative pressure to produce the following graph.

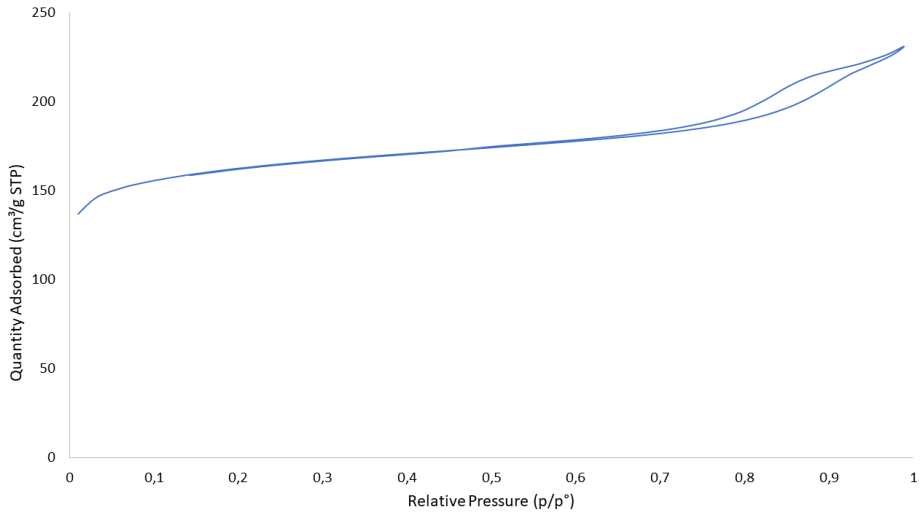

Figure 4.25: Adsorption-desorption isotherm for sample A40-32.5:H_2O-167h (Entry 92 in Table 4.3).

The curve is similar to a combination of a type 1 and a type 4 adsorption-desorption isotherm with what resembles a H4 hysteresis loop, something of which is characteristic for microporous materials.

A total surface area of roughly *528 m^2/g* was found the calcined entry 92 in Table4.3, of which 378 m^2/g was attributed to the micropore area and 150 m^2/g was attributed to the external surface area. This is a bit lower than the value reported by Lima, S. et al. who reported a total surface area of 670 m^2/g of which 60 m^2/g was attributed to the external surface area.[8]

A pore size distribution was also obtained by plotting the fraction of cumulative pore volume against the pore diameter. It can be seen from Figure 4.26 that a larger fraction of pores is located towards the average pore diameter of 10 Å.

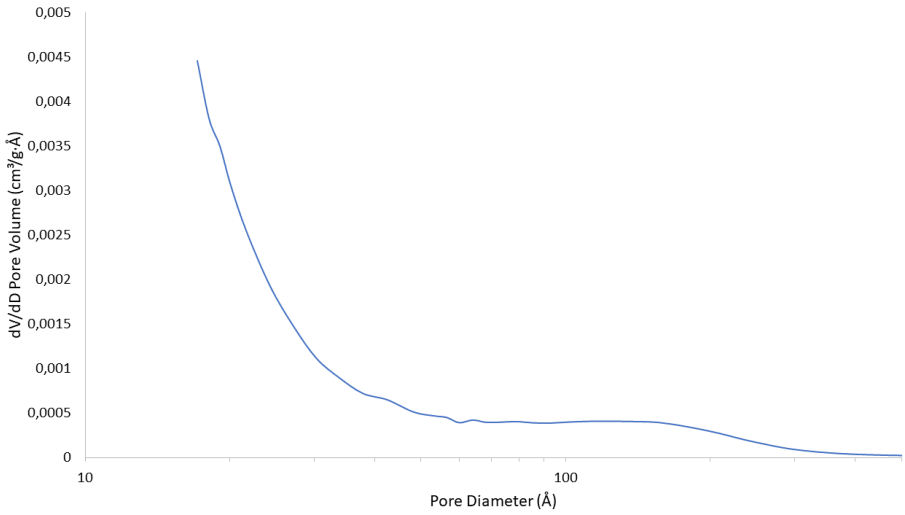

Figure 4.26: Poresize distribution of the A40-32.5:H_2O:167h-cal sample (Entry 92 in Table 4.3).

4.3 CuAlPO-40 results

A small set of copper containing AlPO-40 synthesis were also conducted. It is important to specify that these were conducted before the optimization of the plain AlPO-40 synthesis. Below is a summarizing table detailing all attempted CuAlPO-40 syntheses with important results included.

Table 4.5: Table showcasing all CuAlPO-40 syntheses with pH, colour and zeotypes phase results. Parameters being changed are bolded for easier visibility. A '*' next to the copper amount indicates that the copper source was copper acetate. The filling grade of the liners was always 45 %. In the pH column, B means for "Before", A means for "After".

Entry	Parameter varied	Al	P	H_2O	Cu	TMAOH	TPABr	TPAOH	Ageing [h]	HF wash	T [°C]	t_4 [h]	pH	Colour	Resulting zeotype(s)
93	Copper source and aluminium content	**1**	1	37.5	**0.05**	0.045	0.26	0.71	t_1 : 6 t_2 : 2 t_3 : 17	No	150	23	B: 6 A: 7	Blue	AFR + AFI
94	Copper source and aluminium content	**0.95**	1	37.5	**0.05**	0.045	0.26	0.71	t_1 : 6 t_2 : 2 t_3 : 17	No	150	23	B: 6 A: 7	Blue	AFR + AFI
95	Copper source and aluminium content	**1**	1	37.5	**0.05 ***	0.045	0.26	0.71	t_1 : 6 t_2 : 2 t_3 : 17	No	150	23	B: 5.5 A: 7	Blue	AFI
96	Copper source and aluminium content	**0.95**	1	37.5	**0.05 ***	0.045	0.26	0.71	t_1 : 6 t_2 : 2 t_3 : 17	No	150	23	B: 5.5 A: 7	Blue	AFI + AFR
97	Cryst. temp.	1	1	37.5	0.05	0.045	0.26	0.71	t_1 : 6 t_2 : 2 t_3 : 17	**Yes**	**150**	23	B: 6.5 A: 7	Blue	AFI

Table 4.5: Table showcasing all CuAlPO-40 syntheses with pH, colour and zeotypes phase results. Parameters being changed are bolded for easier visibility. A '*' next to the copper amount indicates that the copper source was copper acetate. The filling grade of the liners was always 45 %. In the pH column, B means for "Before", A means for "After".

Entry	Parameter varied	Al	P	H_2O	Cu	TMAOH	TPABr	TPAOH	Ageing [h]	HF wash	T [°C]	t_4 [h]	pH	Colour	Resulting zeotype(s)
98	Cryst. temp.	1	1	37.5	0.05	0.045	0.26	0.71	t_1 : 6 t_2 : 2 t_3 : 17	**Yes**	**170**	23	B: 6.5 A: 7	Blue	AFI

In order to get a better overview when comparing results, the synthesis entries where given longer, more descriptive names in order to highlight differences better. These are presented in the table below.

Table 4.6: Table detailing all entries of the CuAlPO-40 syntheses and their respective descriptive names.

Entry	Sample
93	CuA40-S-CuO-1:Al
94	CuA40-S-CuO-0.95:Al
95	CuA40-S-Cu(Ac)2O-1:Al
96	CuA40-S-Cu(Ac)2O-0.95:Al
97	CuA40-S-Hfwash-150 °C
98	CuA40-S-Hfwash-170 °C

The first set sought to investigate the effect of both the copper source and the copper to aluminium ratio. The obtained results are given in the diffractogram below. The alumina content specified in the sample name is the total amount of alumina in the synthesis.

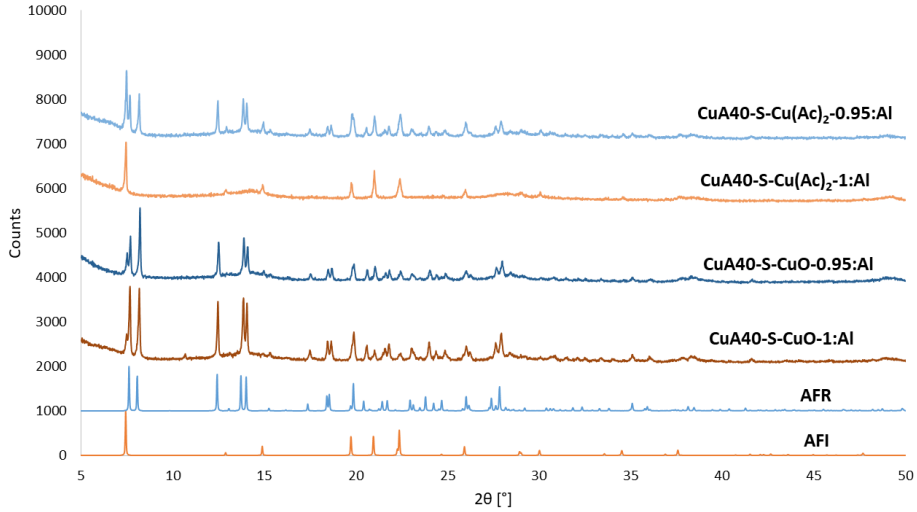

Figure 4.27: Diffractogram showcasing the effect both copper source and the total amount alumina in the system. The syntheses reported corresponds to entries 93 to 96 in Table 4.5.

No phase pure sample was obtained when using either copper oxide (CuO) or copper acetate $Cu(Ac)_2$. Decreasing the total amount of aluminium in the gel did not promote phase purity either. The samples using copper oxide as the copper source produced the largest fractions of the AFR phase, while the samples using copper acetate only produced an AFR phase when the aluminium content was lowered. All samples had a comparatively low crystallinity. All samples had a light blue colour, indication the presence of the hexaquacopper(II) complex.

Sample CuA40-S-CuO-1:Al (Entry 93 in Table 4.5) was calcined in order to see if the AFI impurity could be suppressed. The following diffractogram was obtained.

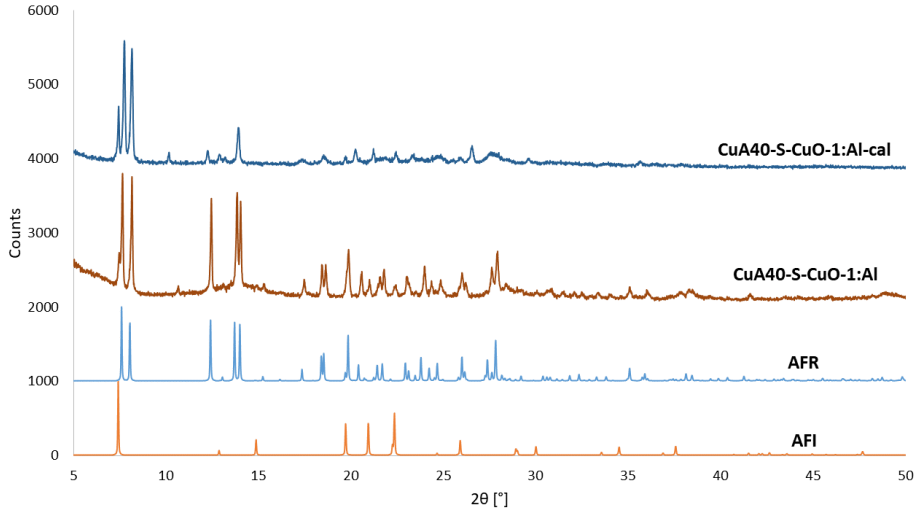

Figure 4.28: Diffractogram showcasing the effect of calcining sample CuA40-S-CuO-1:Al. The synthesis reported corresponds to entry 93 in Table 4.5 and its calcined version.

Calcining the sample did not yield any significant favouring of one phase over the other, nor did it improve the crystallinity in any discernible amount. Upon calcination, the sample turned from a light blue colour to a olive green colour, indicating tetrahedral geometry of the copper and successful incorporation.

After the discovery of the necessity of washing with HF, and the report from Sierra, L. et al[41] stating that increasing the temperature can facilitate framework incorporation of metals into AlPO-40, a small test of both parameters was run. The data obtained are given in the diffractogram below.

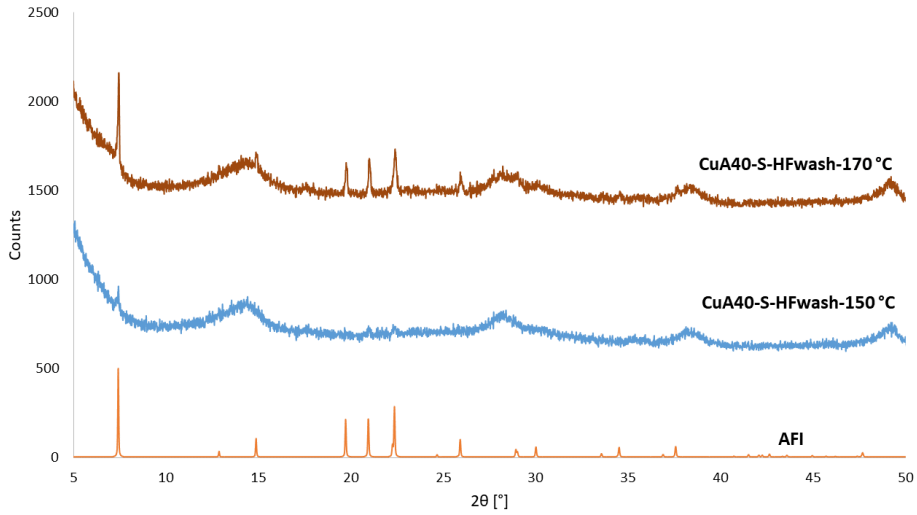

Figure 4.29: Diffractogram showcasing the effect of washing the liners with HF as well as increasing the crystallization temperature. The syntheses reported corresponds to entries 97 and 98 in Table 4.3.

No AFR phase was obtained when the liners were washed with HF, the crystallinity did increase when the temperature was increased.

Chapter 5

Discussion

The overall aim of this thesis was to investigate synthesis strategies for making SAPO-40, AlPO-40 and CuAlPO-40 and this was done with mixed results. The in-depth discussion of each material is handled in their respective sections. The syntheses of AlPO-40 were the most successful, and the most critical parameters for formation of AlPO-40 are detailed in Table 5.1 below.

Table 5.1: Table listing the most important parameters for producing AlPO-40.

Parameter	Change	Effect
Washing of liner	HF wash	Removes AFI traces
Water content	Decrease to 32.5	Promotes AFR
Cryst. time	Increase to 167h	Promotes AFR
Ageing time	Decrease	Impedes reaction
Cryst. temp	Increase	Increase crystallinity

SAPO-40 and CuAlPO-40 did not produce enough AFR containing results to obtain a full parameter map.

Most work on the AFR system in general, was performed by the research groups of Sierra, L. et al.,[38,41] Lourenço, J. P. et al.,[12,14] and Dumont, N. et al.[39] in the 1990's. This collection of work was the main source of synthesis conditions tested in the thesis and their findings were used as basis for many of the parameter and probing studies that were conducted.

As shown by multiple results presented in Figures 4.1, 4.2, 4.8 and 4.10; replication of published literature was difficult and did not yield the same reported

100 % reproducibility of a completely phase pure AFR phase. Instead, almost unequivocally, all reproduction syntheses yielded the AFI phase as either the only phase or the majority phase. There was one exception to this, sample A40-S-reprod1 presented a clear AFR phase with only a small contamination from an unknown zeotype. This success was at a later point attributed to the cleaning of the liner with HF, removing any possible AFI seeds in the liner. This seeding effect had been documented, not necessarily with the AFR system, but it was highlighted as a general problem in the work of Casci, J. et al.[24]

Several reasons may exist as to why the literature reported results could not be reproduced. Differences in physical laboratory conditions such as temperature and humidity, storage of chemicals, their individual sources and shelf life, and accumulation small human errors which add up to a greater errors. Another factor was small, unreported methods used in the original work such as washing procedures which could have impacted the final result.

5.1 SAPO-40

SAPO-40 was never synthesized with a clear AFR phase present. In sample S40-D-39.8:H_2O (entry 5 in Table 4.1), an AFR phase was present, but it was partially obscured by the broader and taller AFI peaks in the diffractogram. The role of water content in the synthesis was a documented case, where an increase in gel dilution was stated to increase the amount of AFR phase and the ease of its selective crystallization. This was suspected to be due to dilution increasing the pH of the gel into a more favourable domain. However, in the probe synthesis, an increase did not favour an AFR phase formation within the range tested, this might have been due to the pH already being too high and with further dilution it was pushed out of the domain of SAPO-40 formation.

Addition of TMAOH to the gel was also stated to favourable when forming an AFR phase. When only 0.01 molar equivalents of TMAOH was added while maintaining a constant OH^-, a combination of an AFI phase and a FAU phase formed. TMAOH, while able to suppress the AFI phase, also readily templates the FAU phase, rendering even the smallest addition of TMAOH to the standard Dumont synthesis unsuitable for synthesizing a pure AFR phase.

It was suggested by Dumont, N. et al. that the AFR phase was the thermodynamic phase in the reaction, meaning it should have been favoured at longer crystallization times combined with lower crystallization temperatures. Several synthesis sets were performed in order to study the full effects of internal pressure, crystallization time and crystallization temperature. No synthesis was successful in producing a detectable AFR phase, with no zeotype phases forming below 200 °C. In the case of the test of a synthesis adapted from Lourenço, J. P. subjected to the crystallization time and temperature tests, a definite AFI phase forms even

at temperatures below 200 °C. The lack of any visible AFR signal indicates that there was some unknown, critical parameter which had not been accounted for and resulted in an erroneous phase formation despite efforts to promote the AFR phase.

Finally for the SAPO-40 synthesis, the effect of changing the silicon source and method of mixing did not seem to promote the synthesis of an AFR phase. Using a one-pot mixing scheme seemed to lower the overall obtained crystallinity; most likely caused by grade of availability of reactants, their momomerization grade and thereby ability to react properly. The one-pot scheme might have a lesser grade of homogeneity due to all reactants being mixed in the same vessel instead of separately and at the relevant gel composition this might have been sub-optimal.

5.2 AlPO-40

The first AlPO-40 reproduction of the synthesis from Sierra, L. et al.[41] was partially successful in obtaining an AFR phase. There was a small unidentified zeotype peak that did not disappear upon calcination, indicating either heavy interconnected growth or irreversible phase formation. The reproduction of the synthesis from Lourenço, J. P. et al.[14] was not as successful, only yielding a small AFR peak when the crystallization time was increased from 120 hours to 144 hours. This might indicate that in the case of the Lourenço synthesis, an even longer crystallization time was favoured due to the supposed thermodynamic stability of the AFR phase when compared with the AFI phase.

To see if an AFR phase could form without the harsh conditions of an HF-based washing procedure, several experiments were set up. Initial probing and parameter testing of chemical factors such as total TPA^+ content, the Br^-/OH^- ratio, and TMAOH content did not yield any significant results. Whether this was due to the lack of HF washing masking the overall potential beneficial effect, or the adjustments not being extreme enough is difficult to say exact. Theoretically, a change in pH should alter the dissolution of reactive species and thereby alter the kinetics and favour one phase over the other. Without knowing the exact kinetics of the reaction under these specific circumstances due to the black.box nature of the reaction, establishment of the accepted well domain in regards to pH for successful AFR formation is impossible. The TMAOH content was only tested as a lower value due to the high risk of creating a FAU phase when increasing it as was evidenced by the aforementioned SAPO-40 samples. An increase of the crystallinity of the AFI phase was observed when the TMAOH content was lowered, indicating a possible suppression effect.

Moving to physical parameters, ageing, crystallization time and crystallization temperatures were all varied. Increasing the crystallization time from 23 to 47

hours did produce an AFR phase in lieu of an HF wash, but it is was heavily contaminated with several other zeotype phases. This suggests that the AFR phase is indeed the thermodynamic phase in the system and could possibly be partially promoted with an increase in crystallization time. A repeat of the same increase in crystallization temperature did not yield the same result, as can be seen when comparing entries 14 and 16 in Table 4.3. Furthermore, no AFR was obtained when the crystallization temperature was increased, but no conclusive evidence for what favours the formation of the AFR phase could be obtained.

Increasing the ageing time did produce a very small AFR peak, almost indistinguishable from the overall noise in the diffractogram in Figure 4.14. An increase in the ageing time also seems to give more favourable kinetics, possibly due to increased dissolution of materials or increased levels of homogeneity even at a micro scale.

In turn, a general lowering of the ageing times of both the two reactant solutions as well as the gel, seems to hinder any crystallization of a zeotype phase. Easily explained by insufficient homogenization, less dissolution of reactants and less initial nucleation due to too short of times being utilized. Still, a low ageing sample batch was exposed to longer crystallization times as had been previously seen to be beneficial. Indeed did an AFI phase start to form with time, but no AFR phase was present in the samples. Short ageing times thus seem to favour a kinetic product with any small nuclei formed primarily being AFI nuclei which growth and dominate at longer crystallization times. A final test, with only a reduction in the actual gel ageing, no discernible AFR could be observed, confirming that the AFR phase is more favoured at higher ageing times, at least when the liners are not washed with HF.

Correspondence with Lourenço, J. P. confirmed the suspicion of the need for an HF-based wash of the liners in order to sufficiently remove any trace of AFI nuclei present in small grooves in the liner. Thus, a test to see if an AFR phase could be easily reproduced when equipment was washed properly was conducted. No trace was observed at either crystallization temperature, as can bee seen in Figure 4.17. From this it can be seen that even with perfect conditions, the reported synthesis is not 100 % reproducible.

Another point of discussion was the source of the TPAOH solution used in the synthesis. Both claimed by Dumont, N. et al.[39] and Lourenço, J. P. et al., the source of the template used, matters. At the time of writing their reports on the synthesis, the TPAOH sourced from Sigma Aldrich had about ten times as much alkali metal cation contaminants as the template sourced from Alfa Aesar. Until this point in the thesis, the Sigma Aldrich template had been used due to economical reasons. As such, tests looking into the influence of the TPAOH source in the Lourenço synthesis were conducted. These tests were combined with crystallization time tests, as the increase in time had been seen to be beneficial.

No effect could be observed when the templates were investigated. The original reports were at this point over 20 years old and the contamination grade of the samples could have changed throughout the years. Additionally, an increase in the crystallization time in the Lourenço synthesis did not yield any increase in the AFR phase that could be seen forming in Figure 4.10. For the sake of completion, the template source effect was investigated in the Sierra synthesis as well, with no effect. Without an in-house report on the elemental composition of the different templates, it is difficult to say if they are different at this point in time.

Moving on, the crystallization time was also investigated in the Sierra synthesis when the liners where washed with HF. Now, the crystallization time was pushed longer than before to see effect at more extreme lengths. Initially, no phase forms; but as the time increases, so does the AFR peak. And at 167 hours of crystallization time, it can be clearly identified.

Due to crystallization times prolonged beyond 7 days (168 hours) being impractical, other methods to increase the AFR phase were investigated. The gels up until this point where generally not very viscous and at times they resembled liquids more that gels. As such, a further dilution was deemed unnecessary and the water content was lowered instead. A lower water content should in theory lower the pH in the initial alumina mixture and possibly facilitate better dissolution of the pseudoboehemite. Regardless of theoretical predictions, a clear AFR phase was obtained when the water content was lower sufficiently. With an almost pure AFR phase being obtained with a molar equivalent water content of 32.5. Lowering this produced an AFI minority phase, indicating the existence of a well domain for water as well.

Attempting to synthesize the same AFR phase with a lower content and no HF wash did not yield the same result, cementing the need for an HF wash.

Finally, the two positive results of increasing the crystallization time and decreasing the water content were combined in a final synthesis scheme. Here that dual effect was clearly seen, with a highly crystalline AFR sample with only a small AFI contaminant was obtained. The water content and crystallization time were therefore identified as the critical parameters for the formation of the AFR phase in the Sierra based synthesis with HF washed liners.

Sample A40-S-32.5:H_2O-167h was also calcined to see if the impurity could be removed. This did not succeed as the impurity was probably too inter-grown in the majority matrix to be sufficiently suppressed. Moreover, BET and BJH analysis were performed on the calcined sample in order to study the physical properties and investigate if it was comparable to other materials. With a relatively high surface area of 528 m^2/g of 378 m^2/g could be attributed to micropore area, the sample readily compared to other reported AlPO-40 materials. A distinctive hysteresis loop was present in the isotherm and the shape correlated well with data observed in general for microporous materials. When combined with

the very broad area in the pore size distribution at pore diameters approaching 10 Å could possibly indicate the presence of interconnected large and medium pore channels, but this would need to be examined further.

To conclude, a phase pure sample of AlPO-40 was not obtained. However, a sample which had a comparatively low contamination grade of only 13 % was obtained when the water content was decreased in tandem with an increase in crystallization temperature.

5.3 CuAlPO-40

It appears that synthesizing a copper containing AFR phase is possible. And while the crystallinity is low, the phase seems to readily form at 150 °C. Based on the few results available, copper oxide seems to be better suited as the copper source when attempting to make framework incorporated copper AlPO-40. This could be due to the buffering effect of the acetate ion lowering the pH of the gel, something which can be seen in the pH levels, as the obtained pre-reaction pH for the acetate-containing gels was slightly lower.

The copper to aluminium ratio, at least within the range tested for, seems less important. While it seemed to give rise to an AFR phase when the aluminium content was lowered, it Further studies would be needed in order to gain any conclusive evidence into the optimal ratio.

When the synthesis was repeated with HF washed liners, only an AFI phase was obtained. There was not positive effect of raising the crystallization temperature except a small increase in crystallinity. This might suggest that the HF wash is not strictly necessary under these circumstances and that the synthesis is not 100 % reproducible. The aforementioned benefit, stated by Sierra, L. et al of increasing the crystallization temperature to facilitate obtaining phase pure AFR phases with framework incorporated metals, did not seem to have an effect for copper. This was partially predicted due to copper favouring different geometries than zinc and cobalt, and therefore might be favourable under different thermodynamic conditions.

There seems to be a good indication that CuAlPO-40 is possible to obtain phase pure, and that the parameters just have to be tweaked in order to sufficiently suppress the AFI phase formation.

Chapter 6

Conclusion and Future work

6.1 Conclusion

Neither SAPO-40 nor AlPO-40 could be reliably reproduced from literature. In the case of SAPO-40, none of the investigated parameters were found to be promoting of the AFR phase as no AFR phase was obtained in almost all samples. Synthesis conditions never yielded any crystalline phases below 200 °C.

An AlPO-40 phase was obtained, but with a 13% contamination grade of AlPO-5, and only the Sierra sourced synthesis produced any significant AFR phase in the samples. A parameter study was conducted in order to determine the critical parameters for the successful formation of the AFR phase in AlPO-40 samples. These are listed below in order of importance.

- Washing liners with HF to remove AFI traces and prevent seeding effects.
- Decreasing the water to aluminium ratio from 37.5 to 32.5 to reduce the pH. Identified as a well domain, further decrease was not beneficial.
- Crystallization time increase from 23 hours to 167 hours in order to improve crystallinity and favour the thermodynamic phase.

The sample with the lowest amount of contamination at only 13 % was calcined and analysed in order to investigate the surface area. A micropore area of about 380 m^2/g was found, a value comparable to other zeotypes such as AlPO-5, but lower than reported values for the AFR system.

Only a few CuAlPO-40 syntheses were conducted, but the results were promising. The sample using copper oxide as a copper source and with a 0.05 copper to aluminium ratio, produced a blue powder where the AFR phase was the majority phase.

6.2 Future work

There are many things still left undone that could be worth investigating. The most important, is a further study of thermodynamics of the water-reduced AlPO-40 samples. The crystallization time should be extended further beyond the now 168 hours (7 days). This should ideally be coupled with a decrease in crystallization temperature, to get a better understanding on when the AFR phase readily forms. Furthermore, the extended crystallization time with the reduced water content experiment should be repeated without the HF-wash, to see if time can have an effect. Other, smaller experiments include increasing the ageing time at lower water content to see if the thermodynamics of the system, in regards to early nucleation of the AFR phase in the gel, is affected in this step.

Once a phase pure AlPO-40 synthesis has been established; the findings from the plain AlPO-40 experiments should be translated to the CuAlPO-40 synthesis in order to map the systems response. It could also be interesting to do an in-depth, pH evolution study across an entire experiment. With regular and accurate measurements of the pH in the system as the reaction progresses in order to the change across time. This should ideally be done at both 32.5 and 37.5 molar equivalents of water.

The findings from the AlPO-40 synthesis should be adopted to the SAPO-40 synthesis as well, especially the HF washing. This should be done for both the Dumont synthesis and Sierra synthesis of SAPO-40. Effects of water content can also be interesting to investigate, this should be done in extreme variations in both directions.

Finally, analyses of reactants could be interesting to study innate water content as well as potential template decomposition during gel ageing.

Bibliography

(1) Krautkraemer, J. A. et al. *Journal of Economic literature* **1998**, *36*, 2065–2107.

(2) Change, I. C. et al. *Contribution of Working Group III to the Fifth Assessment Report of the Intergovernmental Panel on Climate Change* **2014**, *1454*.

(3) Fogler, S. H., *Essentials of chemical reaction engineering*; Prentice Hall: 2011; Vol. 4.

(4) Yang, W.; Parr, R. G. *Proceedings of the National Academy of Sciences* **1985**, *82*, 6723–6726.

(5) Gordon, R. B.; Bertram, M.; Graedel, T. E. *Proceedings of the National Academy of Sciences* **2006**, *103*, 1209–1214.

(6) Hartmann, M.; Kevan, L. *Chemical reviews* **1999**, *99*, 635–664.

(7) Baerlocher, C.; McCusker, L. B. Database of Zeolite Structures., `http://www.iza-structure.org/databases/` (accessed 10/21/2018).

(8) Lima, S.; Fernandes, A.; Antunes, M. M.; Pillinger, M.; Ribeiro, F.; Valente, A. A. *Catalysis letters* **2010**, *135*, 41–47.

(9) Periana, R. A.; Taube, D. J.; Gamble, S.; Taube, H.; Satoh, T.; Fujii, H. *Science* **1998**, *280*, 560–564.

(10) Wulfers, M. J.; Teketel, S.; Ipek, B.; Lobo, R. F. *Chemical Communications* **2015**, *51*, 4447–4450.

(11) Zhu, Z.; Hartmann, M.; Kevan, L. *Chemistry of materials* **2000**, *12*, 2781–2787.

(12) Lourenco, J.; Ribeiro, M.; Borges, C.; Rocha, J.; Onida, B.; Garrone, E.; Gabelica, Z. *Microporous and mesoporous materials* **2000**, *38*, 267–278.

(13) Lourenço, J.; Fernandes, A.; Bértolo, R.; Ribeiro, M. *RSC Advances* **2015**, *5*, 10667–10674.

(14) Lourenco, J.; Ribeiro, M.; Ribeiro, F. R.; Rocha, J.; Onida, B.; Garrone, E.; Gabelica, Z. *Zeolites* **1997**, *18*, 398–407.

(15) Corma, A.; Díaz-Cabañas, M. J.; Jordá, J. L.; Martinez, C.; Moliner, M. *Nature* **2006**, *443*, 842.

(16) Sing, K. S. *Pure and applied chemistry* **1985**, *57*, 603–619.

(17) Wilson, S. T.; Lok, B. M.; Messina, C. A.; Cannan, T. R.; Flanigen, E. M. *Journal of the American Chemical Society* **1982**, *104*, 1146–1147.

(18) Olsbye, U.; Svelle, S.; Lillerud, K.; Wei, Z.; Chen, Y.; Li, J.; Wang, J.; Fan, W. *Chemical Society Reviews* **2015**, *44*, 7155–7176.

(19) Wilson, S. T. In *Studies in Surface Science and Catalysis*; Elsevier: 2001; Vol. 137, pp 229–260.

(20) Sastre, G.; Lewis, D. W.; Catlow, C. R. A. *The Journal of Physical Chemistry* **1996**, *100*, 6722–6730.

(21) Sastre, G.; Lewis, D.; Catlow, C. *Journal of Molecular Catalysis A: Chemical* **1997**, *119*, 349–356.

(22) Ward, J. W. *Journal of Catalysis* **1968**, *11*, 259–260.

(23) Lourenço, J.; Ribeiro, M.; Ribeiro, F. R.; Rocha, J.; Gabelica, Z. *Applied Catalysis A: General* **1996**, *148*, 167–180.

(24) Casci, J. L. *Microporous and mesoporous materials* **2005**, *82*, 217–226.

(25) Lok, B. M.; Messina, C. A.; Patton, R. L.; Gajek, R. T.; Cannan, T. R.; Flanigen, E. M. Crystalline silicoaluminophosphates., US Patent 4,440,871, 1984.

(26) Jansen, J. *ChemInform* **2002**, *33*, 242–242.

(27) Mortlock, R.; Bell, A.; Radke, C. *The Journal of Physical Chemistry* **1993**, *97*, 775–782.

(28) Mortlock, R.; Bell, A.; Radke, C. *The Journal of Physical Chemistry* **1993**, *97*, 767–774.

(29) Prasad, S.; Liu, S.-B. *Chemistry of materials* **1994**, *6*, 633–635.

(30) Elanany, M.; Larin, A. V.; Su, B.-L.; Vercauteren, D. P. In *Studies in surface science and catalysis*; Elsevier: 2006; Vol. 162, pp 339–346.

(31) Solomons, G.; Fryhle, C.; Snyder, S., *Organic Chemistry International Student Version*; Wiley: 2014; Vol. 11.

(32) Lok, B.; Cannan, T.; Messina, C. *Zeolites* **1983**, *3*, 282–291.

(33) Mathisen, K.; Nicholson, D. G.; Fitch, A. N.; Stockenhuber, M. *Journal of Materials Chemistry* **2005**, *15*, 204–217.

(34) Wilson, S.; Barger, P. *Microporous and Mesoporous Materials* **1999**, *29*, 117–126.

(35) Kleitz, F.; Schmidt, W.; Schüth, F. *Microporous and Mesoporous Materials* **2003**, *65*, 1–29.

(36) Weller, M.; Overton, T.; Rourke, J.; Armstrong, F., *Inorganic Chemistry*; Oxford University Press: 2014; Vol. 6.

(37) Hu, Y.; Navrotsky, A.; Chen, C.-Y.; Davis, M. E. *Chemistry of materials* **1995**, *7*, 1816–1823.

(38) Sierra, L.; Patarin, J.; Deroche, C.; Gies, H.; Guth, J. In *Studies in Surface Science and Catalysis*; Elsevier: 1994; Vol. 84, pp 2237–2244.

(39) Dumont, N.; Gabelica, Z.; Derouane, E. G.; Di Renzo, F. *Microporous Materials* **1994**, *3*, 71–84.

(40) Lourenço, J.; Ribeiro, M.; Ribeiro, F.; Rocha, J.; Gabelica, Z.; Derouane, E. *Microporous Materials* **1995**, *4*, 445–453.

(41) Sierra, L.; Patarin, J.; Guth, J. *Microporous materials* **1997**, *11*, 19–35.

(42) Weyda, H.; Lechert, H. *Zeolites* **1990**, *10*, 251–258.

(43) Ojo, A. F.; Dwyer, J.; Dewing, J.; Karim, K. *Journal of the Chemical Society, Faraday Transactions* **1991**, *87*, 2679–2684.

(44) Höchtl, M.; Jentys, A.; Vinek, H. *Microporous and mesoporous materials* **1999**, *31*, 271–285.

(45) Naeem, A.; Mustafa, S.; Rehana, N.; Dilara, B.; Murtaza, S. *Journal of colloid and interface science* **2002**, *252*, 6–14.

(46) Corà, F.; Alfredsson, M.; Barker, C. M.; Bell, R. G.; Foster, M. D.; Saadoune, I.; Simperler, A.; Catlow, C. R. A. *Journal of Solid State Chemistry* **2003**, *176*, 496–529.

(47) Nicholson, D. G.; Nilsen, M. H. *Journal of Materials Chemistry* **2000**, *10*, 1965–1971.

(48) Gao, F.; Walter, E. D.; Washton, N. M.; Szanyi, J.; Peden, C. H. *Applied Catalysis B: Environmental* **2015**, *162*, 501–514.

(49) Lee, C. W.; Chen, X.; Kevan, L. *Catalysis letters* **1992**, *15*, 75–81.

(50) Djieugoue, M.-A.; Prakash, A.; Kevan, L. *The Journal of Physical Chemistry B* **1999**, *103*, 804–811.

(51) Pastore, H.; Coluccia, S.; Marchese, L. *Annu. Rev. Mater. Res.* **2005**, *35*, 351–395.

(52) Muñoz, T.; Prakash, A.; Kevan, L.; Balkus, K. J. *The Journal of Physical Chemistry B* **1998**, *102*, 1379–1386.

(53) Mathisen, K.; Nicholson, D. G.; Stockenhuber, M. *Microporous and mesoporous materials* **2005**, *84*, 261–274.

(54) Trouillet, L.; Toupance, T.; Villain, F.; Louis, C. *Physical Chemistry Chemical Physics* **2000**, *2*, 2005–2014.

(55) Moen, A.; Nicholson, D. G. *Journal of the Chemical Society, Faraday Transactions* **1995**, *91*, 3529–3535.

(56) Martínez-Franco, R.; Moliner, M.; Franch, C.; Kustov, A.; Corma, A. *Applied Catalysis B: Environmental* **2012**, *127*, 273–280.

(57) Lee, C. W.; Brouet, G.; Chen, X.; Kevan, L. *Zeolites* **1993**, *13*, 565–571.

(58) Callister Jr., W. D.; Rethwisch, D. G., *Materials Science and Engineering*; John Wiley and Sons Pte. Ltd.: 2015; Vol. 9.

(59) Butt, H. J.; Graf, K.; Kappl, M., *Physics and Chemistry of Interfaces*; Wiley-VHC: 2016; Vol. 3.

(60) Brunauer, S.; Emmett, P. H.; Teller, E. *Journal of the American chemical society* **1938**, *60*, 309–319.

(61) Barrett, E. P.; Joyner, L. G.; Halenda, P. P. *Journal of the American Chemical society* **1951**, *73*, 373–380.

Appendix A

Extra data

A.1 SAPO-40 diffractograms

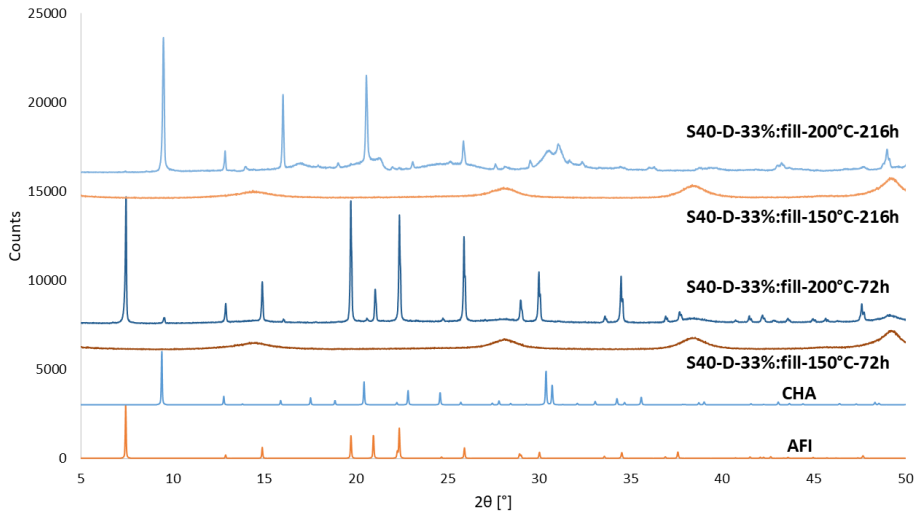

Figure A.1: Diffractogram showcasing the effect of a 33 % fill grade combined with variations in crystallization temperature and time. The syntheses reported corresponds to entries 16 to 19 in Table 4.1.

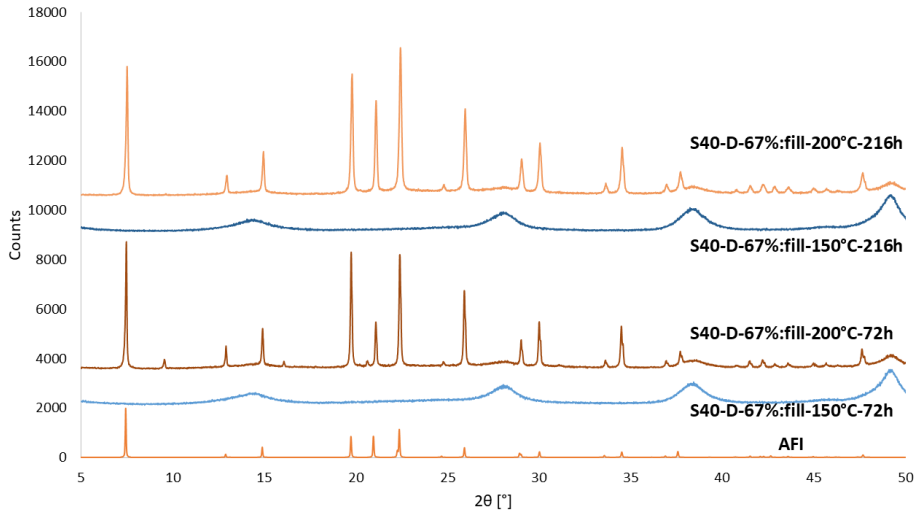

Figure A.2: Diffractogram showcasing the effect of a 67 % fill grade combined with variations in crystallization temperature and time. The syntheses reported corresponds to entries 20 to 23 in Table 4.1.

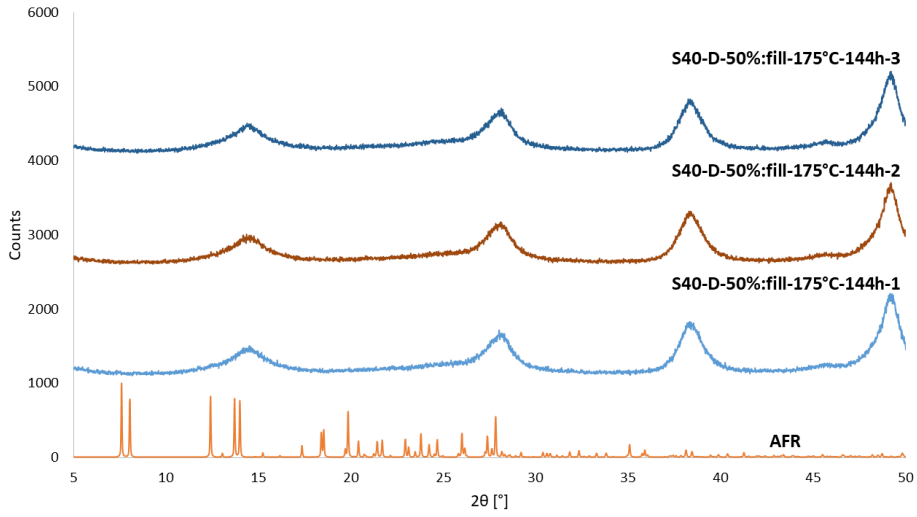

Figure A.3: Diffractogram showing the effect of a 50 % fill grade combined with a crystallization time of 144 hours and a crystallization temperature of 175 °C. The syntheses reported corresponds to entries 24 to 26 in Table 4.1.

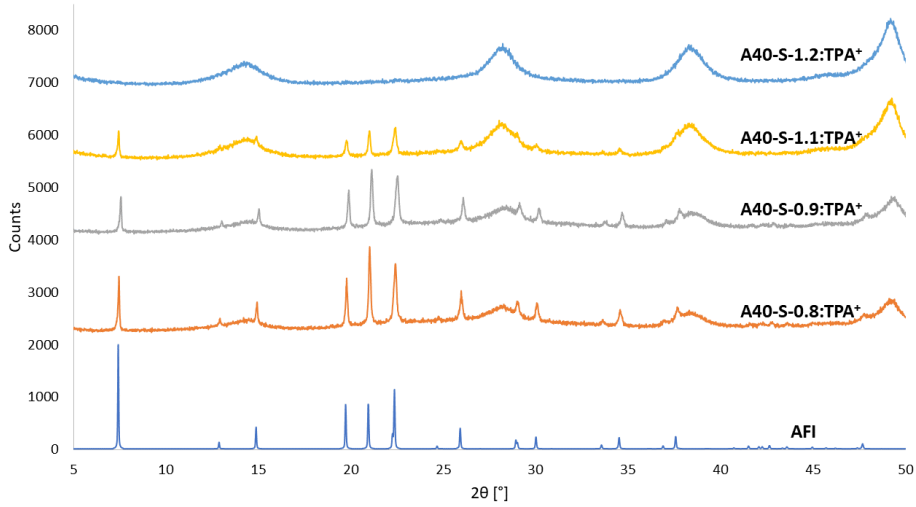

Figure A.4: Diffractogram showing the response of the Sierra based synthesis, when the total TPA^+ concentration is altered to both increase and decrease the pH. The syntheses reported corresponds to entries 40 to 43 in Table 4.3.

A.2 AlPO-40 diffractograms

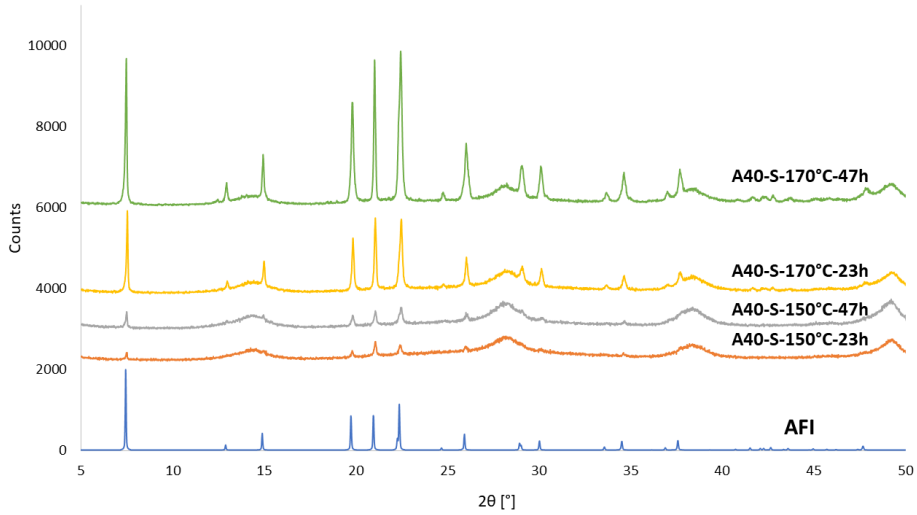

Figure A.5: Diffractogram showcasing the individual and combined effects of increasing crystallization time and temperature. The syntheses reported corresponds to entries 45 to 48 in Table 4.3.

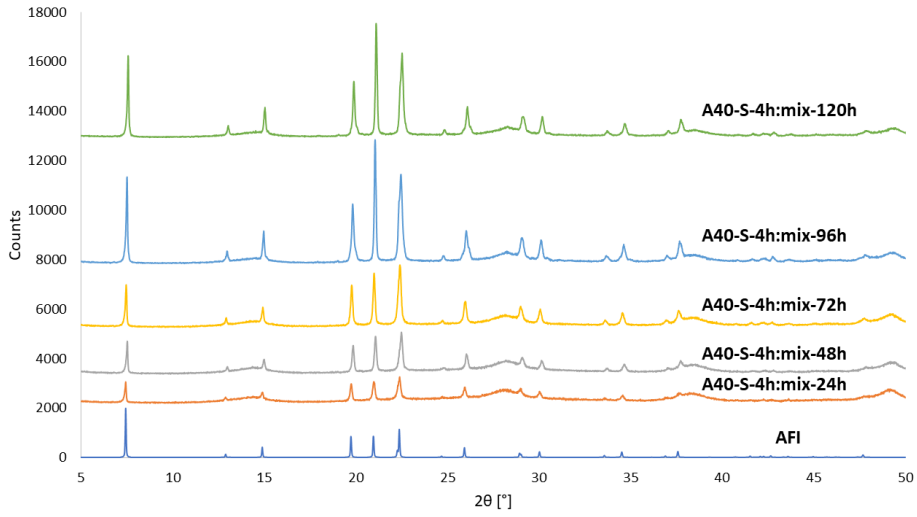

Figure A.6: Diffractogram showcasing the effect of extending the crystallization time at a low ageing time relative to the reported synthesis. The syntheses reported corresponds to entries 53 to 57 in Table 4.3.

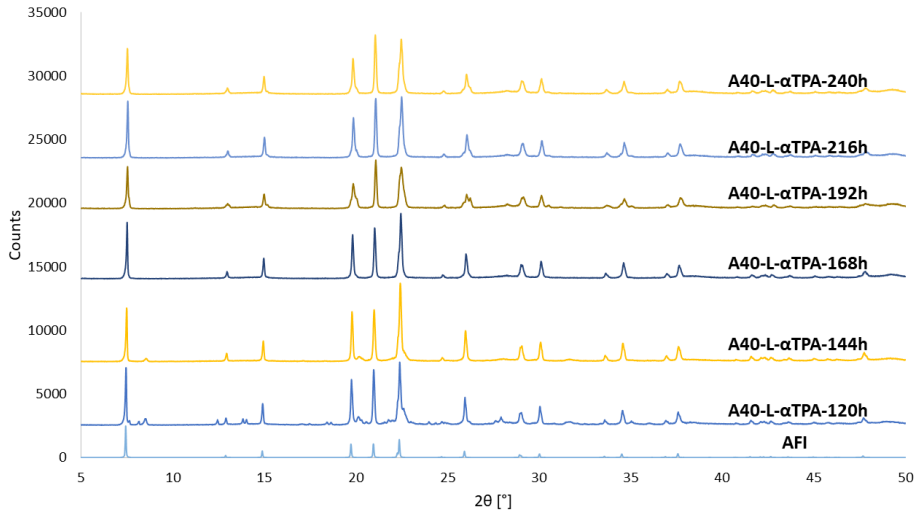

Figure A.7: Diffractogram showing the effect of using TPAOH sourced from Alfa Aesar in the Lourenço based synthesis when liners were washed with HF. The syntheses reported corresponds to entries 61 to 66 in Table 4.3.

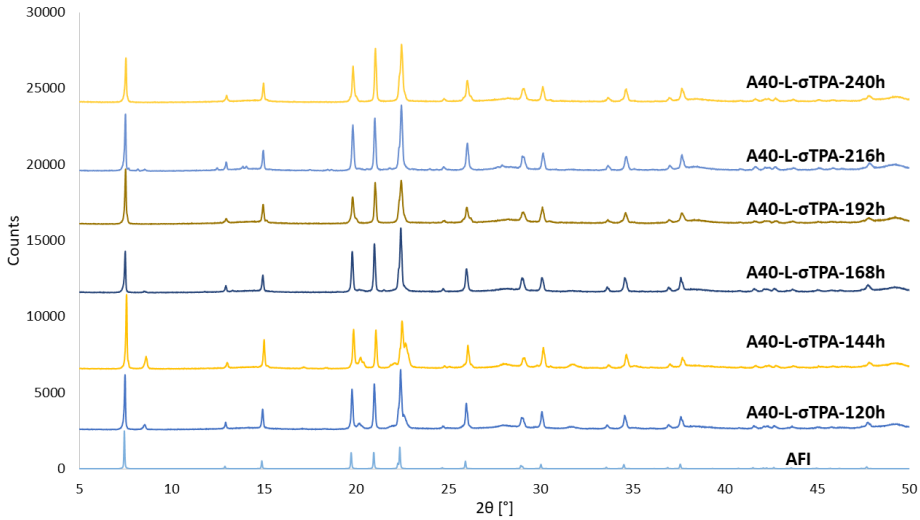

Figure A.8: Diffractogram showing the effect of using TPAOH sourced from Sigma Aldrich in the Lourenço based synthesis when liners were washed with HF. The syntheses reported corresponds to entries 67 to 72 in Table 4.3.

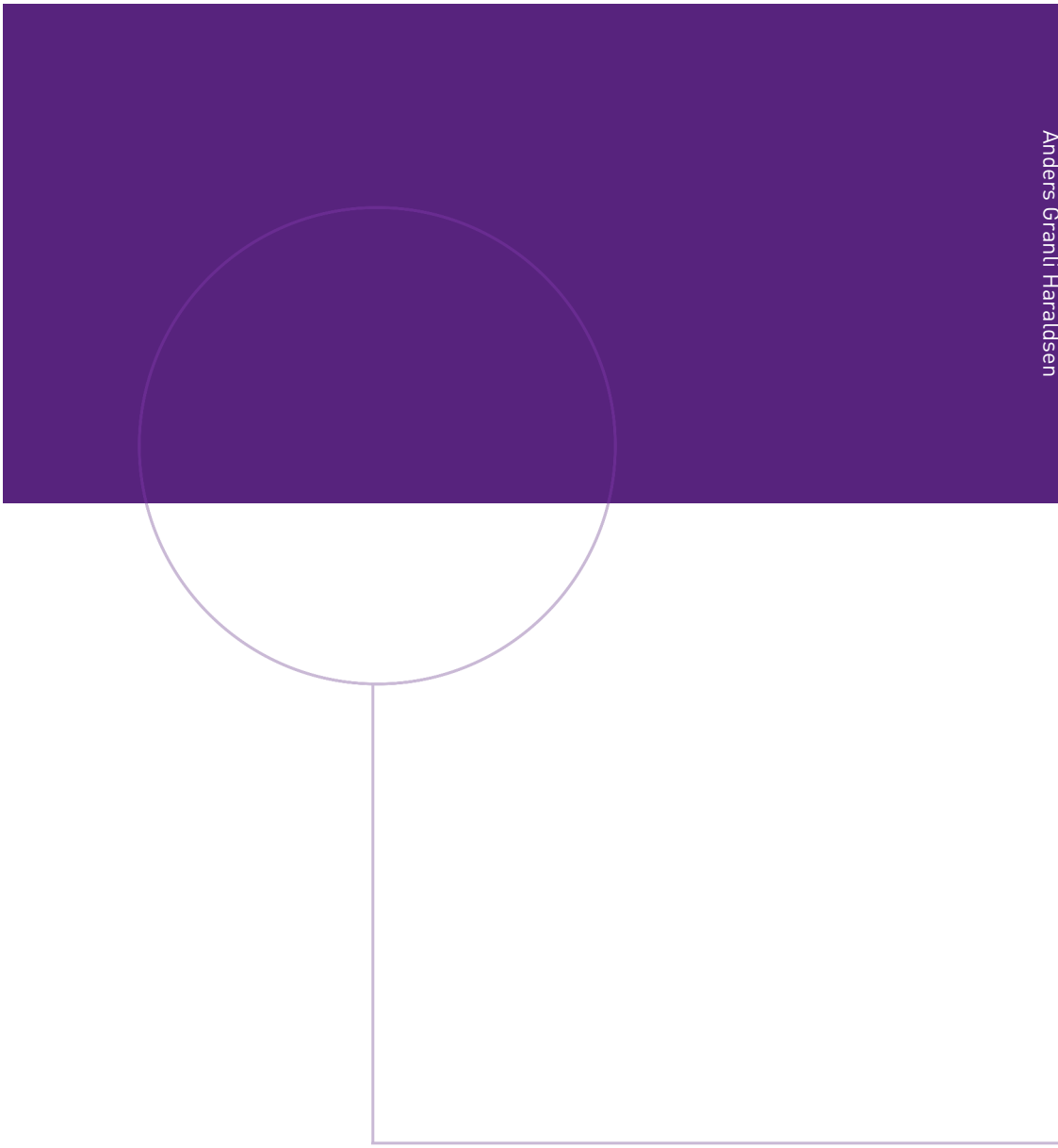

Anders Granli Haraldsen

NTNU
Norwegian University of
Science and Technology